

**EFFECT OF COLOUR CONVERSION LAYER ON THE
OPTICAL AND THERMAL EFFICIENCY OF LED
BASED LIQUID CRYSTAL DISPLAYS**

A Thesis

by

Emrah BAKAN

Submitted to the
Graduate School of Sciences and Engineering
In Partial Fulfilment of the Requirements for
The Degree of

Master of Science

In the
Department of Electrical and Electronics Engineering

Özyeğin University
May 2018

Copyright © 2018 by Emrah BAKAN

EFFECT OF COLOUR CONVERSION LAYER ON THE OPTICAL AND THERMAL EFFICIENCY OF LED BASED LIQUID CRYSTAL DISPLAYS

Advisor: Asst. Prof. Kadir Durak

Co-Advisor: Dr. Devrim Köseođlu

Approved by:

Asst. Prof. Kadir Durak, Advisor,
Department of Electrical and
Electronics Engineering
Özyeđin University

Asst. Prof. Dr. Ahmet Tekin
Department of Electrical and
Electronics Engineering
Özyeđin University

Asst. Prof. Dr. M. Fatih Toy
Department of Electrical and
Electronics Engineering
Medipol University

Date Approved: May 2018



To my family...

ABSTRACT

In light-emitting diode (LED) lit liquid crystal displays (LCD), the colour gamut is related to the back-light unit (BLU) spectrum. The blue LED light is generally converted to green and red bands with phosphor mixtures. The broad emission spectrum of phosphors narrows down the colour gamut because of the incompatibility between the converted spectra and colour filters. Quantum dot (QD) integrated display systems can provide a solution to this problem. In this thesis, we will design a BLU by using high performance blue flip chips. The optical specifications of the BLU will be determined according to the pre-determined colour coordinates and luminance. The BLU components and the LCD panel are characterized to figure out the optical parameters such as the emission spectrum of LEDs, transmittance of optical films, spectrum of BLU and LCD, luminance uniformity, mura level, luminance, colour coordinates and gamut. In addition, the effect of colour conversion layer on thermal efficiency is investigated for On Chip and Remote Layer Solutions. Finally, all the design parameters are optimized in order to enhance the optical and thermal performance of the display system.

ÖZET

LED ile aydınlatılmış likit kristal ekranlarda, renk gamı (gamutu), arka ışık ünitesinin (backlight unit, BLU) spektrumuna bağlıdır. Genel olarak, BLU yapısındaki mavi LED ışığı, bir katman tarafından dönüştürülerek yeşil ve kırmızı spectrum bölgesinde ışımaya yarar. Fosforların geniş renk spectrumu ile renk filtreleri arasındaki uyumsuzluktan dolayı renk gamutu azalır. Kuantum nokta yapılarının ekranlara entegrasyonu sayesinde bu probleme çözüm sağlanabilir. Bu çalışmada, mavi çevrilmiş çipler (flip-chip) ile BLU tasarımı yapılacaktır. BLU'nun optik özellikleri önceden belirlenen renk koordinatlarına ve parlaklığına göre belirlenecektir. BLU komponentleri ve sıvı kristal ekran (LCD) panelinin karakterizasyonları LED spektrumunu, optik filmlerin geçirgenliği, BLU ve LCD'nin spektrumu, parlaklık dağılımı, mura seviyesi, parlaklık seviyesi, renk koordinatları ve gamut gibi parametrelerin ölçümü ile ortaya konur. Ek olarak, çip üstü ve uzak katman çözümü renk dönüşümü yapılan katmanın ısısal verimliliğinin etkisi açısından incelenir. Çalışmanın sonunda, ekranın optik ve ısısal performansı geliştirmek için tüm tasarım parametreleri iyileştirilir.

ACKNOWLEDGMENTS

I express my sincere respect and gratitude to my adviser Asst. Prof. Kadir Durak and co-adviser Dr. Devrim Köseođlu for their valuable support and guidance. I would like to thank the members of the examining committee Asst. Prof. Ahmet Tekin and Asst. Prof. M. Fatih Toy for their comments and suggestions.

I would like to extend my gratitude to Kıvanç Karşlı providing me with all the facility that was required. I'm also thankful to Mehmet Karaman and Mustafa Cem Lider for their effective support in completing my work on time. Special thanks go to Yusuf Sinan Sezer, Mehmet Salih Kılıç and Orkun Özen who always help during my studies.

This work is supported by Vestel Electronics.

TABLE OF CONTENTS

ABSTRACT	iv
ÖZET.....	v
ACKNOWLEDGMENTS	vi
LIST OF TABLES	ix
LIST OF FIGURES.....	xi
I INTRODUCTION	1
II LED BASED LCD DESIGN.....	4
2.1. Direct-LED and Edge-LED for Back Light Unit (BLU).....	6
2.2 Optical Structure.....	7
2.2.1 LED:	7
2.2.1.1 Vertical LED Chip Packaging.....	9
2.2.1.2 Lateral LED Chip Packaging	10
2.2.1.3 Flip-Chip Packaging	12
2.2.2 Diffuser Plate	13
2.2.3 Light Guide Plate	14
2.2.4 Reflector Sheet	15
2.2.5 Diffuser Sheet	16
2.2.6 Brightness Enhanced Film (Prism Sheet).....	17
2.2.7 Reflective Polarizer Film.....	18
2.3 Liquid Crystal Panel	19
2.4 Critical Optical Parameters of Display Design	21
2.4.1 Colourimetry, Radiometry, and Photometry.....	21
2.4.2 Electromagnetic Spectrum.....	21
2.4.3 Luminance	22
2.4.4 Colour Coordinates and Colour Spaces.....	23
2.4.5 Definition of Wide Colour Gamut	24
2.4.6 Visual Performance	26

III	WIDE COLOUR GAMUT (WCG) SOLUTIONS BASED ON LIGHT CONVERSION LAYERS AND ON CHIP STRUCTURES	27
3.1	Analysis of On Chip Solution	41
3.1.1	YR-1313 CSP Flip Chip Type LED.....	41
3.1.2	YR-3030 Lateral Type LED	49
3.1.3	KSF-3030 POB Package Type Flip Chip LED.....	56
3.1.4	MGF-1313 CSP Flip Chip Type LED.....	63
3.2	Analysis of Light Conversion Layers (Remote Solutions)	69
3.2.1	Cadmium (Cd) based Quantum Dot (QD) Film	72
3.2.2	Cadmium (Cd) free Quantum Dot (QD) Film	77
3.2.3	Phosphor Film.....	80
IV	DISCUSSION	86
V	CONCLUSION	92
	REFERENCES	94
	VITA	98

LIST OF TABLES

1	Specifications of Optical Films	34
2	Effect of DBEF on Remote Colour Conversion.....	36
3	Average Temperatures of Thermal Test Points.....	43
4	Thermal Effect of a single YR1313 LED (LED2)	44
5	Uniformity, Luminance and Colour Coordinates	47
6	Gamut Results of the YR1313.....	47
7	Average Temperatures of Thermal Test Points.....	51
8	Thermal Effect of a single YR3030 LED (LED2)	52
9	Uniformity, Luminance and Colour Coordinates	53
10	Gamut Results of the YR3030.....	55
11	Average Temperatures of Thermal Test Points.....	57
12	Thermal Effect of a single KSF3030 LED (LED2).....	58
13	Uniformity, Luminance and Colour Coordinates	59
14	Gamut Results of the KSF3030	60
15	Average Temperatures of Thermal Test Points.....	64
16	Thermal Effect of a single MGF1313 LED (LED2)	65
17	Uniformity, Luminance and Colour Coordinates	66
18	Gamut Results of the MGF1313.....	66
19	Average Temperatures of Thermal Test Points.....	71
20	Thermal Effect of a single Blue 1313 LED (LED2).....	72
21	Uniformity, Luminance and Colour Coordinates	73
22	Gamut Results of the Cd based QD	74
23	Uniformity, Luminance and Colour Coordinates	77

24	Gamut Results of the Cd based QD	78
25	Uniformity, Luminance and Colour Coordinates	81
26	Gamut Results of the Phosphor Film	82
27	Colour Gamut, Luminance, Temperatures and Visual Performances	91



LIST OF FIGURES

1	(a) LCP, (b) Direct-lit BLU and (c) Edge-lit BLU Structures [15]	5
2	Edge-LED BLU	6
3	Direct-LED BLU Structure	7
4	Main Components of the SMT LED Package	9
5	Cross sectional view of Vertical LED chip packing	10
6	Packaging of the vertical LED chip	10
7	Cross sectional view of Lateral LED Structure	11
8	Package of Lateral Chip	11
9	Cross sectional view of Flip-chip Structure	12
10	Flip-chip Package	13
11	Surface of a Diffuser Plate	14
12	LGP Working Principle	15
13	Illuminated LGP by LED	15
14	Reflector Sheet Working Principle	16
15	Moire Effect	16
16	Diffuser Sheet Working Principle	17
17	Prism Sheet Working Principle	18
18	DBEF Working Principle	19
19	Electromagnetic Spectrum Diagram	22
20	(a) CIE 1931 (b) CIE 1976 Colour Spaces	23
21	Mac Adam Ellipses in CIE 1931 (left) and CIE 1976 (right)	24
22	Colour Gamut Standards [43]	25
23	(a) Different Types Phosphors and (b) QD Structure	27

24	Triangles of DCI-P3 and BT2020 in CIE 1976 Colour Space.....	29
25	On Chip Solution (OCS).....	30
26	Remote Colour Conversion Mechanism.....	31
27	Measurement System.....	32
28	Uniformity Measurement Points of LCD	32
29	BLU Structure	33
30	Effect of LCL with DBEF on Colour Conversion.....	35
31	(a) POB 3030 and (b) CSP 1313	36
32	Colour Filter Spectrum	37
33	Assembled LED Bars on Metal Back-cover	39
34	Blue LED Spectrum.....	39
35	Thermal Measurement Points.....	40
36	Thermal Test Point of 1313 CSP	41
37	YR1313 Thermal Test Results	42
38	Thermal Effect of a single LED	44
39	BLU Luminance Distribution of YR1313	45
40	Display Luminance Distribution of YR1313	46
41	Colour Gamut Schema of YR1313 on BT2020 Standard.....	48
42	Colour Gamut Schema of YR1313 on DCI-P3 Coverage Standard.....	49
43	Thermal Test Point of YR3030 POB	50
44	YR3030 Thermal Test Results	50
45	BLU Luminance Distribution of YR3030	52
46	The BLU Spectrums of YR1313 and YR3030 with CFs of Panel	54
47	Colour Gamut Schema of YR3030 on BT2020 Standard.....	55

48	Colour Gamut Schema of YR3030 on DCI-P3 Coverage Standard.....	56
49	KSF3030 Thermal Test Results.....	57
50	BLU Luminance Distribution of KSF3030.....	59
51	The BLU Spectrums of KSF3030 with CFs of Panel.....	61
52	Colour Gamut Schema of KSF3030 on BT2020 Standard.....	62
53	Colour Gamut Schema of KSF3030 on DCI-P3 Coverage Standard.....	63
54	MGF1313 Thermal Test Results.....	63
55	BLU Luminance Distribution of MGF1313.....	65
56	The BLU Spectrums of MGF1313 with CFs of Panel.....	67
57	Colour Gamut Schema of MGF1313 on BT2020 Standard.....	68
58	Colour Gamut Schema of MGF1313 on DCI-P3 Coverage Standard.....	68
59	Thermocouples Connections between Colour Conversion Layer and DP.....	69
60	Thermal Test Point of 1313 Blue LED.....	70
61	Blue LED 1313 Thermal Test Results.....	70
62	BLU Luminance Distribution of Cd based QD Film.....	73
63	The BLU Spectrums of CD based QD with CFs of Panel.....	75
64	Colour Gamut Schema Value of Cd based QD on BT2020 Standard.....	76
65	Colour Gamut Schema of Cd based QD on DCI-P3 Coverage Standard.....	76
66	BLU Luminance Distribution of Cd free QD Film.....	77
67	The BLU Spectrums of CD free QD with CFs of Panel.....	79
68	Colour Gamut Schema of Cd free QD on BT2020 Standard.....	79
69	Colour Gamut Schema of Cd free QD on DCI-P3 Coverage Standard.....	80
70	BLU Luminance Distribution of Phosphor Film.....	81
71	The BLU Spectrums of Phosphor Film with CFs of Panel.....	83

72	Colour Gamut Schema of Phosphor Film on BT2020 Standard	84
73	Colour Gamut Schema of Phosphor Film on DCI-P3 Coverage Standard	85
74	Spectrums of All Solutions	86
75	Crosstalk Regions (a) blue to green (b) green to red	88
76	Visual Performances	90



CHAPTER I

INTRODUCTION

In thin film transistor (TFT) liquid crystal displays (LCD), back light unit (BLU) and LCD characteristics determine the colours [1]. The blue LED light is generally converted to other bands with a layer inside the BLU. This layer can be located on chip or remote place. The location, process and thermal efficiency of conversion materials are critical parameters in terms of optical performance and life time. The implementation of quantum dots (QDs) and phosphors to the BLU makes it possible to widen the colour gamut. Additionally, the life time of LED and conversion layer can be expanded by inhibiting thermal exposure to quantum dots, LEDs and phosphors [2, 3].

Today, increasing the colour gamut has a big role in developing display technologies in the market as well as designing cost effective wide display products with high resolution. Wide colour gamut aims to provide better colour perception by users. In order to provide wide colour gamut, generally QDs, phosphor mixture and their applications are studied [4].

Phosphors are the materials that create a luminescence when it is excited by photons that have appropriate energy. In display design, phosphors are powders having 2-20 μ m granule size. The phosphor materials include impurity ions or activators. These ions or activators when excited produce emission spectra in the visible range. Additionally, they should have high quantum efficiency. If these conditions can be arranged well, conversion mechanism works efficiently [5].

Quantum dots (QDs) have been one of the foregoing materials used in applications in diverse fields ranging from optoelectronics and photovoltaics to sensors, and bio-imaging. This is due to their tunable optoelectrical properties and potential applicability for low cost production. However, common synthesis methods require sensitive, precise injection of volatile and reactive materials, which are not suitable for mass production at the moment [6]. The most prevalent materials that have been used to synthesize QDs are cadmium (Cd) and lead (Pb). However, the use of such compounds, due to toxicity issues, may be a challenge for scaled-up synthesis for large area applications [7, 8]. Furthermore, in electronic industry materials are controlled by RoHS in terms of restriction of hazardous substances. In contrast, indium phosphide (InP)-based QDs, have attracted considerable attention due to their wide range tunability, low bandgap, and lower toxicity.

On chip phosphor converted LED (pcLED) solutions are widely available in the market for both general lighting and display applications. Blue GaN LED light is generally converted to green and red bands by a layer to obtain white light after the BLU [9]. It can be achieved using one or more types of light converting materials. In order to obtain white light, only yellow phosphor can be excited by blue LED such as YAG. In addition to this technique, red and green phosphors can be coated on the LED chip instead of yellow phosphor. In this way, colour gamut of the display is getting larger. However, the disadvantage of this method is expensive. Recently, studies are focused on integrating the QDs on LED chips. However, the thermal inconsistency of QDs is the challenge of these studies. On the other hand, the usage of remote light conversion mechanism is relatively low in general lighting due to high cost of phosphors and inapplicability of QDs under high intensity excitation. However, for

display applications, the mainstream wide colour gamut (WCG) solutions and thermal efficiency are based on photo-enhanced films of QDs or phosphor blends [10].



CHAPTER II

LED BASED LCD DESIGN

In display design, there are generally two main subjects of interest. The first one is the BLU, where the light sources are located. The second one is the liquid crystal panel (LCP), which manipulates the colours and changes the luminance level for each pixel to create images. As a matter of fact, all LCPs need to be illuminated by BLUs [11].

BLUs can be illuminated either directly or from the edges as shown in Figure 1-b and Figure 1-c. In each case, the light output of the LEDs should be uniformly distributed over the surface of the BLU. In order to achieve this, diffuser plates are used in direct-lit type configuration, while a light guide plate (LGP) is used for edge-lit. Diffuser sheets, brightness enhanced films (BEF), dual brightness enhanced films (DBEF) are used together both in direct-lit and edge-lit configurations. In addition, the back reflected light is regained by using a reflector sheet covering the inner surface of the BLU. [12, 13]

LCPs control the liquid crystal polarization via thin-film transistors (TFT), so that the luminance level of each pixel can be controlled. In addition, these pixels also determine the light to be directed to the colour filters to generate coloured images. However, in this mechanism, approximately 5 – 10 % of the BLUs flux passes through the LCPs, therefore the luminance level is considerably decreased. For this reason, transmittance of LCPs is critical for the luminance level of displays. [14]

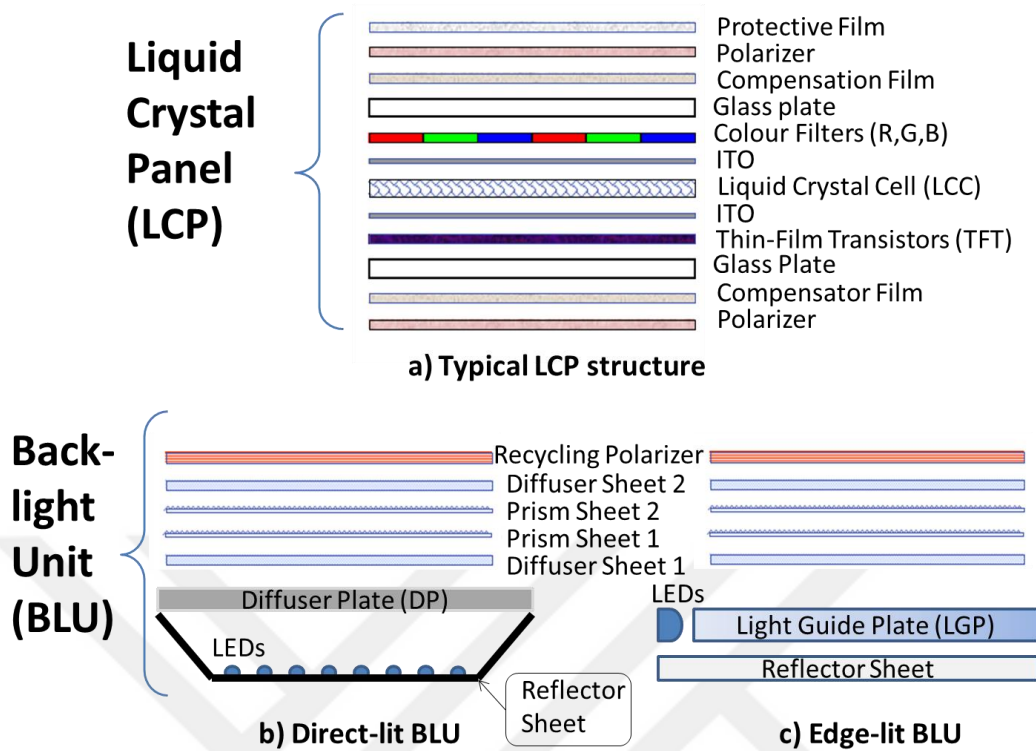


Figure 1: (a) LCP, (b) Direct-lit BLU and (c) Edge-lit BLU Structures [15]

LCPs consist of several layers in Figure 1-a. The first layer on the BLU side is the polarizer. Then, compensator film is used. These are followed by glass plates in between the encapsulation of liquid crystals, colour filters, Indium-Tin Oxide (ITO) coatings and TFTs are sandwiched in Figure 1-a. Here, blue, green and red colour filters are integrated to the LCP in order to generate colours on each pixel areas. After this sandwiched structure, a compensation film and a polarizer are placed similarly [16].

The light source of LCD is BLU which consumes 90% power of the TV. In addition, it shares 40% cost of TV [17]. Nowadays, approximately 400 nit luminance is necessary for TVs. In order to achieve this, BLU should provide about 4000-8000 nit. For ultra-high resolution LCP and big sizes, it is more difficult because of lower transmittance [18]. BLU design has critical optical parameters such as luminance,

colour gamut, colour coordinate, power consumption and uniformity. BLU consists of some mechanical, optical and electrical structures.

Liquid crystal displays (LCDs) are used frequently in daily life in mobiles, e-book readers, video displays, game watches, kiosks, ATMs and automotive displays to televisions. For these reasons, developments on LCDs and related technologies have become an important research interest.

2.1. Direct-LED and Edge-LED for Back Light Unit (BLU)

Direct-LED (DLED) and edge-LED (ELED) are named based on LED locations on the backlight unit. DLED consists of LED which is located under the liquid crystals panel (LCP) as well as LEDs output way is directed to LCP. On the other hand, ELED's light sources are placed on the side of panel. Generally, direct LED is thicker than edge-LED because of their design structures. Despite of the edge-LED's thinner production, cost is commonly higher than direct-LED [19].

For the DLED design, LEDs, reflector, diffuser plate and optical films are used respectively as main optical components (Figure 3). ELED design doesn't use diffuser plate. Light guide plate (LGP) is used to change the light direction to LCP side (Figure 2).

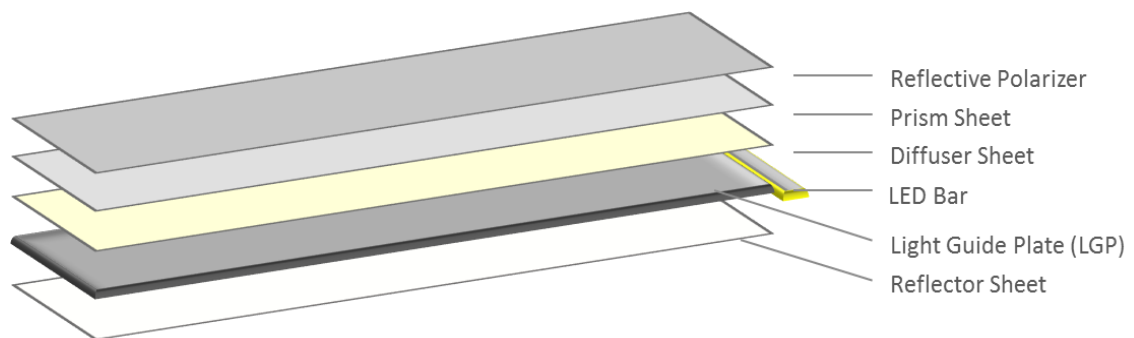


Figure 2: Edge-LED BLU

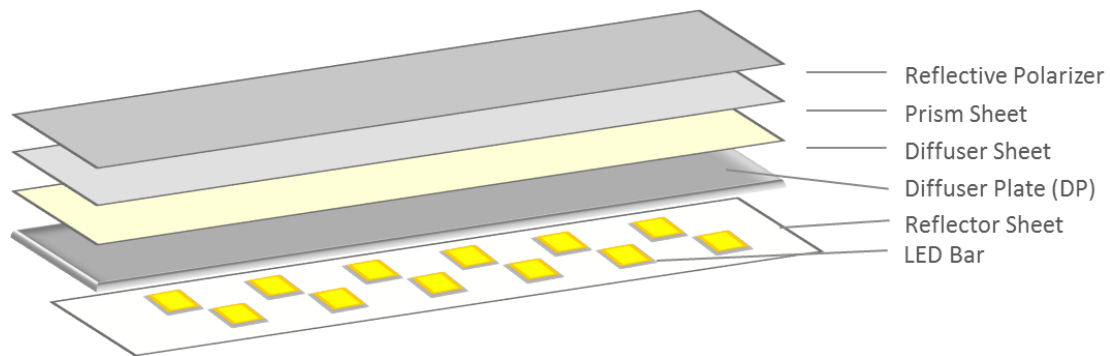


Figure 3: Direct-LED BLU Structure

2.2 Optical Structure

2.2.1 LED:

LED is a semi-conductor device which includes a P-N junction. In 1907, British experimenter Henry Joseph Round, in Marconi labs, applied potential difference to silicon carbide crystal firstly, and showed that SiC emits yellowish light. He announced that diodes of radio receivers emitted light when current was applied to diodes in the middle of 1920s [20]. Working principle of LED was published firstly by a Russian scientist Oleg Vladimirovich Losev in 1927 [21]. In 1962, Nick Holonyak developed first light-emitting diode that emitted red light by growing $\text{GaAs}_{1-x}\text{P}_x$ (an alloy) [22]. In 1993, Shuji Nakamura achieved GaN blue LED [23]. However, it was too expensive for commercial usage until 1994. Fairchild Semiconductors reduce the LED cost using new packing methods and planar process for LED chip. After these studies, blue chip encapsulated with yellow phosphor was used to generate white light emitting LED. In addition, red and green phosphors are also excited by blue LED to get white spectrum [24].

LEDs can be produced from InGaN, GaN, GaP, SiC, GaP, AlGa, AlGaAs ... etc. [25]. Since, compounds have specific spectrum ranges and peaks, the spectrum of the LED depends on the used compounds. In this way, it is possible to produce different coloured LED emission by changing compounds or mixture [25].

Life time of LEDs is higher when compared with other light sources as well as it's lower forward voltage (V_f). Furthermore, it has a short response time, durability, reliability. Therefore, there are many advantages of integrating LEDs to BLU as light sources. There are four practical methods of generating white LED for BLU which are blue LED with yellow phosphor, blue LED with RG phosphor, UV LED with RGB phosphor and single coloured RGB LEDs [17].

LED packaging methods are very critical for stability, thermal conditions and efficiency. Generally, surface-mount technology (SMT) based packing is preferred because of having low cost process in TV technology. As shown in Figure 4, the heat sink platform does not only provide electrical contacts for the SMT LED packing, but also decreases the heat on the chip. In order to gain back scattered light, the top of the heat sink is coated with silver. Additionally, silver or gold is coated on the bottom of the system for soldering. Phosphor is inorganic powder which is mixed with the polymeric binder like silicone. According to the viscosity of the mixture, 10-100 micrometer thickness is obtained [25].

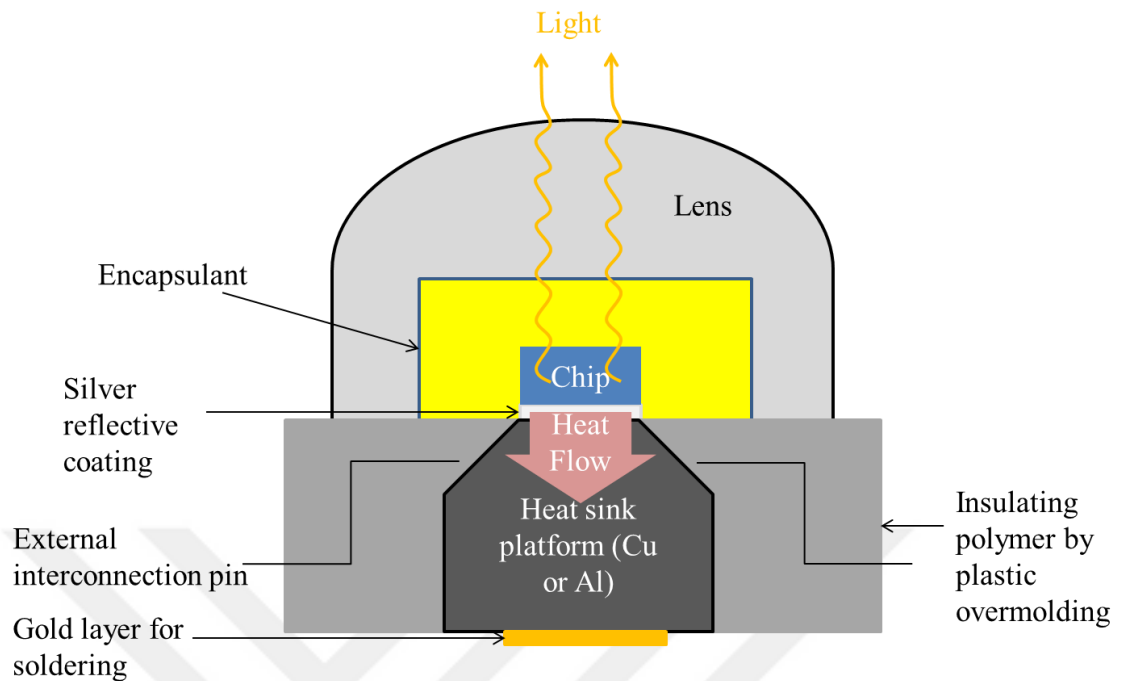


Figure 4: Main Components of the SMT LED Package

SMT packing process consists of three type packing which is vertical LED chip packaging, lateral LED chip packaging and flip-chip packaging.

2.2.1.1 Vertical LED Chip Packaging

In vertical LED chip, wire is connected to cathode which is located on the top surface of the LED chip which is demonstrated in Figure 6. The layers of the vertical LED can be seen in cross sectional view in Figure 5. Anode is placed at the bottom of the structure. Additionally, host silicone, p type GaN, active region and n type GaN are laminated layer by layer from bottom to top.

In order to provide efficient heat transmission, polarity can be applied to heat sink to polarize latter. However, it is unacceptable for some applications. In addition to this method, interposer, which is dielectric and thermally conductive, may be added

between the LED chip and heat sink. To avoid electrostatic discharge (ESD), zener diodes are connected to LEDs [26, 27, 28].

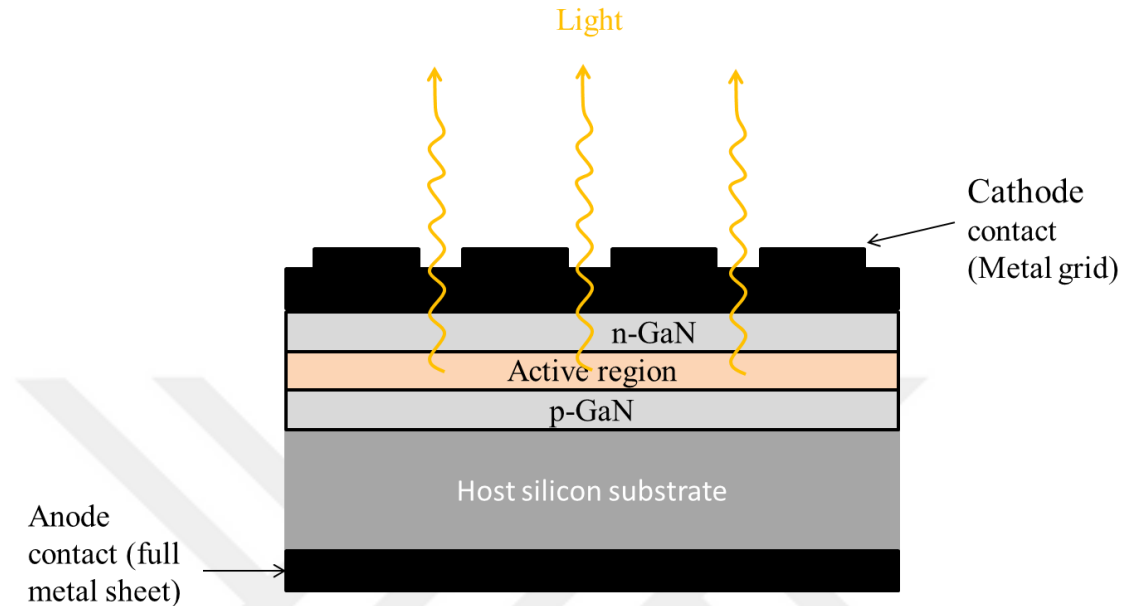


Figure 5: Cross sectional view of Vertical LED chip packing

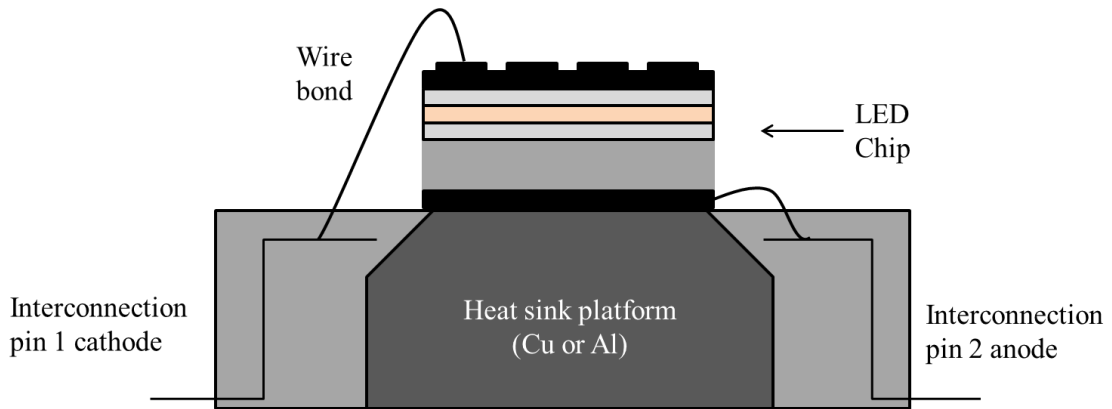


Figure 6: Packaging of the vertical LED chip

2.2.1.2 Lateral LED Chip Packaging

Figure 7 and Figure 8 show the cross-sectional view of lateral LED packaging. In this structure, anode and cathode are placed on the surface of p-type and n-type regions. The wires are linked to these contacts. The sapphire substrate provides

electrical isolation between the chip and heat sink. In this method the shadowing effect may occur due to the nature of wire bonding.

The solder bumps are placed parallel to contact points of the chip. Then, thermal treatment is completed in oven to evaporate the liquid content in order to solidify the solder [26, 27, 28].

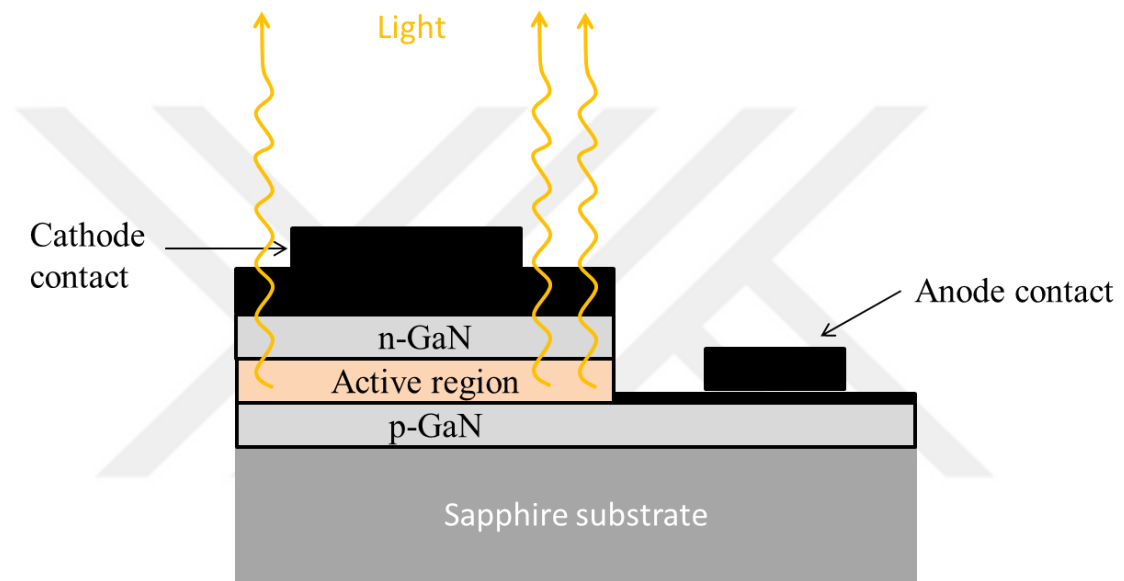


Figure 7: Cross sectional view of Lateral LED Structure

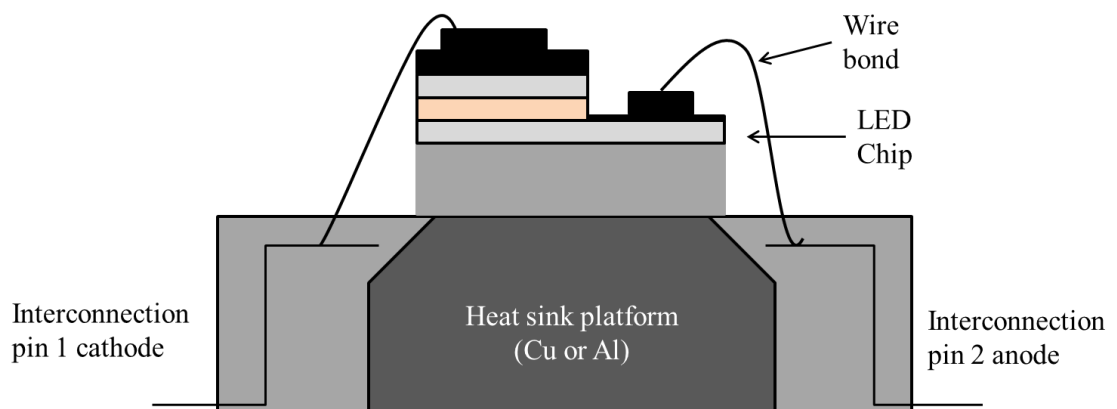


Figure 8: Package of Lateral Chip

2.2.1.3 Flip-Chip Packaging

Flip-chip is assembled upside-down on ceramic or organic circuit boards as indicated in Figure 9 and Figure 10. In contrast to Vertical and Lateral packing methods, wire connections are not necessary for Flip-chip packaging (Figure 10). Interposer can be integrated on package or circuit board.

Locations of solder bumps are adjusted via contact pads. Then, the structure is exposed to thermal treatment in an oven to stabilize the solder. The epoxy is implemented by dispensing along to the sides of LED. The epoxy, which has low viscosity, is filled into the gaps. In the end, the epoxy is cured by a heat source [26, 27, 28].

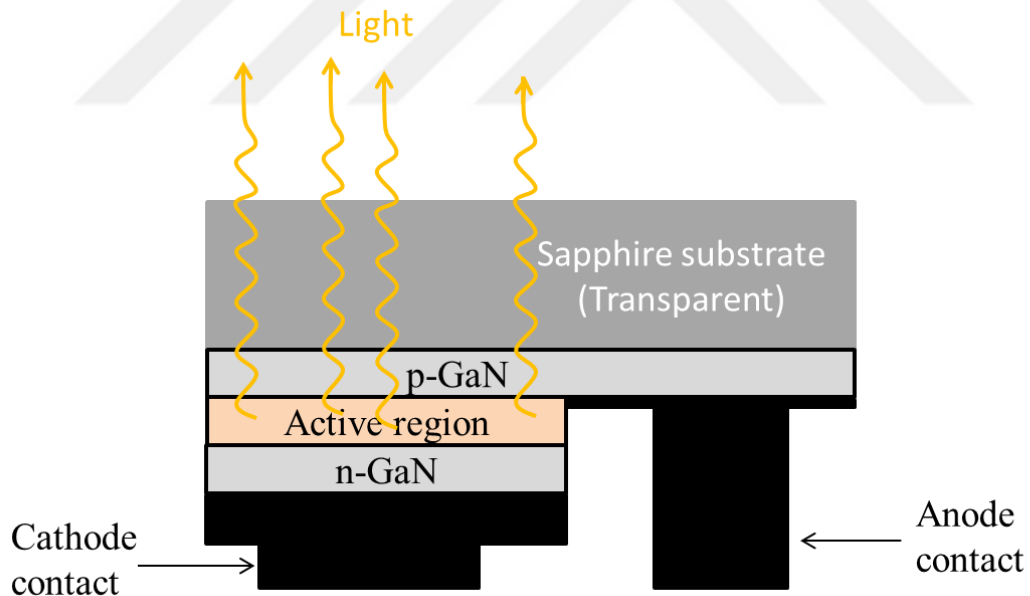


Figure 9: Cross sectional view of Flip-chip Structure

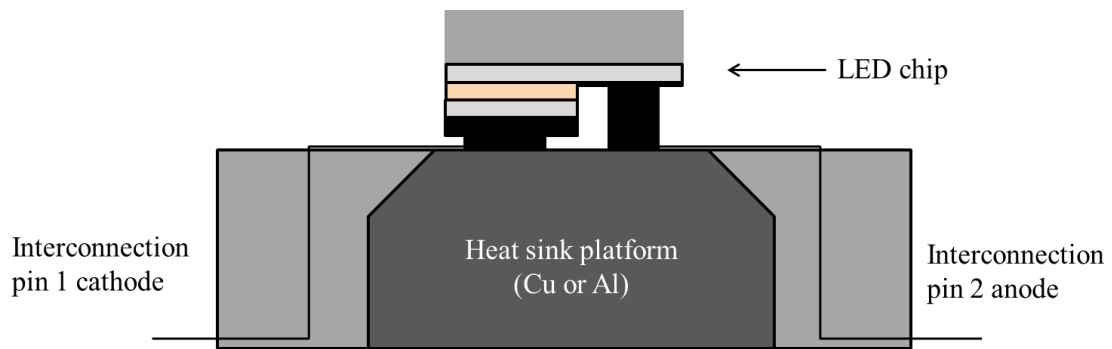


Figure 10: Flip-chip Package

2.2.2 Diffuser Plate

Diffuser plate (DP) spreads out the light over a large area which is reflected from the reflector sheet and received directly from light sources. It is used generally for direct-LED BLU in order to provide uniform light distribution. Besides, the optical films over the DP improve the uniformity of the light before reaching to the LCP. Mostly, it is made of polymeric materials such as polystyrene (PS) or polycarbonate (PC).

DPs contain only diffuser agents to diffuse incident light. This diffusivity largely depends on the difference in refractive index between the particle and the matrix, and the diameter of the light diffuser agent. When spherical diffuser agents are used in the diffuser plate, diffusing performance can be analyzed using Mie scattering. If refractive index of particles is increased, back scatter light and intensity at wide angles will be dominant. In fact, since different sized particles are used for diffusion, multiple scattering should be taken into account [29].

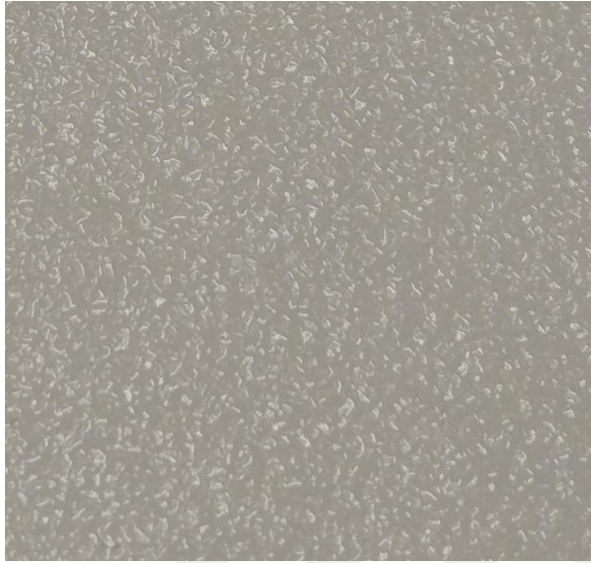


Figure 11: Surface of a Diffuser Plate

2.2.3 Light Guide Plate

Light guide plate (LGP) is used generally in edge-LED BLU which uses dot patterns to provide uniform light distribution. The dots are made from chemical mixture coated on the polymethyl methacrylate (PMMA). Besides this method, it can be created by forming shapes on the PMMA using hot roll stamping machines. Both of them aim to achieve uniform light distribution by designing dot size and shapes [30].

Incident light from the source is reflected and refracted to panel direction. Furthermore, incident light propagates from source to the opposite side of the panel by total internal reflection in the LGP. Diffuser, prism and polarization sheets are typically placed above the light guide plate as shown in Figure 12 in order to collimate the output beam and provide good light contrast [31, 32]. For such systems, high power efficiency and high beam uniformity are essential to achieve overall low power consumption and a high quality illumination of the LCD panel [32]. In addition, thinner LGP designs enable slimmer BLU as well as reduce the cost.

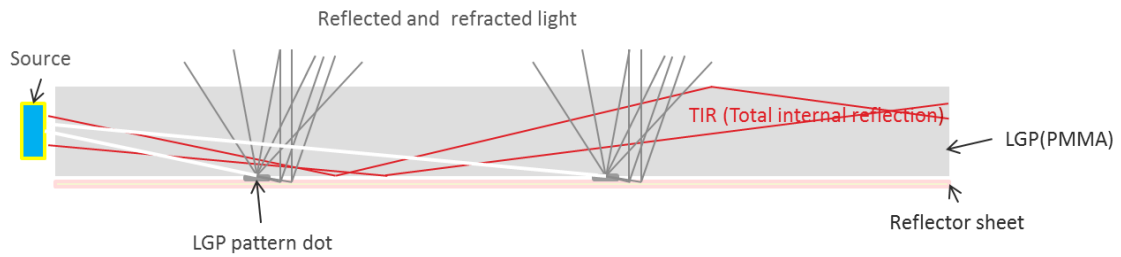


Figure 12: LGP Working Principle

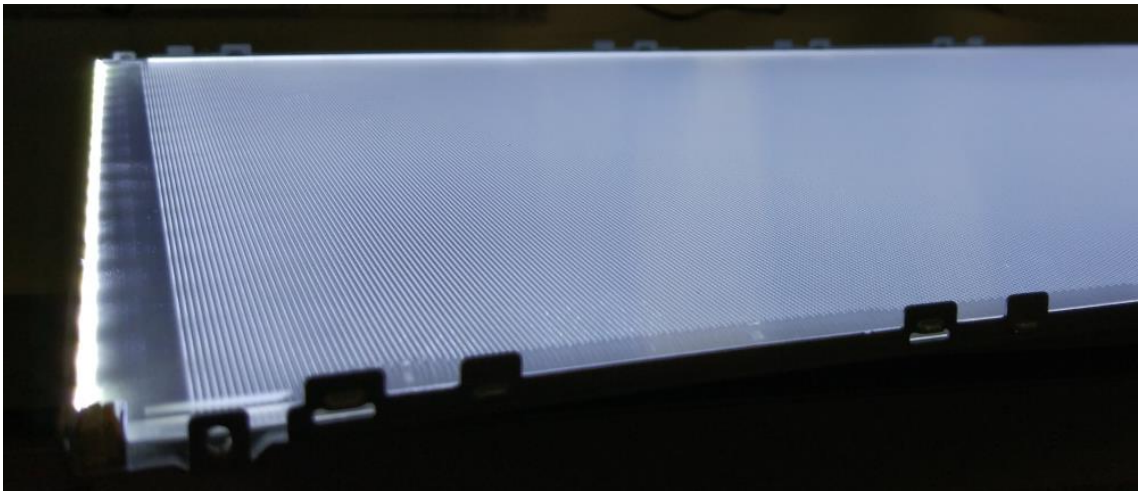


Figure 13: Illuminated LGP by LED

2.2.4 Reflector Sheet

Using a reflector in BLU aims to gain back scattered light. The reflector is located on the BLU metal in order to direct the light efficiently to the panel. Generally, polyethylene terephthalate (PET) are used as substrate which includes holes to reflect the light by means of their refractive index difference. These design and materials are cost effective solution for most of the reflector manufacturer.

In display design, luminance and visual performance are two important parameters for a successful design. Reflector's reflectance, haze and gloss have big role in achieving a successful display design. These characteristics are related with reflector design, raw materials, and additive materials as well as whether it is coated or not.

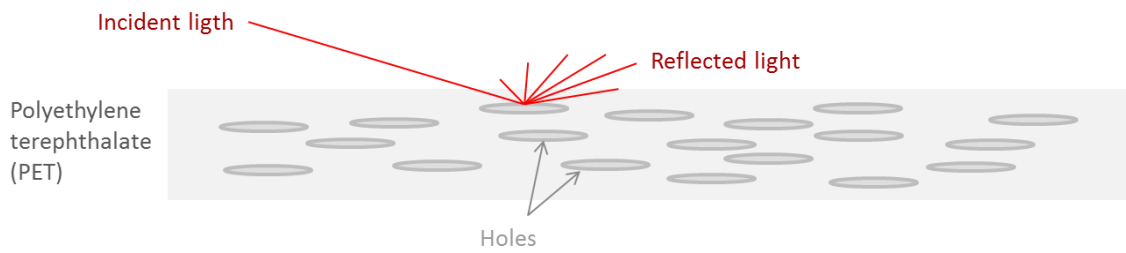


Figure 14: Reflector Sheet Working Principle

2.2.5 Diffuser Sheet

Diffuser sheets are used to scatter the light in BLU. Simply, the working principle of diffuser sheet is given in Figure 16. The light is scattered by the beads located on the surface of the sheet to acquire a homogeneous distribution. It can be used for many visual performance solutions such as increasing the view angle, avoiding moire effect and getting more uniform light distribution. The reason of moire effect is the overlapping of two prismatic structures which is represented in Figure 15.

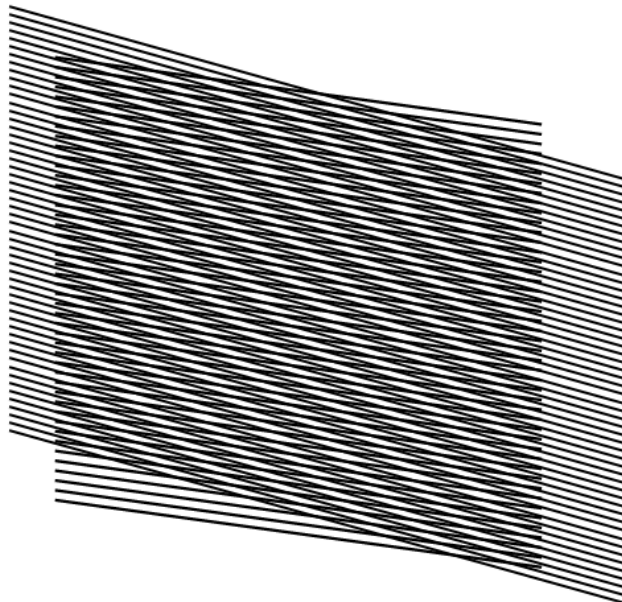


Figure 15: Moire Effect

Critical optical specifications of the diffuser sheets are haze and transmittance values. Increasing the haze provides smoothness for the light distribution problems such as light leakage and dark areas. Luminance is critical parameter in the market which is closely related with transmittance of all optical films.

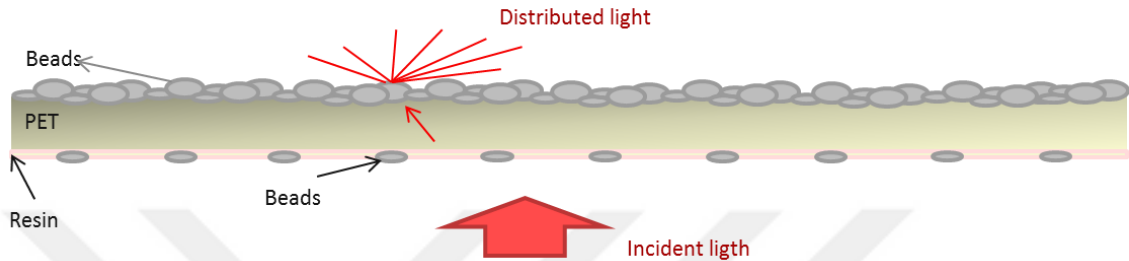


Figure 16: Diffuser Sheet Working Principle

2.2.6 Brightness Enhanced Film (Prism Sheet)

Basically, prism sheet is obtained by processing prismatic structures on PET. Brightness Enhanced Film (BEF) is integrated into BLU for luminance gain. Incident light is directed to liquid crystal panel to increase the luminance (gain) level of BLU. Prismatic structure determines whether light is reflected or not according to its angles. Reflected light is returned back via reflector sheet to provide proper angle. Other rays are directed and refracted to direction of LCP by prismatic structures [33].

The components of regular shape of prism sheet and LCP may lead to moire effect at certain angles which can be seen in Figure 15. This effect can be avoided by using irregular shapes on prism sheet or tilted prism sheet.

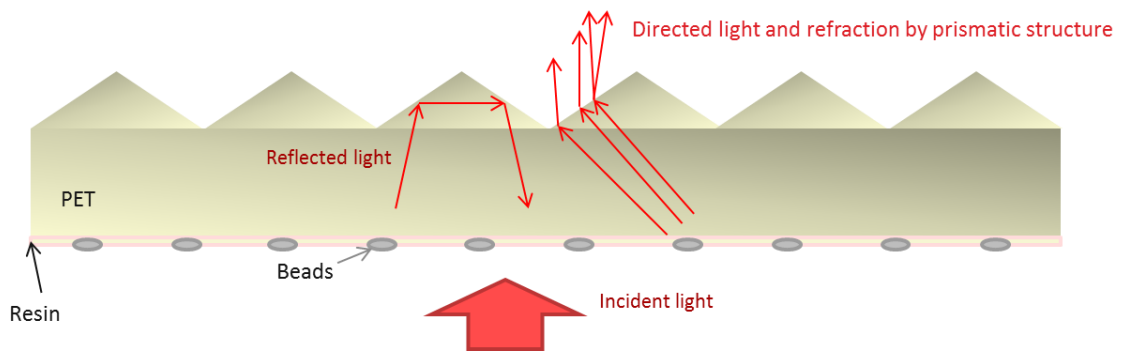


Figure 17: Prism Sheet Working Principle

2.2.7 Reflective Polarizer Film

Reflective polarizer film transmits the correctly polarized light and reflects back the orthogonally polarized light into BLU. The polarizations of reflected lights are changed by scattering from the micro-beads on the surfaces of prism sheets and reflector sheets. These loops are repeated increasing the proper polarization which is transmitted by reflective polarizer. As a result, reflective polarizer film increases the amount of correctly polarized light to pass through the liquid cell. Therefore, it contributes to luminance gain. This solution provides significant luminance gain without higher power consumption. The luminance gain process is depicted in Figure 18 comparing a panel with reflective polarizer and without polarizer [34].

Reflective polarizer films allow only one linear polarization to pass through the LCD; the other polarized rays are not allowed to propagate. This polarization is calculated according to bottom polarizer located on the determined liquid crystal cell. The disallowed polarizations are reflected to backward.

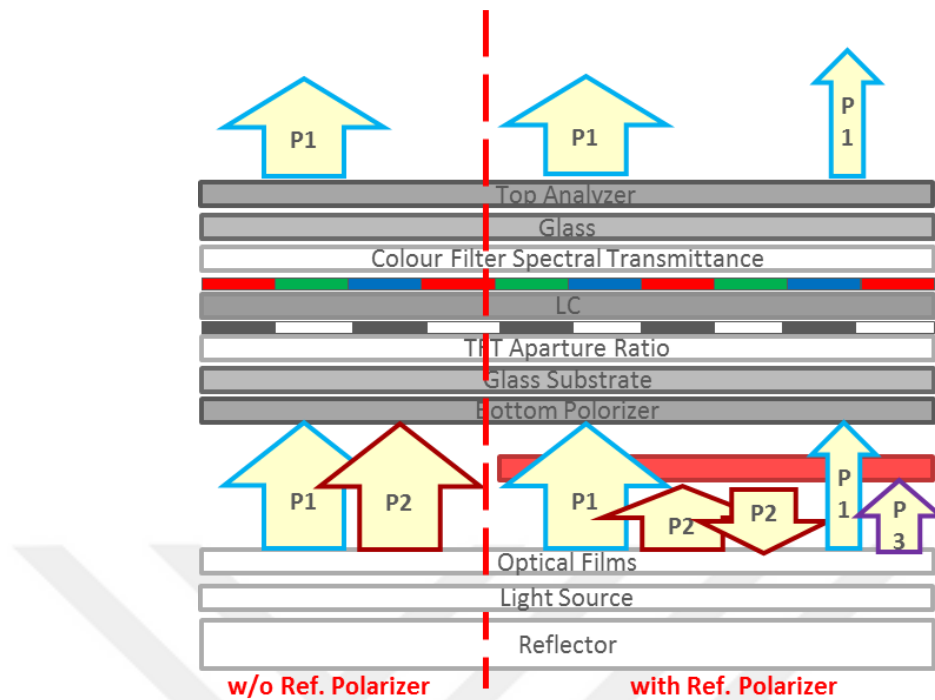


Figure 18: DBEF Working Principle

2.3 Liquid Crystal Panel

Liquid Crystal Panels (LCPs) utilize liquid crystals between two polarizing sheets (Figure 1-a). Alignment and modulation of the liquid crystals are managed by electrical field and thus light polarizations can be arranged. In this way, intensity of incident light passing through LCP can be controlled. For controlling each pixel, TFTs should be driven one by one. Therefore, thin film transistors (TFT) are used to manipulate the intensity of each pixel. TFT based LCP displays need to be illuminated by a light source. At this point, LEDs are preferred due to power consumption and cost advantages.

The final image on LCP with different colours is obtained by processing the BLU light through the CFs. Furthermore, the colour filters in LCP can be adjusted to get wider colour gamut and also it helps improving the properties of BLU spectrum.

There are many criteria that affect the LCP performances such as response time, contrast value, viewing angle, colours, transmittance, uniformity and resolution. Improvements are mostly focused on these criteria in LCP industry. In this manner, developments on LCP technologies have a big role on the performance criteria. The first LCD technology was introduced by Joseph Castellano in 1968 [35]. In 1990s, twisted nematic cell technology was being used widespread in the display industry [36]. After the developments on twisted nematic structure, in plane switching (IPS) and vertical alignment (VA) cell technologies emerged in the display market. IPS and VA names are inspired by their liquid crystal structures. [37].

LCPs include two layers between polarizers. These layers are separated with spacers whose inside is filled with liquid crystals [37]. It also includes the TFT array deposited on a substrate by a complex processes chain of plasma enhanced chemical vapor deposition (PECVD), photo-lithography, sputter deposition, dry and wet etching and other processes [37].

Amorphous silicon (a-Si) or polycrystalline (p-Si) silicon are used to produce thin film transistors generally. A-Si and p-Si can be deposited by using physical vapor deposition (PVD) and chemical vapor deposition (CVD) methods mostly. Doping and lithography processes of silicon thin films are finalized as thin film transistors (TFT) on integrated circuit (IC). It is a simple and useful technology. However, p-Si provides better colour performance as well as low temperature process [37].

2.4 Critical Optical Parameters of Display Design

2.4.1 Colourimetry, Radiometry, and Photometry

Colourimetry and related devices are interested in colour measurements. Radiometry is associated with optical radiation which is an electromagnetic radiation that includes the wavelength range between 0.01 μm and 1000 μm . Photometry is related to brightness in the range of visible light which is limited by human eye. In this manner, since photometry covers 0.360 μm and 1000 μm spectrum range, it is distinct from radiometry. In addition, it involves only the luminous flux perceived by human eye which is measured in lumens and defined as efficacy (lm/W). In contrast, radiometry is defined by radiant flux measured in watt as efficiency (%), which is related to real power [25].

2.4.2 Electromagnetic Spectrum

Electromagnetic spectrum covers wide wavelengths range from radio wave to gamma ray. From radio wave to gamma ray, as the energy and frequency increases, wavelength decreases.

White light can be separated to different wavelengths via a prism. Different materials have distinct light-material interaction characteristics. Emission and absorption spectrums depend on the energy band structure of the materials. Furthermore, all materials have characteristic electromagnetic emission over the temperatures absolute zero [25].

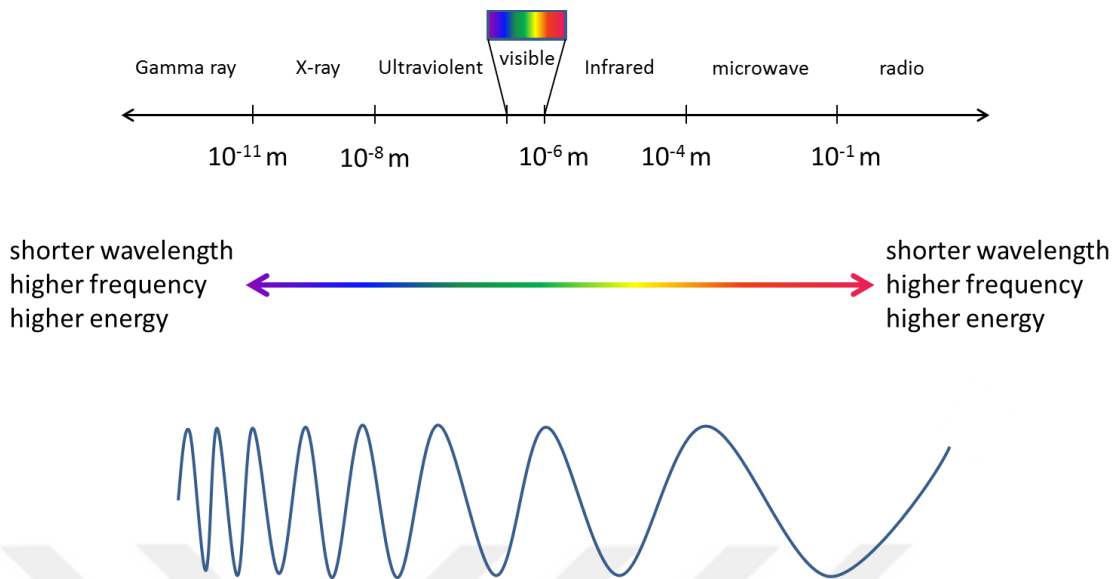


Figure 19: Electromagnetic Spectrum Diagram

2.4.3 Luminance

Since most people prefer displays with high luminance in terms of human perception, luminance is a critical parameter in display industry. Luminance of a display depends on the backlight luminance and transmittance of liquid crystal panel.

Luminance can be increased by designing the BLU components such as prism sheet, reflective polarizer films. In addition, the driving current of LEDs has a big role on the luminance level. However, increasing the luminance may lead to some complications like view angle performance, high power consumption, cracking of LED, life time and thermal problems. Therefore, according to the targets and restrictions, optimization of BLU design is carried out simultaneously with the luminance studies. On the other hand, liquid crystal panel has a big role on the luminance since it has a certain transmittance. Transmittance decreases from HD (high definition) to FHD (full-high definition) because of aperture ratio. For instance, HD has approximately 15% higher aperture ratio than FHD [17].

2.4.4 Colour Coordinates and Colour Spaces

Colour spaces and colour coordinates are critical parameters in order to define the colour perception. In other words, several colour space models have been introduced in the visible colour spectrum. For example, Commission internationale de l'éclairage (CIE) spaces were developed to map colours such as chromaticity and luminance. Both CIE 1931 and 1976 are commonly used ones. Colour spaces represent all colours whose borders are limited by the average human eye visibility [38].

Generally, CIE 1931 is preferred in display industry since it is the traditional way of colour mapping and have been adapted to analysis techniques for many years [39]. The CIE 1931 diagram, in Figure 20-a, is created by points that have different colours. The edges of the diagram shows pure colour region which is the most saturated. This saturation is decreased towards the center of the diagram. Some critical optical parameters are determined on the colour spaces such as colour gamut, colour coordinates. It provides a standard for measurements and comparisons.

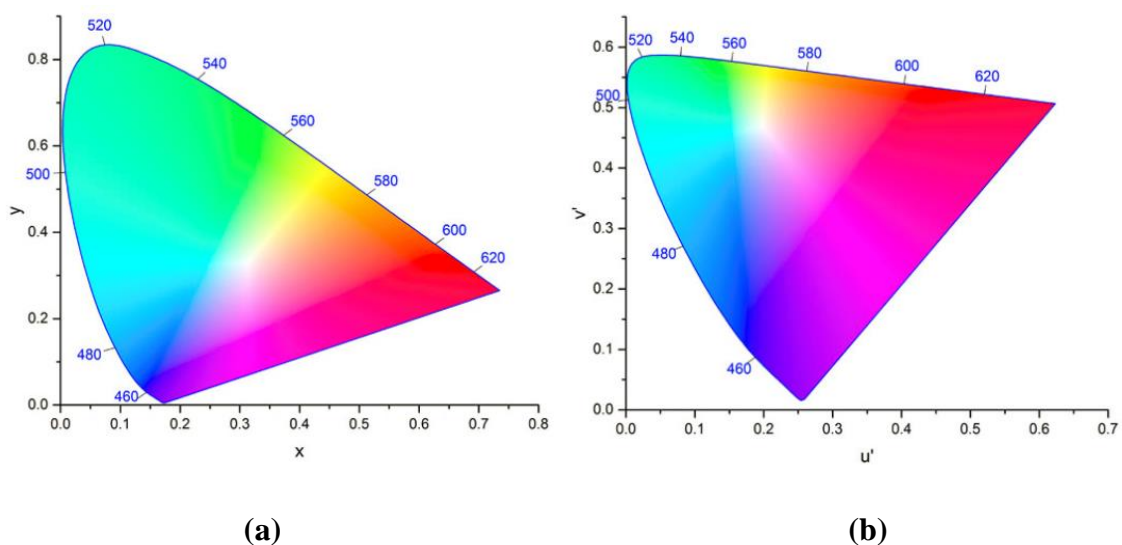


Figure 20: (a) CIE 1931 (b) CIE 1976 Colour Spaces

In 1942, MacAdams integrated ellipses on the colour systems to optimize the colour space according to human eye [40]. However, the ellipses used in CIE 1931 indicate a large variation in colour. In the CIE 1976 (Figure 20-b), MacAdams used the different colour mapping and minimized the colour variations in the ellipses. The difference between CIE 1931 and 1976 approach can be seen in Figure 21. Essentially, CIE 1976 approach gives rise to all MacAdam's ellipses seems to have circles with equal radius, and would provide the framework for accurate and consistent colour difference calculations [41]. As a result, coordinates of a specific colour can be differentiated much better in CIE 1976 than CIE 1931.

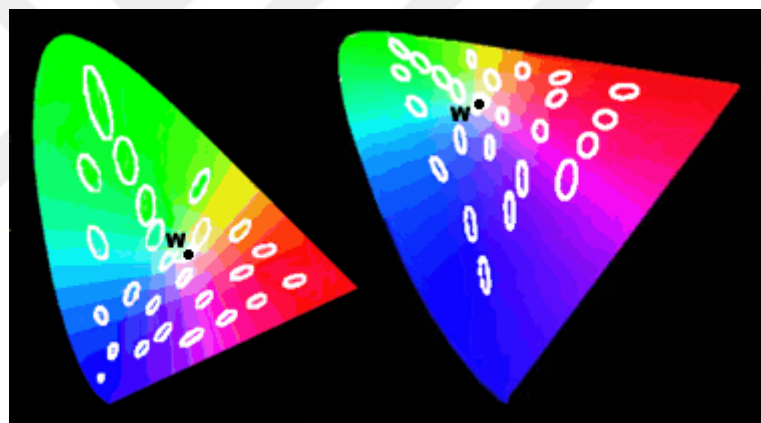


Figure 21: Mac Adam Ellipses in CIE 1931 (left) and CIE 1976 (right)

2.4.5 Definition of Wide Colour Gamut

The colour gamut specifies colour range which can be sensed by human eye. Generally, this parameter is evaluated based on some standards such as national television system committee (NTSC), standard red, green, blue (sRGB), Adobe red, green, blue (Adobe RGB), Digital Cinema Initiatives (DCI-P3) and BT2020 (Rec2020). Every individual space is defined by triangles that include blue, green and red coordinates on colour space. The target colour space is evaluated with respect to these

standards by calculating the direct intersection area or the area ratios of the triangles [42].

In TV industry, NTSC standard was used generally which is defined according to cathode ray tube (CRT) TVs before the emergence of LCD TVs. However, as the display technologies are being improved, new standards with larger colour gamut on the colour space will be necessary in order to evaluate the output. Recently, BT2020 has the largest defined area among the other colour gamut standard. In Figure 22, the colour gamut standards are given with the corresponding relative size.

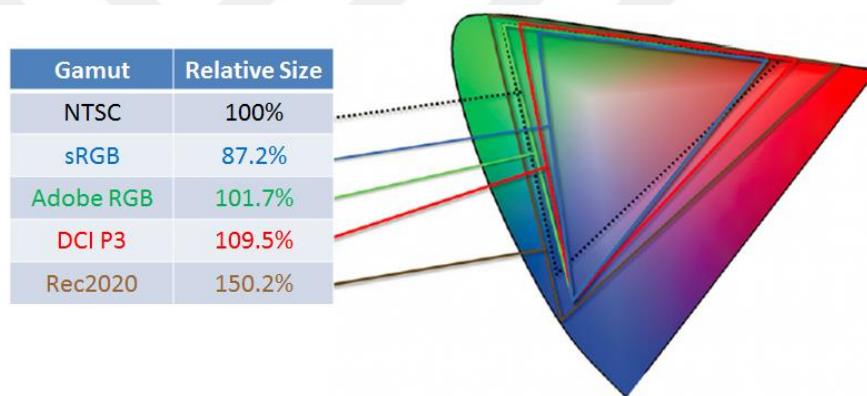


Figure 22: Colour Gamut Standards [43]

Colour gamut evaluation also can be determined by using different shapes apart from triangle. However, general trend uses triangle systems. To increase the colour gamut, triangle area should be enlarged. However, since enlarging the colour gamut may not increase the coverage area in the specified standard, increasing only the area does not refer to large colour gamut.

2.4.6 Visual Performance

The other significant assessment for a display is the visual performance test. Since the visual performance is sensed by human eye, the evaluation may be relative which makes performance test difficult. However, visual tests are necessary for display manufacturers to determine the problems such as skin tones, BLU mura, cell defect that cannot be analyzed by optical measurement devices. These issues are disruptive problems for users.



CHAPTER III

WIDE COLOUR GAMUT (WCG) SOLUTIONS BASED ON LIGHT CONVERSION LAYERS AND ON CHIP STRUCTURES

In LCD based LED displays, one or more conversion layers are excited by blue LED light to get white light. Yellow phosphor $\text{Ce}^{+3}:\text{YAG}$ is preferred in terms of cost advantage. However, colour gamut with yellow phosphor is around 67-72% of NTSC, 75-80% of DCI-P3 and 55-60% of BT2020 standards. Wider colour gamut can be achieved by using different type phosphors of (Figure 23-a) or quantum dots (QDs) (Figure 23-b). RGB LEDs also extend the colour gamut triangle. However, this solution is not preferred because of its high cost.

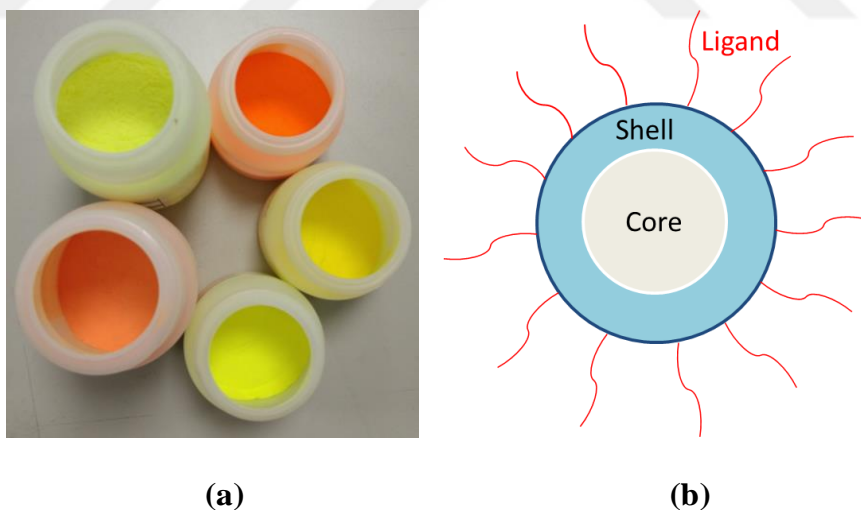


Figure 23: (a) Different Types Phosphors and (b) QD Structure

QDs can provide promising solutions in order to get wider colour gamut for LCDs [44, 45]. Their narrow emission spectrum creates pure colours and low intensity in crosstalk regions of CFs as well [46, 47]. Since, QDs are thermally very sensitive

materials, their usage directly on the LED is not suitable [48]. The optical structures of QDs can be destroyed due to the heat coming from LED chip. Remote QD films or plates, which include quantum dot particles, provide solution for wide colour gamut.

Wide colour gamut is one of the most critical parameters for display design. There are various colour conversion systems and materials for wider colour gamut solutions. However, they have many advantages and disadvantages in terms of process, material, location of layer, thermal efficiency and light convertors.

We have compared different type systems and materials in terms of wide colour gamut and thermal efficiency while targeting optical specifications such as luminance, colour coordinates and luminance uniformity. Furthermore, Remote Solutions (Figure 25) and On Chip Solutions (OCS) (Figure 26) are evaluated in terms of optical efficiency and thermal efficiency as well as luminance distribution and uniformity. Different particles for wide colour gamut solutions were studied such as KSF ($\text{K}_2\text{SiF}_6:\text{Mn}^{4+}$), MGF ($\text{Mg}_4\text{Ge}_2\text{O}_3\text{F}_2:\text{Mn}^{4+}$) and YR (yellow phosphor) based on chip solutions. Furthermore, Cd based QD, Cd free QD and phosphor films are also investigated. Finally, optimum solutions have been proposed for LED based LCD.

Colour gamut of the display has been analyzed with respect to two different standards. One of them is DCI-P3 coverage standard which is critical in terms of getting Ultra High Definition Premium (UHD Premium) logo provided by Ultra High Definition Alliance (UHDA). This logo requires over 90% DCI-coverage colour gamut of displays. DCI-coverage specifies the covered area in DCI-P3 standard. So, this standard is not only related with larger area but also it is related with the location of DCI-P3 in colour space. The second standard is BT2020 which will be commonly used

standard over the next few years. Schemes of the triangles are shared in Figure 24.

Achieving DCI-P3 colour gamut standard is easier than BT2020 standard.

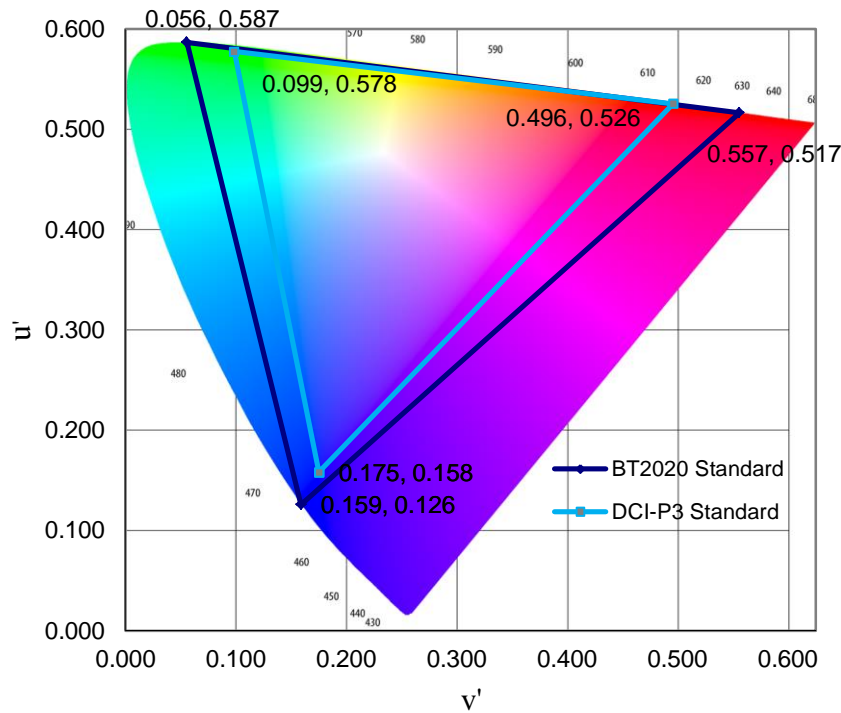


Figure 24: Triangles of DCI-P3 and BT2020 in CIE 1976 Colour Space

In our experiments, conversion layers are first studied as on chip solution (OCSs). Colour conversion layer of OCSs generate more back reflection and heat which in turn reduce the chip performance and life time [15, 49]. Since, silicone must be used with the polymer for on chip solution, the thermal resistance on the chip is increased due to the silicone material which absorbs the heat. Besides, different refractive indexes are also formed between the conversion layer and chip which leads to more back reflection. Even if the refractive indexes of these layers are same, due to the manufacturing nature of LED, an unintentional space between the polymer mixture and chip increases the back reflection. As a result, QD usage in LED package is an

inappropriate and ineffective for application BLU performance. For this reason, the remote colour conversion type BLU design is becoming more preferable for on chip colour conversions especially after the introduction of QDs to the display industry [50].

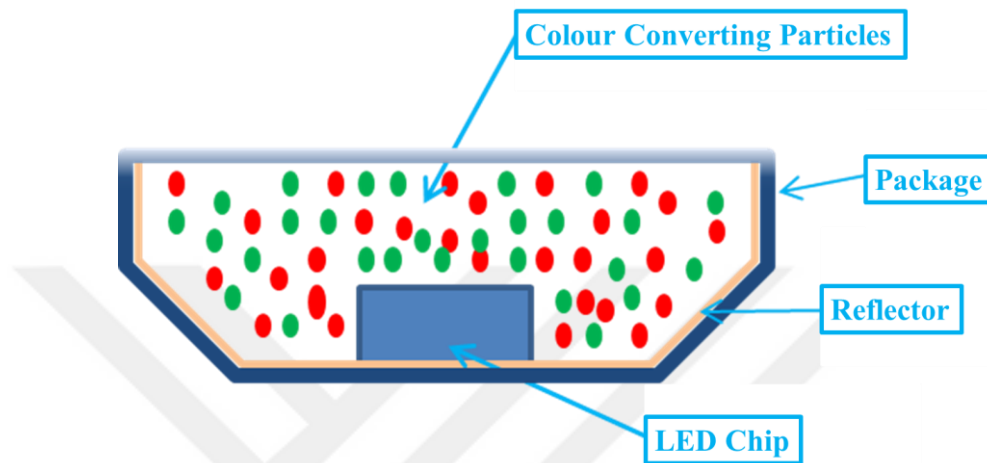


Figure 25: On Chip Solution (OCS)

QD colour conversion layer can be coated on an optical film or a plate in order to integrate BLU. For such a system, the distance between the LED and colour conversion layer depends on the optical distance (OD) of the panel as shown in Figure 26. The displays which have 15mm, 25mm, 30mm and 40mm optical distance are general used in the market. We used 30mm optical distance for our studies since, it has better visual performance with flip chip in combination with top emitting lens which is made of PMMA. However, flip chip with top emitting lens is not suitable for OD 40 mm because of poor visual performance. In addition, OD 15 mm and OD25 mm structures are also not appropriate to use with top emitting lens which may result in LED visibility during the visual performance test.

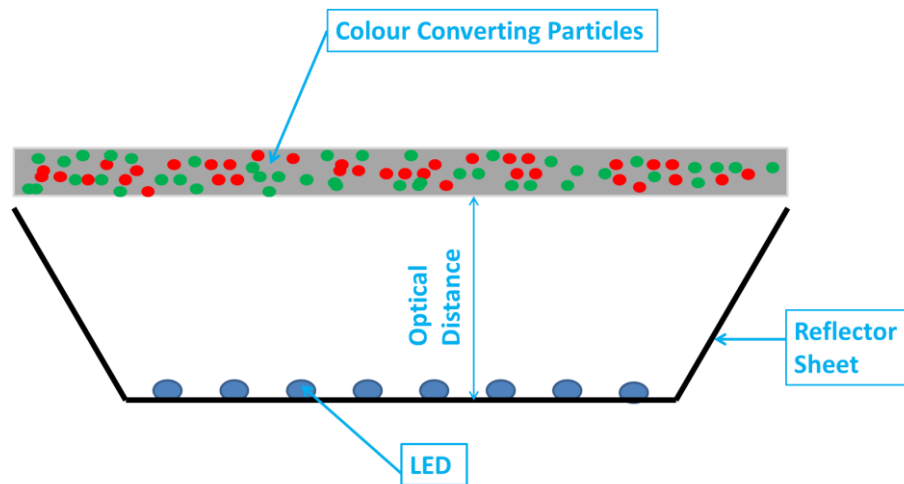


Figure 26: Remote Colour Conversion Mechanism

The usage of photo-enhanced films for WCG solutions is practical, reliable and suitable for mass production, since this kind of films can be manufactured using roll-to-roll systems [15]. The conversion particles are immersed in an optical polymer such as silicone. Generally, protection layers are obtained by this way on the both sides of colour converting layer. The protection layers also blocks the moisture and oxygen diffusion into the conversion layer. The composition of this colour converting composite structure is critical in determining the optical specifications such as colour gamut, colour coordinates and luminance of the display.

In this thesis, for the luminance and colour measurements, Topcon SR-LEDW spectroradiometer was used 50 cm away from TV in Figure 27. Spectrum of BLU and TV were also analyzed using SR-LED. The measurement should be executed in a stable, windless and dark room 60min after lighting the back light at room temperature for stabilization of the back light. This should be measured from the center of screen.

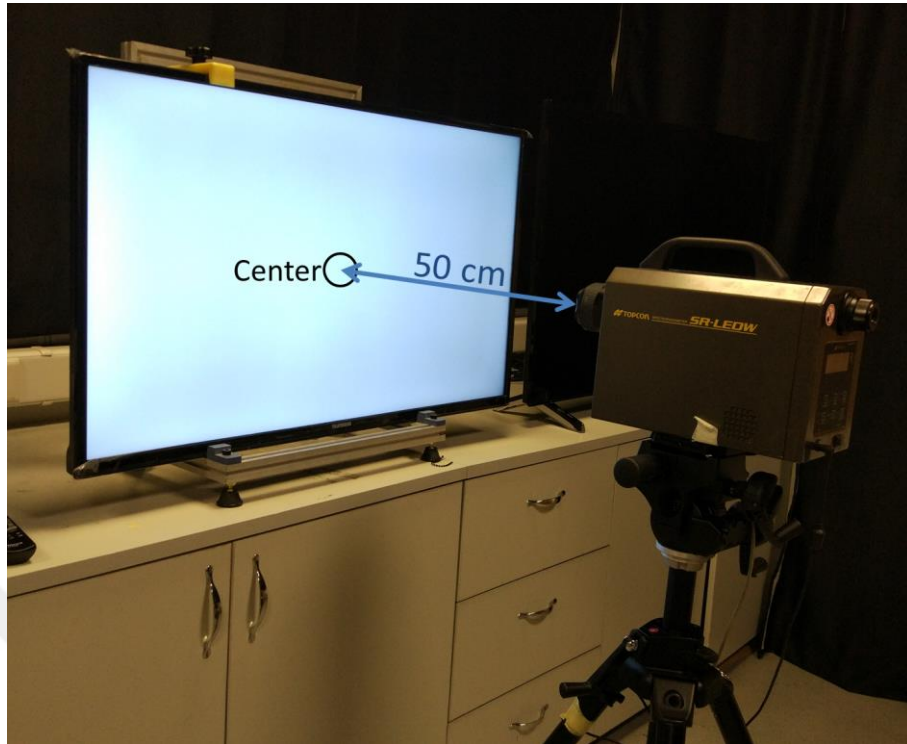


Figure 27: Measurement System

Luminance is used as design parameter for BLU. Luminance of nine points, as shown in Figure 28 are measured by SR-LEDW. The measurement setup (camera) and panel are separated with a distance of 50 cm during the measurement to calculate luminance uniformity as indicated in Figure 27.

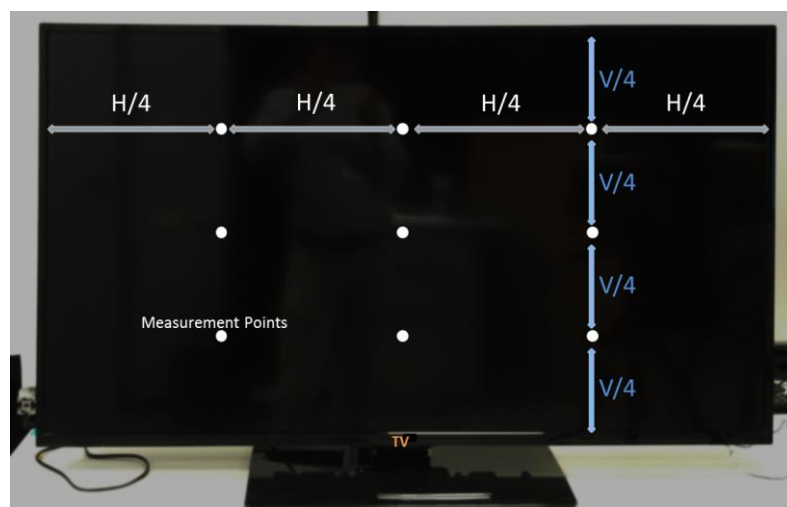


Figure 28: Uniformity Measurement Points of LCD

Minimum and maximum luminance were found from nine points. Minimum luminance is divided by maximum luminance to calculate the percentage of uniformity. Generally, the minimum acceptable value of uniformity is 75%.

$$\frac{\text{Luminance Min.}}{\text{Luminance Max.}} \geq \%75 \quad (1)$$

In this study, we used photo-enhanced optical films and On Chip Solution (OCS) in BLU. Their BLU spectrums are compatible with the colour filter (CF) of the LCP. We have compared the performance of different light conversion layers (LCLs) and OCSs which is evaluated on same BLU. Colour coordinate's targets are arranged to CIE-x=0.280 and CIE-y=0.280 for display. 65" direct-lit BLU is used for all studies. This BLU includes reflector sheet, LEDs, diffuser plate (DP), LCL, prism on prism (POP) and DBEF from bottom to top, respectively (Figure 29).

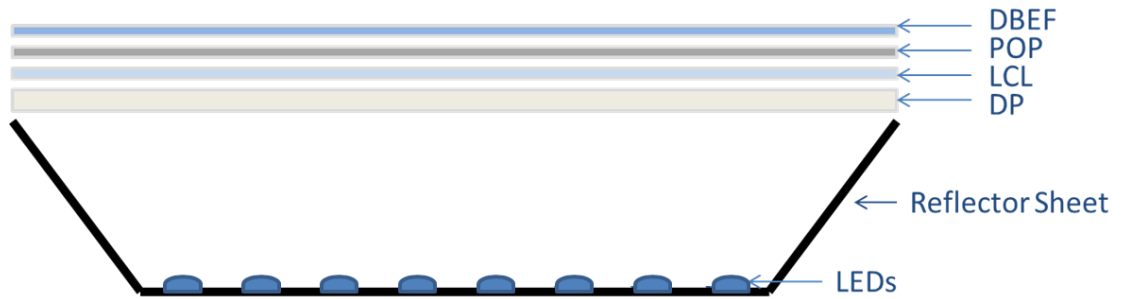


Figure 29: BLU Structure

In order to recover back reflected light, we have used uncoated polyethylene terephthalate (PET) sheet reflectors which includes beads to create different refractive index. The different refractive indexes aim increasing reflectivity. We preferred a lenticular DP made of polystyrene which improves the visual performance issues like LED visibility, BLU mura and light uniformity. However, this lenticular structure decreases the luminance about 5% with regard to the non-lenticular structure. On the

other hand, we introduced a prism-on-prism (POP) film in order to increase the luminance of display. The light is directed to LCP to gain luminance. Then, a dual brightness enhanced film (DBEF) provides around 33 % luminance gain. In addition, it improves colour conversion on remote solutions.

Table 1: Specifications of Optical Films

<i>Product Type</i>	<i>Thickness (mm)</i>	<i>Reflectivity (%) -555nm</i>	<i>Haze (%)</i>	<i>Transmittance (%)</i>	<i>Used Side Gloss (%)</i>
<i>POP</i>	<i>0.33</i>	<i>-</i>	<i>99</i>	<i>3</i>	<i>-</i>
<i>DP</i>	<i>2.0</i>	<i>-</i>	<i>99</i>	<i>31</i>	<i>-</i>
<i>Reflector</i>	<i>0.188</i>	<i>97.5</i>	<i>-</i>	<i>-</i>	<i>20</i>
<i>DBEF</i>	<i>0.260</i>	<i>-</i>	<i>86</i>	<i>47</i>	<i>-</i>

By using this BLU design, we have compared the performance of different LCLs based phosphors and QDs. LCLs are located under the light control films which is POP and DBEF due to diffusive properties of LCL film and effective colour conversion. DBEF creates recycle the light between BLU and recycle film (DBEF). The recycling blue light pass through colour conversion layer several times. In this way, down conversion can be increased using recycling film to improve optical efficiency. These conversions were analyzed with spectral measurement in Figure 30. It shows that DBEF and film order is critical in terms of effective colour conversion.

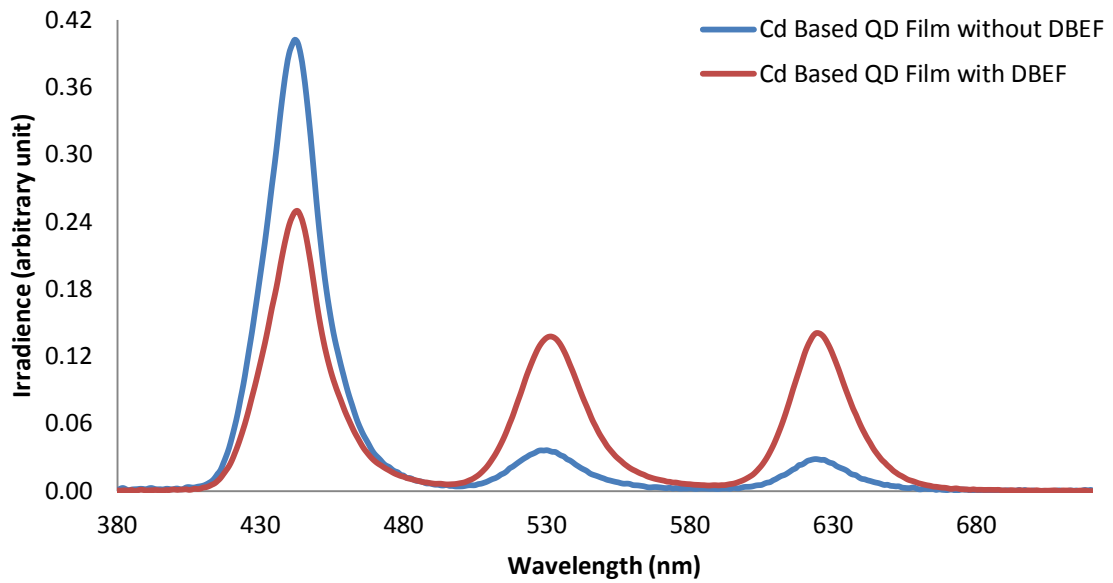


Figure 30: Effect of LCL with DBEF on Colour Conversion

The wavelengths of blue, green and red peaks are 443nm, 531nm and 625 nm respectively for two BLU spectrums. FWHMs of Cd based QD film without DBEF is 21nm, 28nm and 25 nm for blue, green and red peaks. When we added DBEF we observed that intensity of blue decreased while intensities of green and red peaks increased. It shows that colour conversion can be improved using colour conversion layer with DBEF for remote solution. Since, turned back non polarized light by DBEF excite the particles on colour conversion layer. FWHMs of these peaks change to 22nm, 27nm and 24nm for blue, green and red. However, major change was observed for intensity of green and red peaks. After DBEF addition, blue peak reduced 38% while green peak and red peak were rising 280% and 403%, respectively. The intensities and FWHMs of the peaks are shared Table 2.

Table 2: Effect of DBEF on Remote Colour Conversion

	<i>Intensity(Without DBEF)</i>	<i>Intensity (With DBEF)</i>	<i>FWHM(Without DBEF)(nm)</i>	<i>FWHM(With DBEF)(nm)</i>
<i>Blue Peak</i>	0.402	0.249	21	22
<i>Green Peak</i>	0.036	0.137	28	27
<i>Red Peak</i>	0.028	0.141	25	24

The conversion layers were excited with blue flip chip type LEDs. These LEDs are used in two different sizes and structures (LGIT, Korea). One of them has 3.0mm side length whose shape is square. Active size of the blue chip is 1.250mm×0.750mm. This packaged type flip chip is called package on board (POB 3030). Second square shaped has 1.3 mm side length which is named chip scale package (CSP 1313). 1313 CSP LED has 1.100mm×1.100mm active blue chip size. This LED doesn't package like POB 3030 to reduce heat occurred because of encapsulation. However, CSP 1313 is unprotected against the environments such as humidity. Convert materials are environmentally sensitive. Third one is POB3030 lateral chip which has 2 chips in one package and dimensions of them 0.915mm×0.635mm.

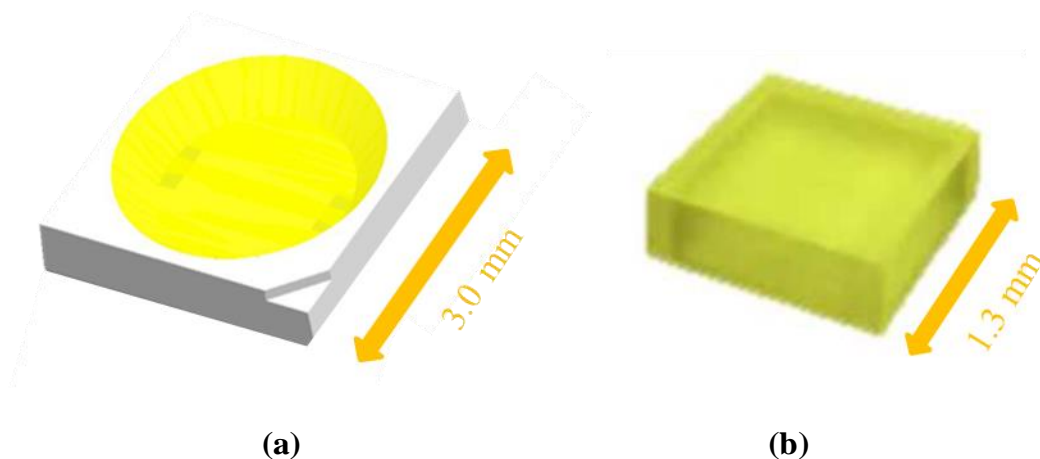


Figure 31: (a) POB 3030 and (b) CSP 1313

In order to observe thermal and optical differences between lateral chip and flip chip, YR3030 lateral chips are analyzed. For YR3030, same package are used with chips of POB 3030 (Figure 31-a). Two chips are integrated to package for YR3030. The dimensions of each chip are 0.915mmx0.615mm.

We have used vertical alignment type liquid crystal which has ultra HD resolution (3840 x 2160 pixels) produced by AOU Company. The model name of the 65” panel is T650QVN06.3. It can display up to 1.07 billion colours. Driver element of the panel is a-Si TFT active matrix. Display operation mode is normally black and its typical transmittance value is 5.3%. It has approximately 11% transmittance when BLU involves DBEF for our display. It is shown in Figure 32 peaks of blue, green and red colour filters are at 450nm, 528nm and 630nm respectively.

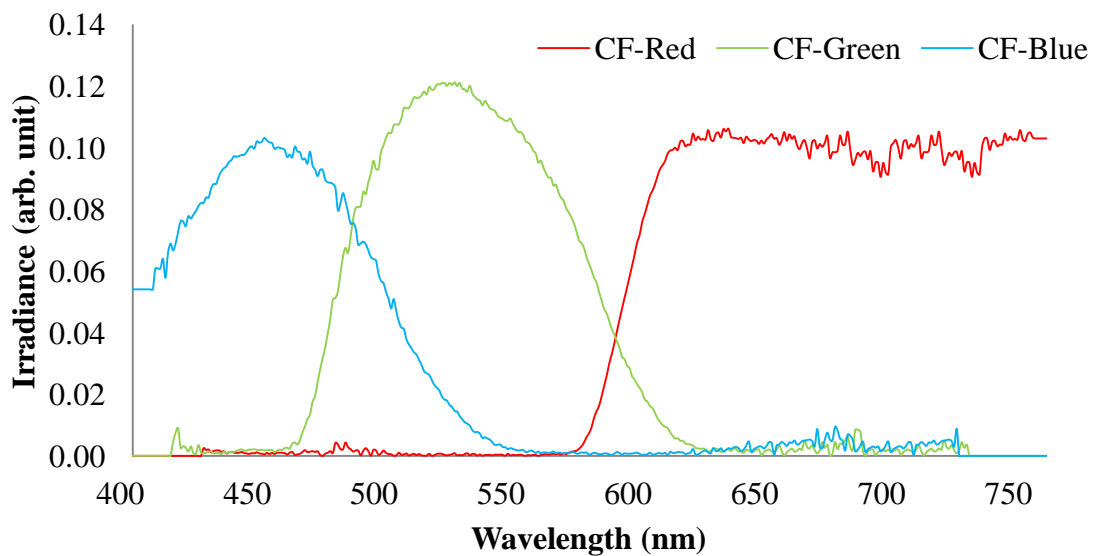


Figure 32: Colour Filter Spectrum

Production of CFs is not as easy as ideal band pass filter. A trade off should be generated for crosstalk areas and peak of the filters. Therefore, the corresponding red, green and blue peaks should be optimized according to related CFs of LCP. QDs are suitable in terms of getting precise peak values because of their conversion mechanism.

Size of QDs specifies the peak value of the spectrum in this mechanism. Matching of the peaks between CF and QDs is easier because of this feature.

The conversion layers were excited with lateral GaN blue LED chips whose center wavelengths and FWHMs are 442nm typically and 21nm (Figure 34), respectively. We have defined the peak wavelength of the blue LED according to the green and blue colour filters (CF). Peak wavelength of blue CF is 462nm and start point of green CF approximately 465nm. If we use 462 nm blue LED, blue spectrum of BLU will be crosstalk with green CF. As a results of crosstalk colour gamut will be decrease because of blue corner of gamut triangle. And the fact that blue corner will be moved to center of the colour space. If the peak wavelength of blue LED shifts lower values than 462nm, luminance will be lower. To get optimum value of peak wavelength, 442nm is preferred. Our design includes 1 B type LED bar and 10 A type LED bars. B type has 8 flip-chip LEDs and A types have 7 flip chip LEDs. Totally, 11 LED bars and 78 LEDs are used for the design (Figure 33). These bars are connected serially as two strings. For each LED, the typical forward voltages (V_f) are 3.1V. And 450mA driving current is used for this design. Copper based CEM-3 PCB type LED bars are preferred because the differences of thermal chip performance can be analyzed better than metal PCB, since metal PCB has better thermal conductivity. Therefore, the differences can be investigated easier on CEM-3 PCB.

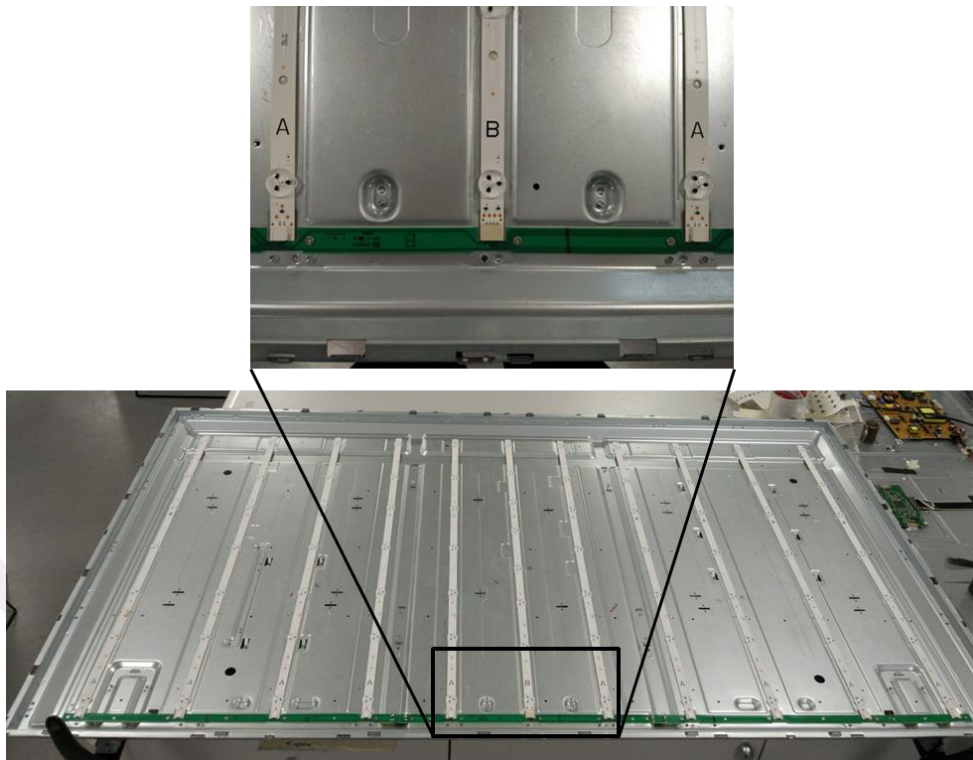


Figure 33: Assembled LED Bars on Metal Back-cover

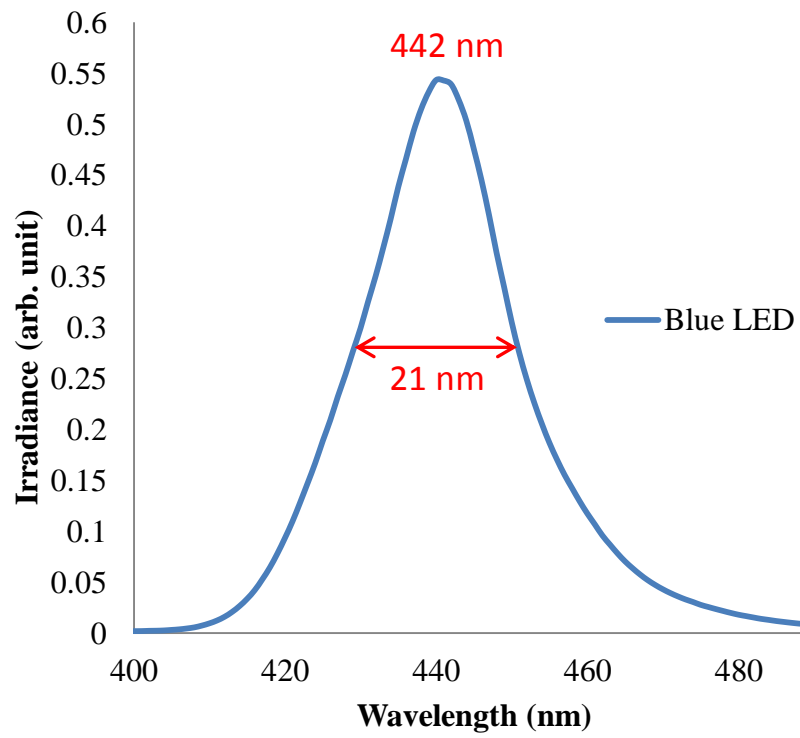


Figure 34: Blue LED Spectrum

In addition to increase the colour gamut, thermal efficiency of On Chip Solution and remote solution were analysed. Data logger, Graphtec GL220, was used with thermocouple for thermal measurements. K type thermocouple produced by OMEGA was used in the studies. Three LEDs were selected out of 78 LED for thermal analysis in Figure 35. Furthermore, in order to investigate conversion layer exposed to heat, two thermocouples were placed between diffuser plate and conversion film in Figure 59. Ambient temperatures were also measured inside and outside of the display.

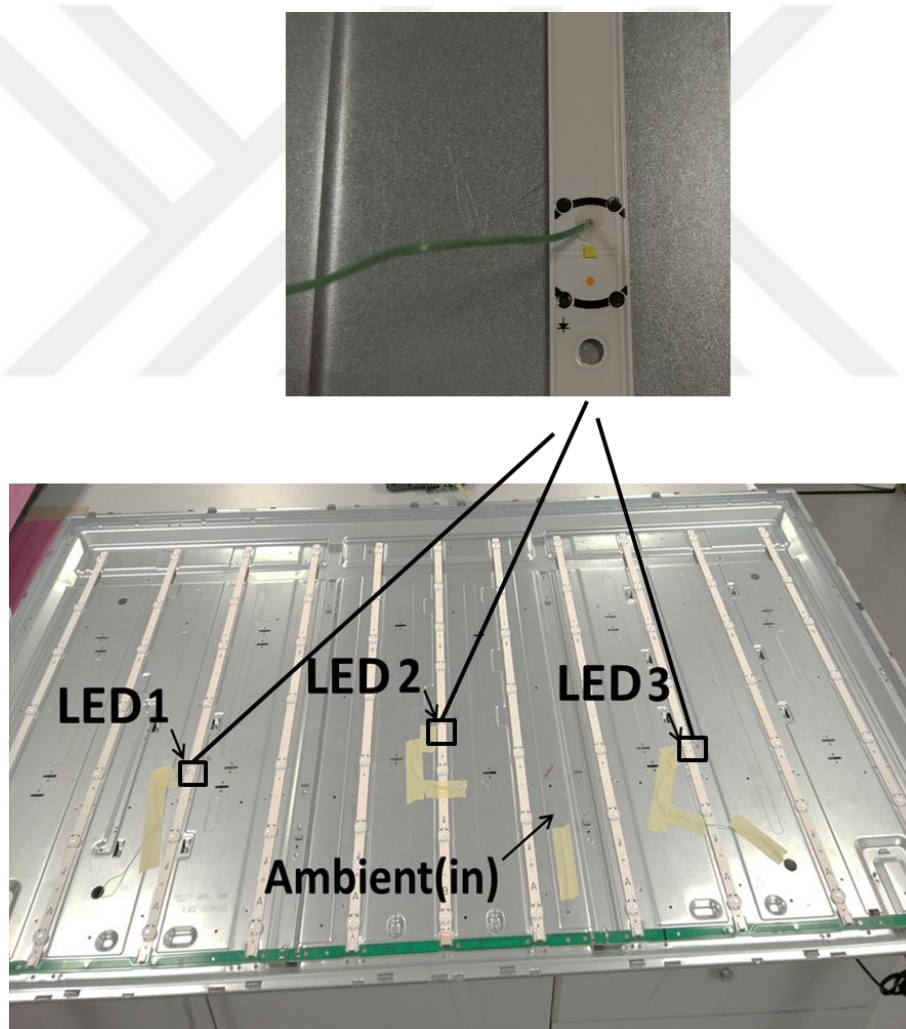


Figure 35: Thermal Measurement Points

3.1 Analysis of On Chip Solution

In this section, different chip solutions were analyzed. For the structure established without LCL film.

3.1.1 YR-1313 CSP Flip Chip Type LED

We used low cost yellow phosphor containing flip chip (YR-1313 CSP LED) which is commonly used LED type for comparison with wider colour gamut On Chip Solution. Lateral chips and POB 3030 flip chips include solder points connected to wires. However, 1313 CSP flip chip is not possible to connect directly to solder points since it is connected to conductive layer on LED bars. Therefore, thermal points of flip chips are defined by the specific distance from the chip rather than lateral chips because of different SMT. We determined the thermal test points 3 mm away from the chip. R^{th} (thermal resistance from test point to junction point) value of the chip was used according to 3 mm distance for our calculation. Thermocouple was connected to thermal test point with glue as shown in Figure 36.

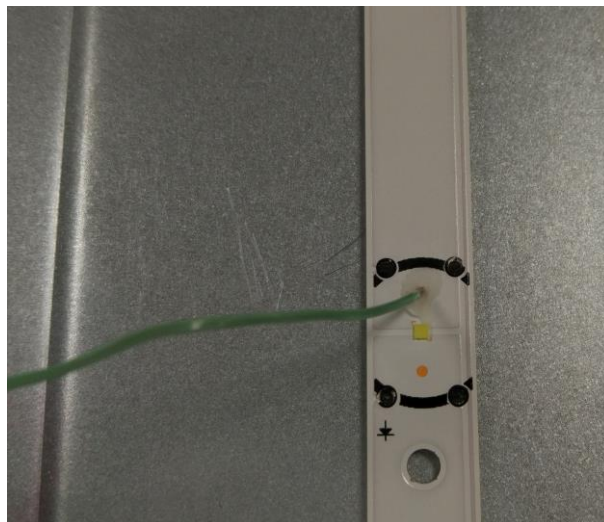


Figure 36: Thermal Test Point of 1313 CSP

Thermal measurements were taken 10 seconds intervals using data logger. Display was powered up at $t=0$. The test took 15570 seconds. Three LEDs were tested which are shown in Figure 35. A contact on the inner assembly platform of display was specified as “Ambient (in)” in (Figure 35). A contact of the outer platform was defined as “Ambient (out)”.

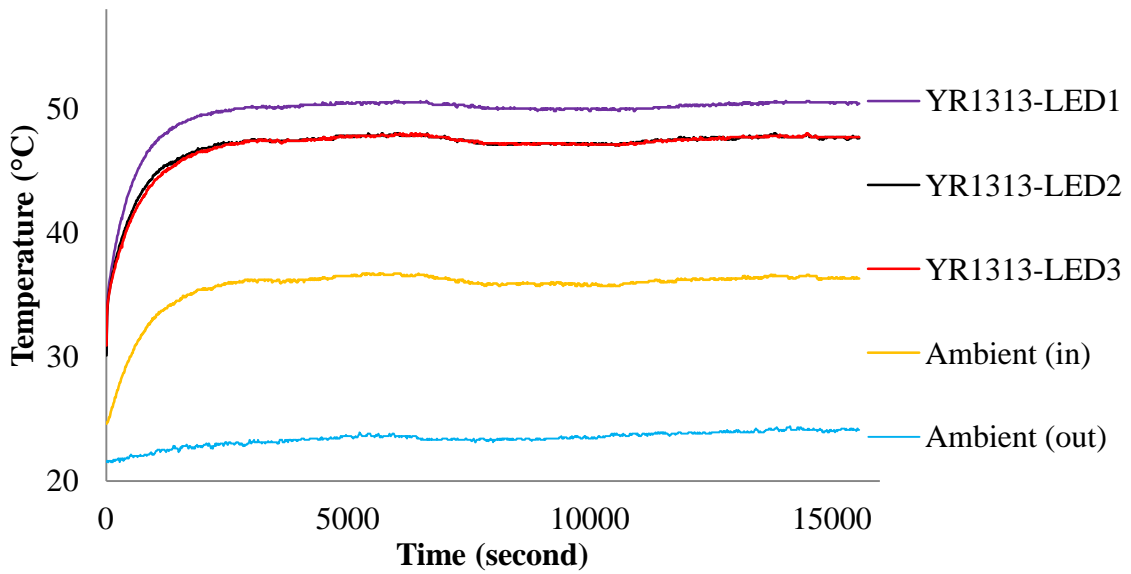


Figure 37: YR1313 Thermal Test Results

The thermal changes on measurement points were presented in Figure 37. We defined the time that the system comes to steady state as 10000th second. We took the average of the thermal measurements from 10000th to 15570th seconds. The results were given in Table 3.

Table 3: Average Temperatures of Thermal Test Points

<i>Test Point</i>	<i>Average Temperature (°C)</i>
<i>YR1313-LED1</i>	<i>50.28</i>
<i>YR1313-LED2</i>	<i>47.54</i>
<i>YR1313-LED3</i>	<i>47.53</i>
<i>Ambient (in)</i>	<i>36.20</i>
<i>Ambient (out)</i>	<i>23.91</i>

Averages of three different LEDs were calculated as 48.45 °C. In order to calculate the junction temperature of LED chip, equation 2 was used. R^{th} value of the 1313 CSP is 14.5 K/W. (where I is driving current and V_f is forward voltage)

$$T_j = T_{test\ point} + [I \times V_f \times R_{th}] \quad (2)$$

$$T_j = 48.45\ ^\circ\text{C} + [0.450\text{A} \times 3.1\text{V} \times 14.5\text{K/W}] = 68.67\ ^\circ\text{C} \quad (3)$$

$$T_j - T_{ambient(out)} = T_{j-a} = 68.67\ ^\circ\text{C} - 23.91\ ^\circ\text{C} = 44.76\ ^\circ\text{C} \quad (4)$$

As a result, average junction temperature of LED is 68.67 °C at ambient temperature (23.91°C). The difference between the junction temperature and ambient temperature was found as 44.76°C. T_{j-a} is defined to remove dependency of ambient temperature. In addition, inside temperature of display was 36.20 °C.

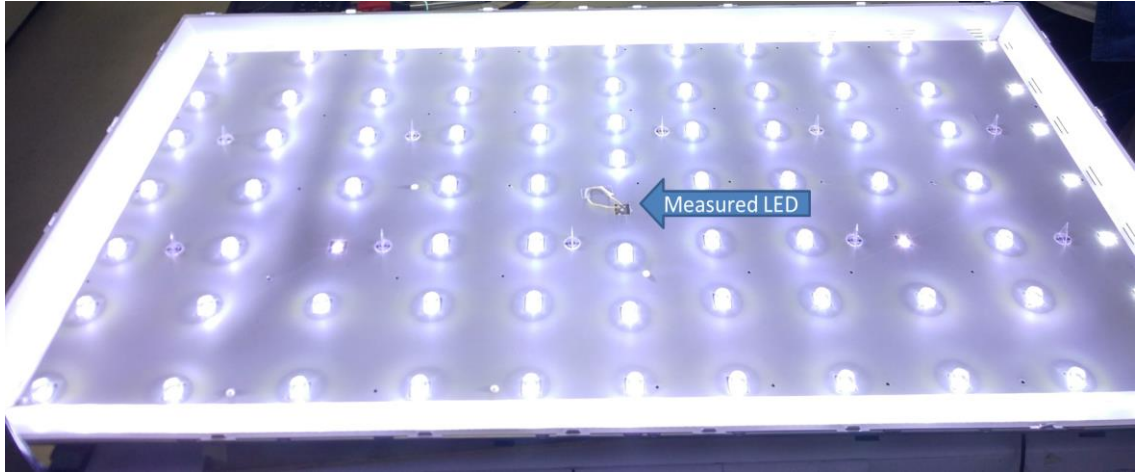


Figure 38: Thermal Effect of a single LED

We have also analyzed the thermal effect of a single LED. In order to detect this effect, we bypassed the selected LED2 (Figure 38). In other words, all the LEDs apart from that one were lighted up. Then, we connected the thermocouple to solder point of this LED. On the other hand, we calculated the junction temperature of the LED by measuring the solder point (Equation 2). As calculated in Equation 7 using the Table 4, the 34.29 °C increase of the junction temperature comes solely from the LED chip itself.

Table 4: Thermal Effect of a single YR1313 LED (LED2)

<i>Test Status</i>	<i>Junction Temperature of the LED (°C)</i>	<i>Ambient Temperature (°C)</i>
<i>YR1313-LED2-Open</i>	<i>67.73</i>	<i>23.91</i>
<i>YR1313-LED2-Close</i>	<i>34.92</i>	<i>25.40</i>

$$\Delta T_{open} = T_{j(open)} - T_{ambient(open)} = 67.73 \text{ °C} - 23.91 \text{ °C} = 43.81 \text{ °C} \quad (5)$$

$$\Delta T_{close} = T_{j(close)} - T_{ambient(close)} = 34.92 \text{ °C} - 25.40 \text{ °C} = 9.52 \text{ °C} \quad (6)$$

$$\Delta T_{open-close} = \Delta T_{(open)} - \Delta T_{(close)} = 43.81 \text{ }^{\circ}\text{C} - 9.52 \text{ }^{\circ}\text{C} = 34.29 \text{ }^{\circ}\text{C} \quad (7)$$

In addition to the thermal investigations, optical specifications were analyzed for notably performance of the colour gamut. Phosphor mixture and ratio were arranged according to optical targets by evaluating colour filters of the used liquid crystal panel. In these measurements, we used a spectroradiometer (SR-LEDW Topcon) which is placed 50cm away from the center of the display platform in a vibrationally isolated, dark and air motion free environment at 25°C. In order to map luminance distribution, the colour meter (Radiant Zemax -IC-PMG2) was used. The measurement of ¼ uniformities of the display and BLU, were done by the spectroradiometer (TOPCON-BM7).

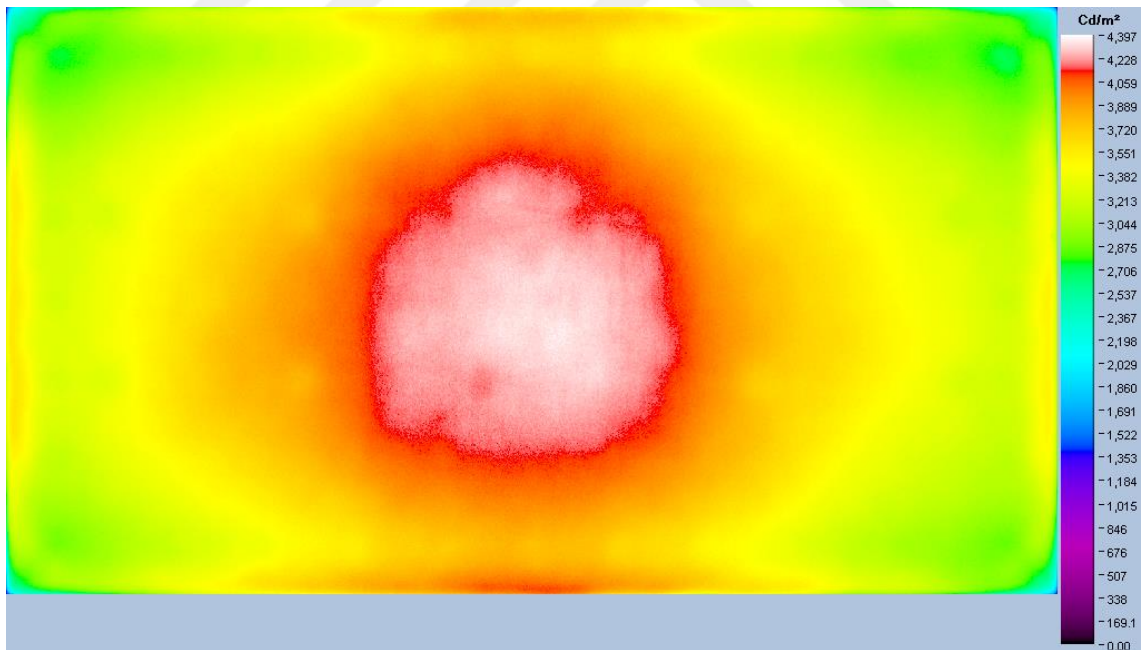


Figure 39: BLU Luminance Distribution of YR1313

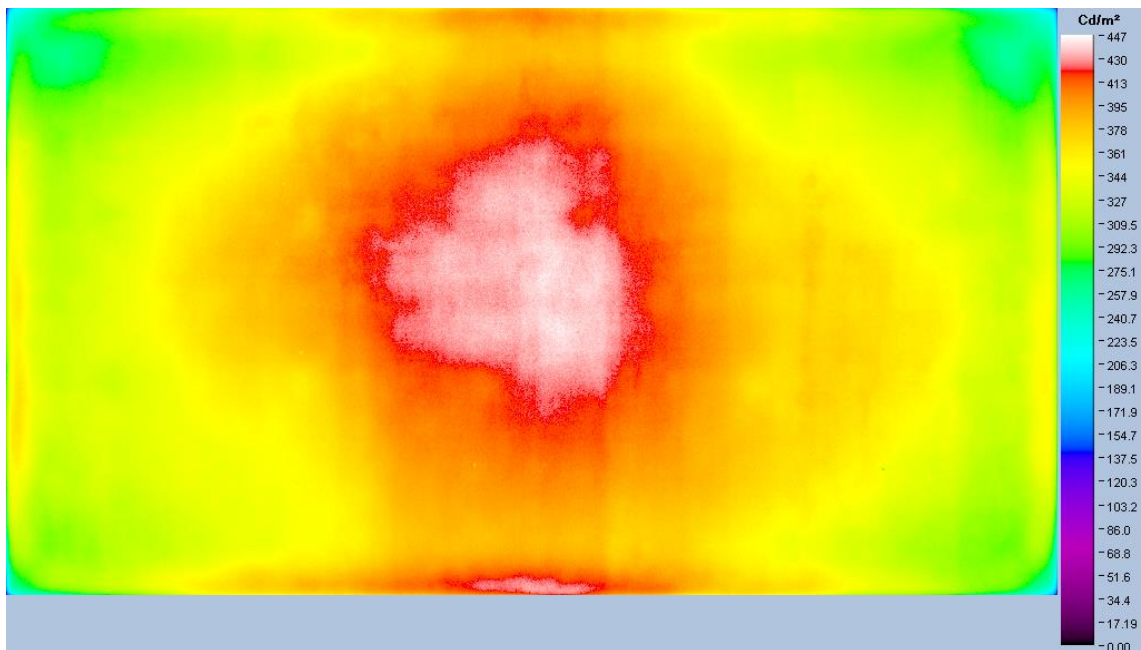


Figure 40: Display Luminance Distribution of YR1313

As we shown in Figure 39 and Figure 40, the luminance of BLU and display are not the same since liquid crystal panel changes the light distribution. We aim to compare light distributions of different solutions using Figure 39 and Figure 40. The luminance distributions are shown. Colours represent the intensities on display. In this way, distributions can be compared easily. For example, we can detect the darker area on the corners than center of the panels by green colours in Figure 39. In addition, between the center and corners, there are also green regions at which regions are darker than the center, yellow areas exist from corners to center. Their luminance are higher than that of green areas. The highest luminance is represented by white colour. When we evaluate sides of the panels, it has light leakages end of the edges. We can detect them by analyzing it from center to edges. Colour change shows that luminance is decreasing from center to edges. However, at the end of the panel it increases again.

Table 5: Uniformity, Luminance and Colour Coordinates

<i>Measured System</i>	<i>¼ Uniformity Result (%)</i>	<i>Luminance of White(nit)</i>	<i>Colour Coordinates</i>
<i>YR1313-BLU</i>	85.95	-	-
<i>YR1313-Display</i>	-	465	<i>x:0.282, y:0.285</i>

According to the colour coordinate results in Table 5, colour coordinate (0.282, 0.285) are so close to our target which have defined at the start point of the study. In addition to the colour coordinates display luminance (465 nit) is higher than most of the displays in this industry. Uniformity is measured as 85.95%. Test method of uniformity measurements were explained in section 2.4.6.

Table 6: Gamut Results of the YR1313

<i>Measured System</i>	<i>Gamut (BT2020)</i>	<i>Gamut (DCI-P3 Coverage)</i>
<i>YR1313-Display</i>	58.34%	79.86%

The colour gamuts of displays were measured as 58.34% and 79.86 for BT2020 and DCI-P3 coverage standards. When we evaluate BT2020 gamut area, its level is too low so, it is not promising solution in terms of colour gamut.

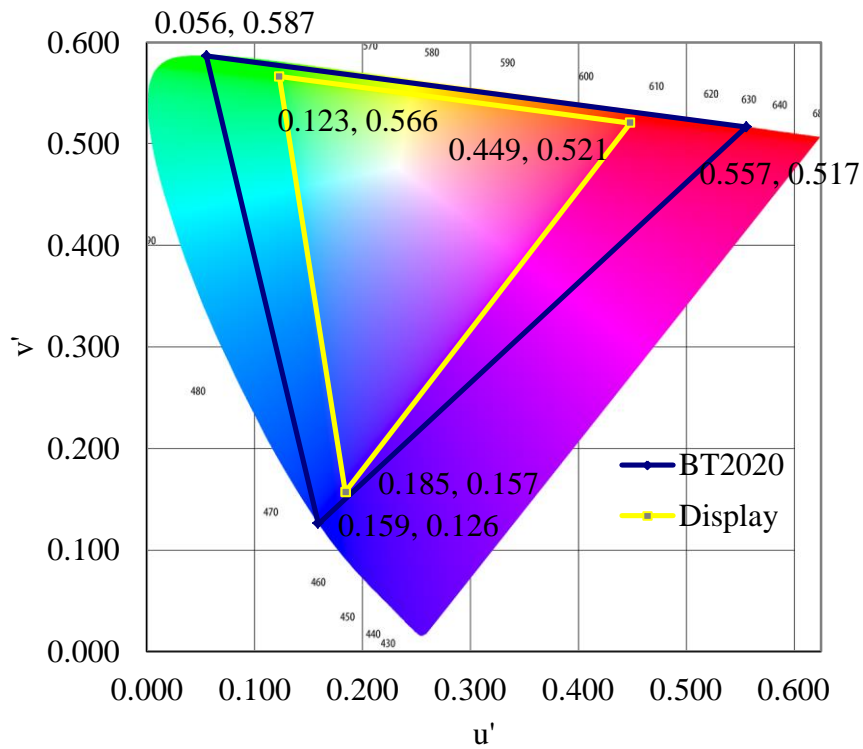
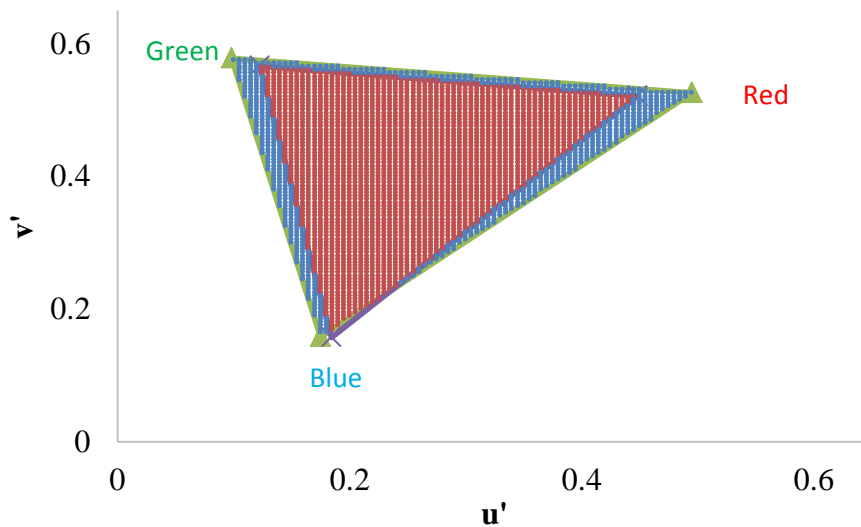


Figure 41: Colour Gamut Schema of YR1313 on BT2020 Standard

YR1313 conventional LED's red and green coordinates are away from the BT2020's ones so, red and green region is not appropriate to achieve colour gamut in BT2020 standard. Blue corner of the display should be improved to get BT2020's corner. It is related with blue LEDs, blue colour filter and green colour filter. If the blue and green CF has narrower FWHM, crosstalk will decrease. However, most effective ones is provided by developing FWHM of blue LED. Since, if blue LED has narrower peak, crosstalk area of colour filter lost its significance.



- DCI-P3 gamut samples interior to the UHDA Device Test Gamut
- DCI-P3 gamut samples exterior to the UHDA Test Device Gamut
- ▲ DCI-P3 UHDA Test Coverage Boundary
- × UHDA Test Device Coverage Boundary

Figure 42: Colour Gamut Schema of YR1313 on DCI-P3 Coverage Standard

Similar to BT2020, green and red points should be developed for wider colour gamut. One of the critical point for DCI-P3 coverage, exterior areas of red and green regions are narrow to get higher gamut value (Figure 42). Furthermore, peak of the blue LED should be narrower. It can be developed by moving to lower wavelength. However, it decreases the luminance because peak of the blue LED moves away from peak of the blue CF.

3.1.2 YR-3030 Lateral Type LED

In this study, we have used yellow phosphor containing package type lateral chips (YR-3030 LED). This LED package consists of two chips. In this study, only YR3030 is used as lateral chip. Its appearance and package dimensions are the same as POB3030. Package type lateral chip includes solder points to measure temperatures.

Therefore, we have used solder points (Figure 43) and its R^{th} value to find junction temperature of chip.

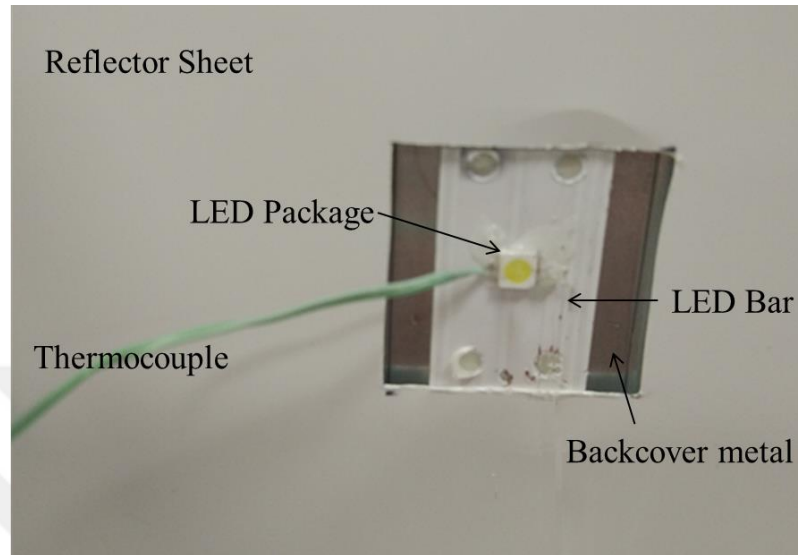


Figure 43: Thermal Test Point of YR3030 POB

Thermal measurements were taken 10 seconds intervals by using data logger. Display was powered up at zero time. The test was finished at 15570th seconds. The results of three LEDs tested are shown in Figure 44. Temperatures of LEDs are well consistent with each other.

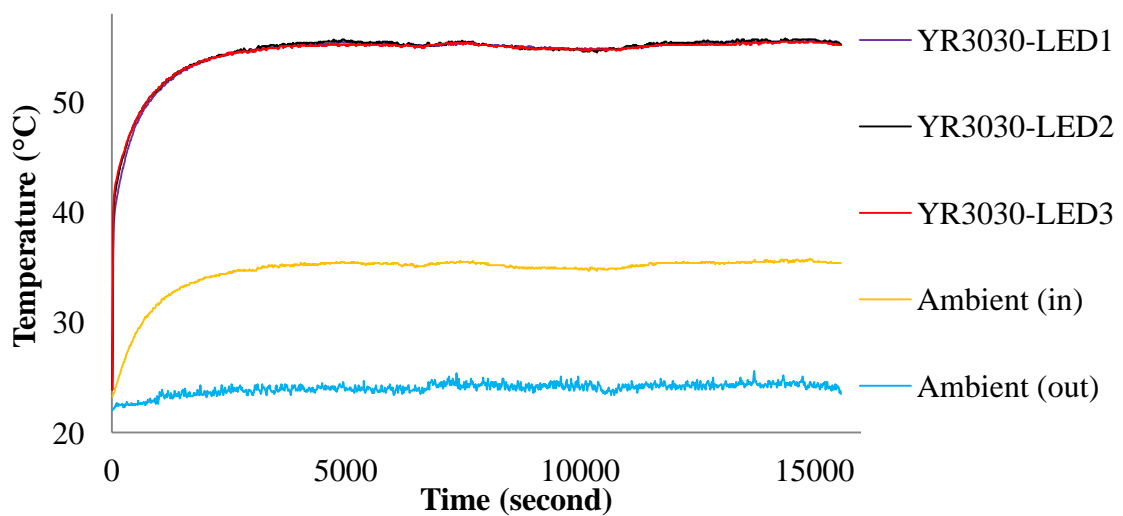


Figure 44: YR3030 Thermal Test Results

We defined the time that the system comes to steady state as 10000th second. The calculated average thermal measurements from 10000th to 15570th seconds are shown in Table 7.

Table 7: Average Temperatures of Thermal Test Points

<i>Test Point</i>	<i>Average Temperature (°C)</i>
<i>YR3030-LED1</i>	<i>55.27</i>
<i>YR3030-LED2</i>	<i>55.34</i>
<i>YR3030-LED3</i>	<i>55.18</i>
<i>Ambient (in)</i>	<i>35.34</i>
<i>Ambient (out)</i>	<i>24.27</i>

Averages of three different LEDs were calculated as 55.26 °C. In order to calculate junction temperature of LED chips, Equation (2) was used. The Rth value of the 3030 lateral chip is 12.0 K/W. (where I is driving current, and V_f is forward voltage)

$$T_j = 55.26 \text{ °C} + [0.450\text{A} \times 3.1\text{V} \times 12.0\text{K/W}] = 72.00 \text{ °C} \quad (8)$$

$$T_j - T_{ambient(out)} = T_{j-a} = 72.00 \text{ °C} - 24.27 \text{ °C} = 47.73 \text{ °C} \quad (9)$$

As a result, the average junction temperature of LED is 72.00 °C at 24.27 °C ambient temperature. The difference between the junction temperature and ambient temperature was found as 47.73 °C where T_{j-a} is defined to remove dependency of ambient temperature. Our comparisons were made on these results which are related with thermal performance of LEDs. In addition, inside temperature of display was measured as 35.34 °C. YR3030 LEDs temperatures are higher than YR1313 approximately 3 °C. It is an expected result because of the package structure and wires of YR3030.

In order to detect thermal effect of single YR3030 LED, we bypassed the selected LED2. As calculated in Equation 12 using the Table 8, the 37.19 °C increase of the junction temperature comes solely from the LED chip itself.

Table 8: Thermal Effect of a single YR3030 LED (LED2)

<i>Test Status</i>	<i>Junction Temperature of the LED (°C)</i>	<i>Ambient Temperature (°C)</i>
<i>YR3030-LED2-Open</i>	<i>71.89</i>	<i>24.27</i>
<i>YR3030-LED2-Close</i>	<i>36.53</i>	<i>26.10</i>

$$\Delta T_{open} = T_{j(open)} - T_{ambient(open)} = 71.89 \text{ °C} - 24.27 \text{ °C} = 47.62 \text{ °C} \quad (10)$$

$$\Delta T_{close} = T_{j(close)} - T_{ambient(close)} = 36.53 \text{ °C} - 26.10 \text{ °C} = 10.43 \text{ °C} \quad (11)$$

$$\Delta T_{open-close} = \Delta T_{(open)} - \Delta T_{(close)} = 47.62 \text{ °C} - 10.43 \text{ °C} = 37.19 \text{ °C} \quad (12)$$

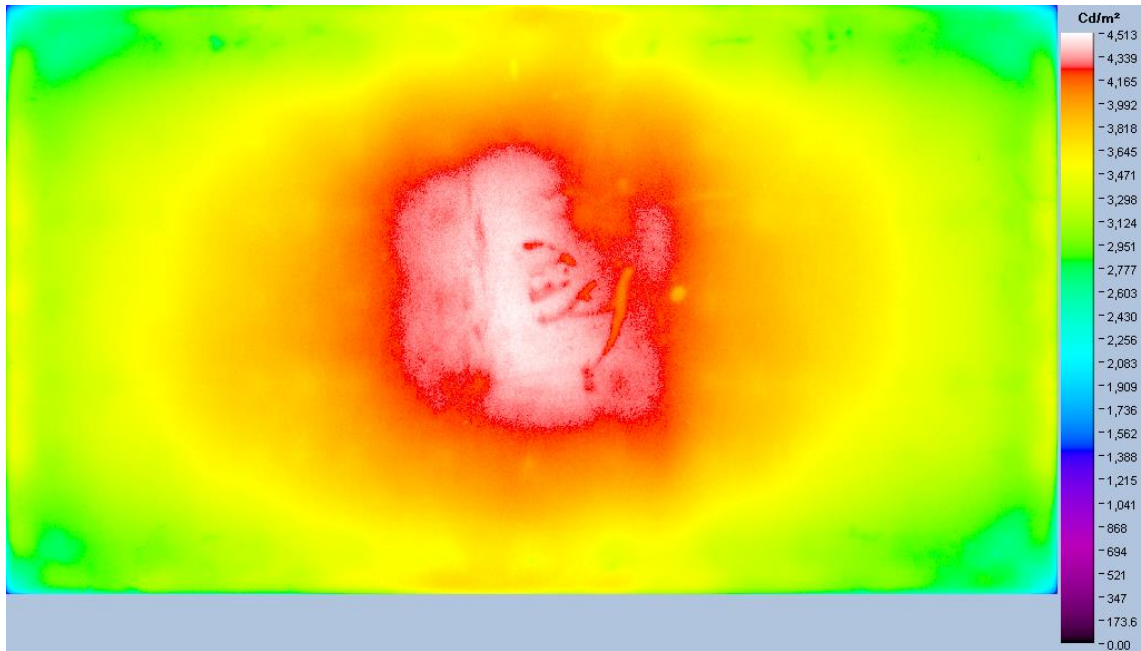


Figure 45: BLU Luminance Distribution of YR3030

Once luminance distributions of YR-3030 (Figure 45) compared with YR-1313 (Figure 39), YR-3030 is worse in regard to performance such as large dark areas, dark corners and smoothness light distribution. We realized the dark corners from cyan colours on corners of the panel and smoothness was analyzed from green to yellow and yellow to green transitions on the pictures. As seen in Figure 45, the transitions exist on the sides of the panel. Comparing YR3030 and YR1313, YR1313 has better performance in terms of darker areas. However, light leakage performance is worse than YR3030 since, red line on the sides is represented that brighter light leakage was seen for YR1313.

Table 9: Uniformity, Luminance and Colour Coordinates

<i>Measured System</i>	<i>¼ Uniformity Result (%)</i>	<i>Luminance of White(nit)</i>	<i>Colour Coordinates</i>
<i>YR3030-BLU</i>	88.45	-	-
<i>YR3030-Display</i>	-	485	<i>x:0.280, y:0.295</i>

Display colour coordinates are close to our target (0.280, 0.280) we have defined at the start point of the study. However, fine tuning calculations are better for comparisons. On the other hand, other optical specifications can be compared directly such as colour gamut, uniformity and light distributions. In order to compare the luminance, we should calculate the luminance if we catch the colour coordinates are determined. When the colour x and colour y are increased 0.005 and 0.01 respectively, the luminance is improved about 3%. The colour coordinates can't be same with each other after calculations for our studies. However, we optimized the results as close as possible. For these measurements, the critical parameter is colour y (CIE-y) coordinates

since luminance of display is a function of CIE-y in CIE 1931. We used this representation as we explained in section 2.4.4.

$$\text{Measured CIE Coordinates} \rightarrow x: 0.280, y: 0.295 \quad (13)$$

$$x: 0.280 - 1 \times 0.005, \quad y: 0.295 - 1 \times 0.01 \quad (14)$$

$$\begin{aligned} \text{For } x: 0.275, \quad y: 0.285 &\rightarrow \text{Luminance will decrease 3\%} \\ &= 485.0 \times \frac{97}{100} = 470 \text{ nit} \end{aligned} \quad (15)$$

After fine tuning, we found the luminance of the display as about 470 nit in Equation (9). Luminance of the display is similar with YR-1313 CSP at same driving current.

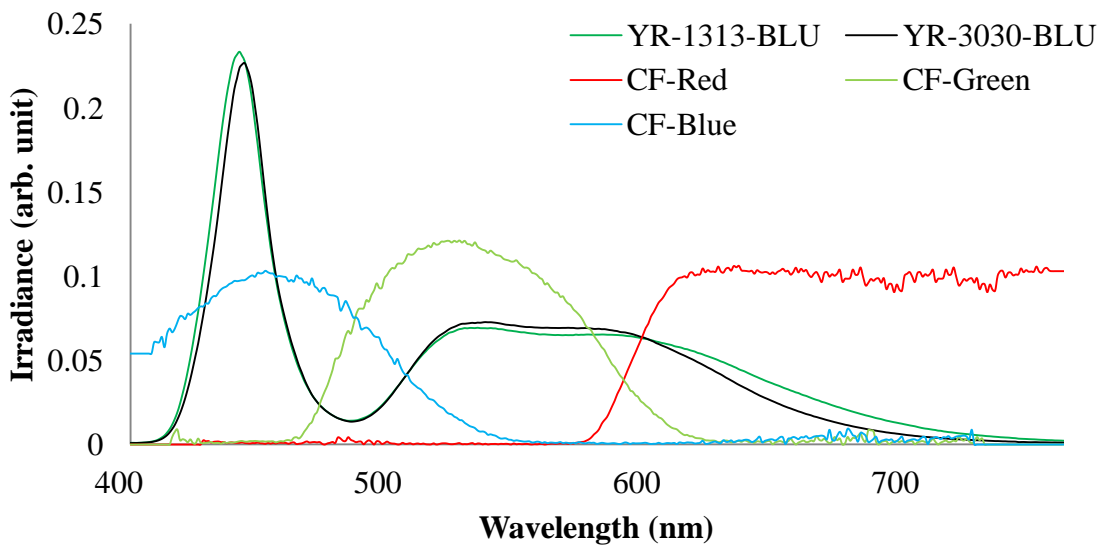


Figure 46: The BLU Spectrums of YR1313 and YR3030 with CFs of Panel

BLU spectrums of YR1313 and YR3030 were shared in Figure 46. As we have expected, these spectrums are similar with each other. The region between 579nm and 615nm is crosstalk region green and red CFs. For blue's CF and green CF which are between 465nm and 535nm have the same effects. These regions decrease the colour

gamut depending on BLU's intensity in these regions. Their effects in the crosstalk regions can be found by multiplying BLU's irradiance with CF's irradiance. On the other hand, peak wavelengths of colours are critical to get wider colour gamut. We can't evaluate for YR3030 because BLU spectrum is continuous from 490 nm to 700nm.

Table 10: Gamut Results of the YR3030

<i>Measured System</i>	<i>Gamut (BT2020)</i>	<i>Gamut (DCI-P3 Coverage)</i>
<i>YR3030-Display</i>	<i>56.89%</i>	<i>78.27%</i>

As we expected, YR-3030's colour gamut is almost the same as YR1313 due to the same colour conversion material.

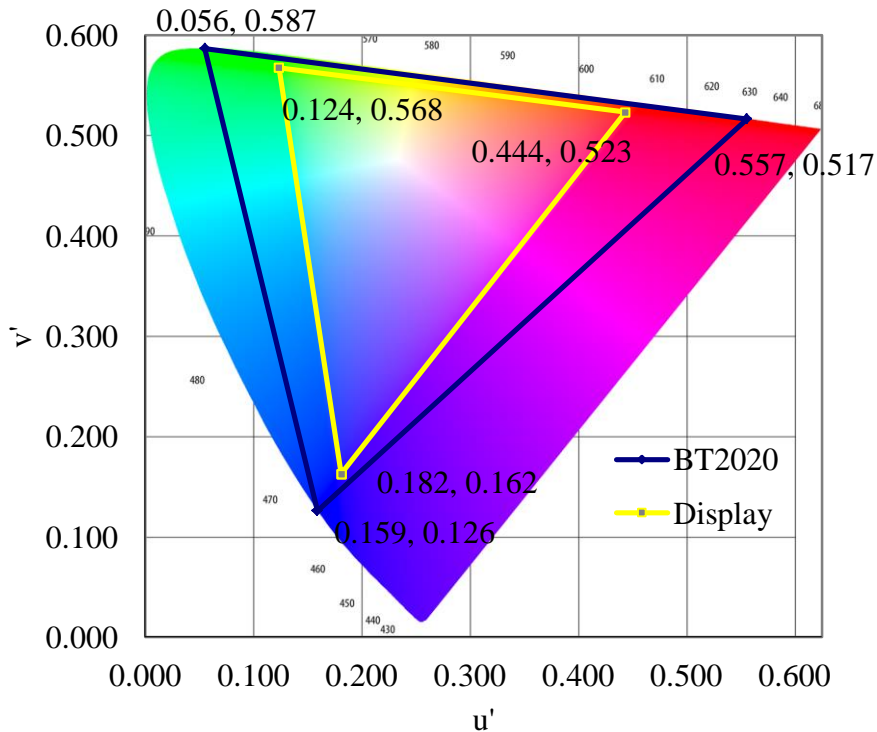


Figure 47: Colour Gamut Schema of YR3030 on BT2020 Standard

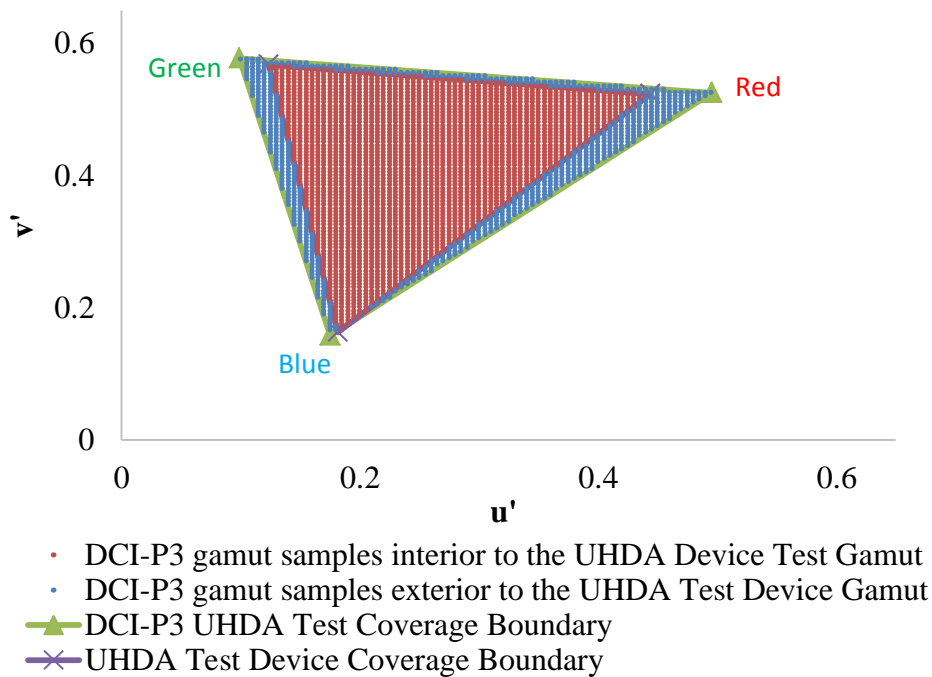


Figure 48: Colour Gamut Schema of YR3030 on DCI-P3 Coverage Standard

In Figure 48, the colour gamut performance of YR3030 is not also satisfactory in DCI-P3 coverage standard. Red and green corners of the triangles are far away from the DCI-P3's corners. Therefore, exterior area is very large to be able to get wider colour gamut.

3.1.3 KSF-3030 POB Package Type Flip Chip LED

In this section, the coated KSF ($K_2SiF_6:Mn^{4+}$), phosphor on blue chip was analyzed in terms of thermal and optical performances. This LED includes package type blue flip chip. KSF3030's thermal connection is same as YR3030 POB in Figure 43. Thermal measurements were taken 10 seconds interval by using data logger. Display was powered up at zero time.

In Figure 49, time dependent temperatures were measured. Measured LEDs results are the not same as each other. LED1 and LED2 are almost the same range from

starting point to 7000th seconds. After this point, temperature of LED1 increases about 1.5 °C. Thermocouple position of LED1 may be changed a little bit due to temperature rise. In order to be tolerated similar differences; three LEDs were defined at the beginning.

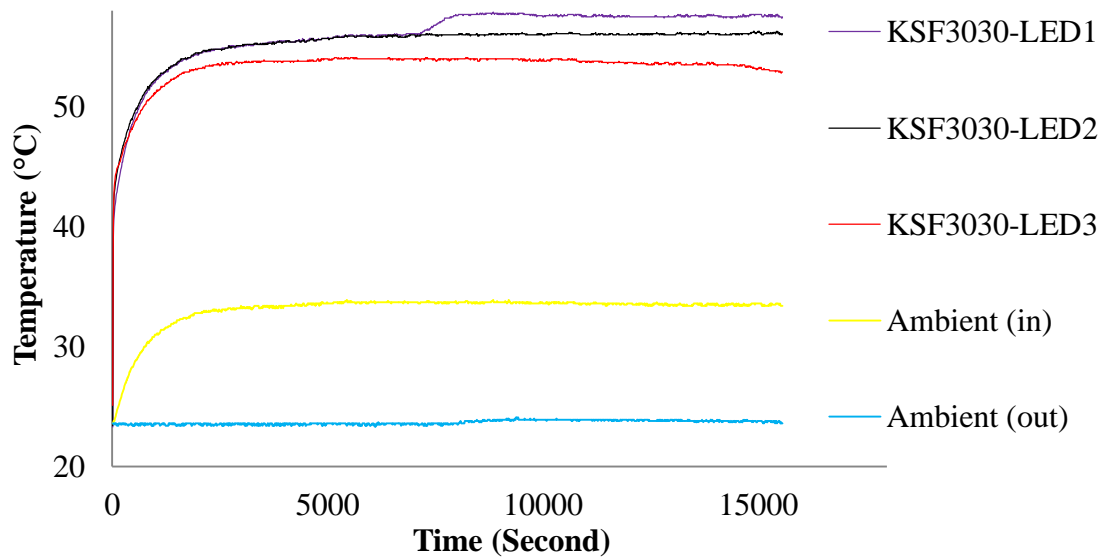


Figure 49: KSF3030 Thermal Test Results

We defined the time that the system comes to steady state as 10000th second. The average thermal measurements from 10000th to 15570th seconds were taken. The results were shown in Table 11.

Table 11: Average Temperatures of Thermal Test Points

<i>Test Point</i>	<i>Average Temperature (°C)</i>
<i>KSF3030-LED1</i>	<i>57.57</i>
<i>KSF3030-LED2</i>	<i>56.07</i>
<i>KSF3030-LED3</i>	<i>53.58</i>
<i>Ambient (in)</i>	<i>33.54</i>
<i>Ambient (out)</i>	<i>23.83</i>

Averages of three different LEDs were calculated as 55.74 °C. In order to calculate junction temperature of LED chips, Equation (2) was used. Rth value of the 3030 POB is 9.0 K/W. (where I is driving current and, V_f is Forward voltage)

$$T_j = 55.74 \text{ °C} + \left[0.450A \times 3.1V \times 9.0 \frac{K}{W} \right] = 68.29 \text{ °C} \quad (16)$$

$$T_j - T_{ambient(out)} = T_{j-a} = 68.29 \text{ °C} - 23.83 \text{ °C} = 44.46 \text{ °C} \quad (17)$$

We calculated the junction temperature as 68.29 °C at 23.83 °C ambient temperature. The difference of junction temperature with ambient temperature was found as 44.46 °C. T_{j-a} was defined to remove dependency of ambient temperature. The temperature of display in the panel was found as 33.54 °C.

According to the results, T_{j-a} of KSF3030 is similar with YR1313 CSP's. The POB3030 KSF flip chip has 1.250mm×0.750mm chip dimensions which has 0.938 mm². The YR1313 flip chip has 1.100mm×1.100mm chip dimensions and its area is 1.210 mm². Despite of the chip bigger chip area of YR1313 CSP, thermal performance is similar with POB3030 KSF.

In order to detect thermal effect of single KSF3030 LED, we bypassed the selected LED2. As calculated in Equation 20 using the Table 12, the 35.06 °C increase of the junction temperature comes solely from the LED chip itself.

Table 12: Thermal Effect of a single KSF3030 LED (LED2)

<i>Test Status</i>	<i>Junction Temperature of the LED (°C)</i>	<i>Ambient Temperature (°C)</i>
<i>KSF3030-LED2-Open</i>	<i>67.97</i>	<i>23.83</i>
<i>KSF3030-LED2-Close</i>	<i>34.49</i>	<i>25.40</i>

$$\Delta T_{open} = T_{j(open)} - T_{ambient(open)} = 67.97 \text{ }^{\circ}\text{C} - 23.83 \text{ }^{\circ}\text{C} = 44.15 \text{ }^{\circ}\text{C} \quad (18)$$

$$\Delta T_{close} = T_{j(close)} - T_{ambient(close)} = 34.49 \text{ }^{\circ}\text{C} - 25.40 \text{ }^{\circ}\text{C} = 9.09 \text{ }^{\circ}\text{C} \quad (19)$$

$$\Delta T_{open-close} = \Delta T_{(open)} - \Delta T_{(close)} = 44.15 \text{ }^{\circ}\text{C} - 9.09 \text{ }^{\circ}\text{C} = 35.06 \text{ }^{\circ}\text{C} \quad (20)$$

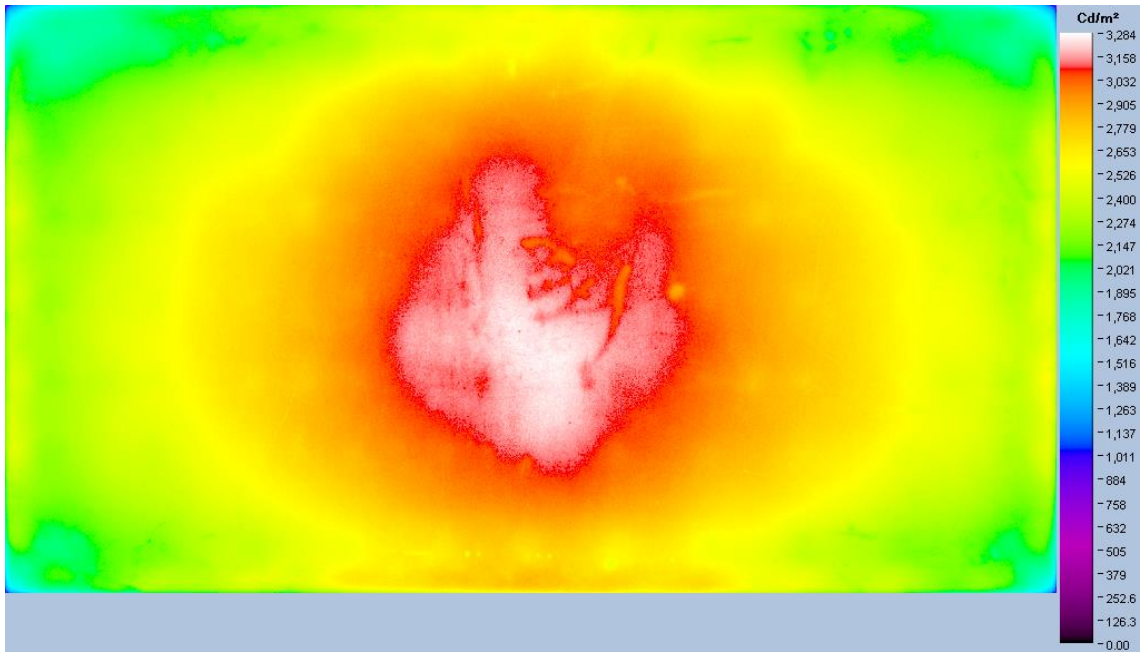


Figure 50: BLU Luminance Distribution of KSF3030

As seen in Figure 50, the light leakages exist on the sides of the panel. However, its level is lower than YR3030. On the other hand, green areas are similar with YR3030.

Table 13: Uniformity, Luminance and Colour Coordinates

<i>Measured System</i>	<i>¼ Uniformity Result</i>	<i>Luminance of White(nit)</i>	<i>Colour Coordinates</i>
<i>KSF3030 -BLU</i>	<i>87.04</i>	<i>-</i>	<i>-</i>
<i>KSF3030-Display</i>	<i>-</i>	<i>444</i>	<i>x:0.297, y:0.317</i>

According to the colour coordinates in Table 13, they are not close to our target (0.280, 0.280) that we have defined at the start point of the study. In order to compare the luminance, we can calculate the luminance if we obtain the desired colour coordinates. If colour x and colour y are increased amount of 0.005 and 0.01 respectively, the luminance improvement is 3%. The calculations are shared operation below.

$$\text{Measured CIE Coordinates} \rightarrow x: 0.297, y: 0.317 \quad (21)$$

$$x: 0.297 - 3 \times 0.005, \quad y: 0.317 - 3 \times 0.01 \quad (22)$$

$$\begin{aligned} \text{For } x: 0.282, \quad y: 0.287 \rightarrow \text{Luminance will decrease 9\%} \\ = 444.0 \times \frac{91}{100} = 404 \text{ nit} \end{aligned} \quad (23)$$

We will use the calculated value of luminance (404 nit) for our target of colour coordinates.

Table 14: Gamut Results of the KSF3030

<i>Measured System</i>	<i>Gamut (BT2020)</i>	<i>Gamut (DCI-P3 Coverage)</i>
<i>KSF3030-Display</i>	<i>68.31%</i>	<i>93.42%</i>

The results of colour gamut in Table 14 show that KSF3030 provides better solution up to this section.

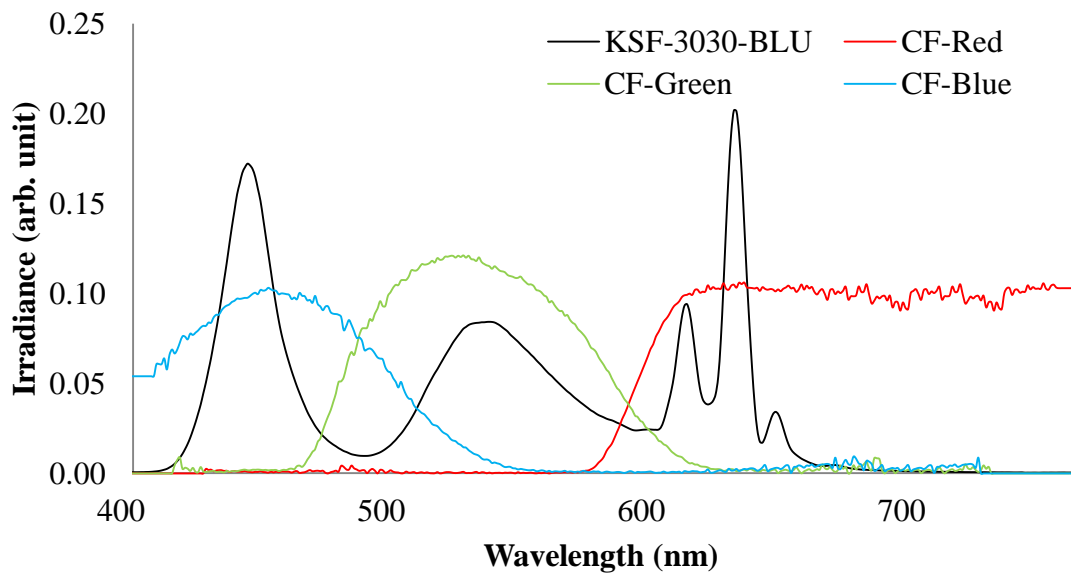


Figure 51: The BLU Spectrums of KSF3030 with CFs of Panel

Between the crosstalk areas of green and red CFs in Figure 51, BLU intensity decreases. Therefore, this effects give rise to increase the colour gamuts. On the other hand, peak wavelengths are at 533nm and 631nm for green and red. Additionally, FWHM of green is 63nm. FWHM of the biggest red peak is 11nm, and second one is 11nm. Green peak is at 532nm. The biggest red peak is 631nm and second peak is at 610nm.

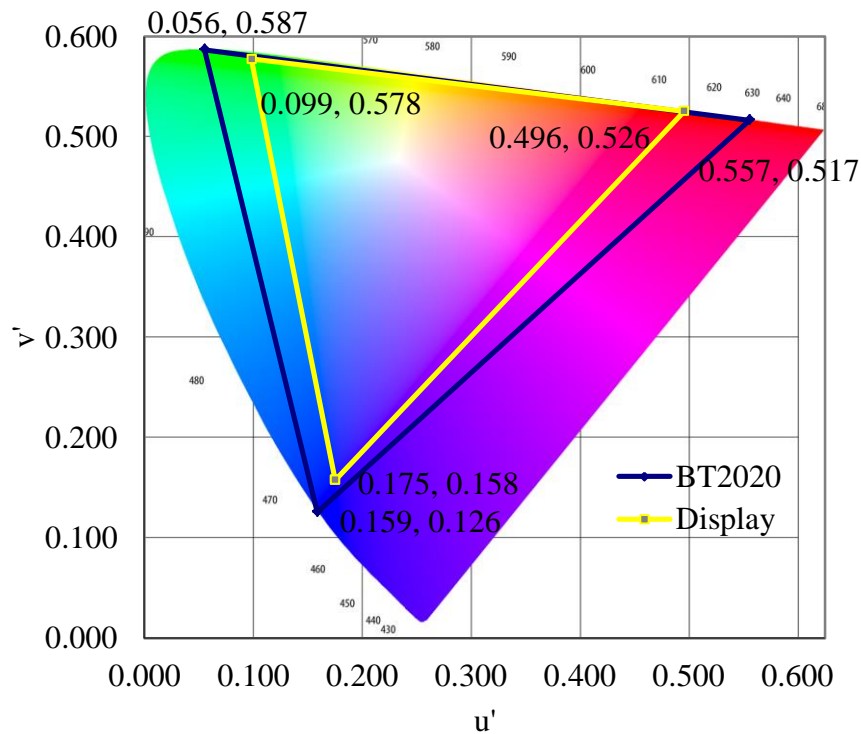
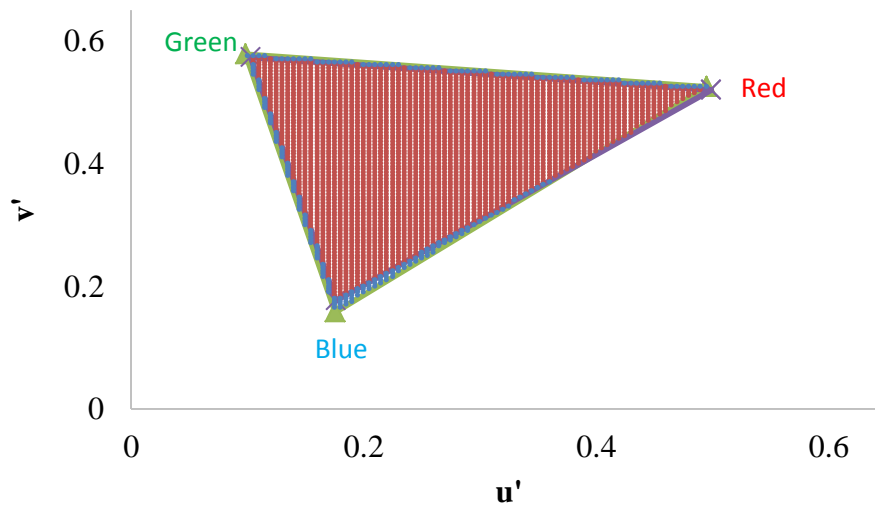


Figure 52: Colour Gamut Schema of KSF3030 on BT2020 Standard

Red and green corners of KSF3030 LED are closer with the BT2020s in Figure 52. Therefore, red and green region is compatible to achieve colour gamut in BT2020 standard. In addition, Blue corner of the display has better performance than YR1313 and YR3030. This improvement was provided by decreasing green luminance of BLU on blue colour filter.

For DCI-P3 coverage colour gamut in Figure 53, green and red corners are close to the DCI-P3 standard. In order to get higher colour gamut, blue LED should be improved. Beside of this improvement, green and red should be slightly improved to achieve 100% DCI-P3 coverage area.



- DCI-P3 gamut samples interior to the UHDA Device Test Gamut
- DCI-P3 gamut samples exterior to the UHDA Test Device Gamut
- ▲ DCI-P3 UHDA Test Coverage Boundary
- × UHDA Test Device Coverage Boundary

Figure 53: Colour Gamut Schema of KSF3030 on DCI-P3 Coverage Standard

3.1.4 MGF-1313 CSP Flip Chip Type LED

Coated MGF ($\text{Mg}_4\text{Ge}_2\text{O}_3\text{F}_2:\text{Mn}^{4+}$) phosphor on blue chip is studied in this section. Chip of the MGF1313 is the same as YR1313. MGF1313’s thermal connection is also same as YR1313 CSP in Figure 36. Thermal measurements were done within 10 seconds intervals using data logger. Display was powered up at zero time.

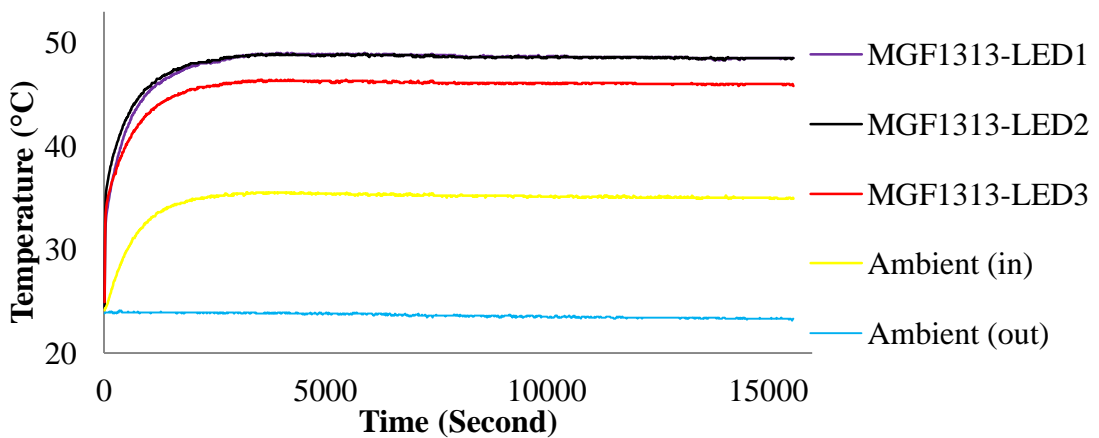


Figure 54: MGF1313 Thermal Test Results

We defined the time that the system comes to steady state as 10000th second. The average thermal measurement from 10000th to 15570th seconds was taken. The results were listed in Table 15.

Table 15: Average Temperatures of Thermal Test Points

<i>Test Point</i>	<i>Average Temperature (°C)</i>
<i>MGF1313-LED1</i>	<i>48.55</i>
<i>MGF1313-LED2</i>	<i>48.53</i>
<i>MGF1313-LED3</i>	<i>46.01</i>
<i>Ambient (in)</i>	<i>35.03</i>
<i>Ambient (out)</i>	<i>23.38</i>

Averages of three different LEDs are calculated as 47.70 °C. In order to calculate junction temperature of LED chips, Equation (2) was used. Rth value of the 1313 CSP was 14.5 K/W. (where I is driving current, and V_f is forward voltage)

$$T_j = 47.70 \text{ °C} + [0.450A \times 3.1V \times 14.5 K/W] = 67.92 \text{ °C} \quad (24)$$

$$T_j - T_{ambient(out)} = T_{j-a} = 67.92 \text{ °C} - 23.38 \text{ °C} = 44.54 \text{ °C} \quad (25)$$

As a result of the calculation, the average junction temperature of LED is 67.92 °C at 23.38°C ambient temperature. The difference between the junction temperature and ambient temperature was calculated as 44.54 °C. T_{j-a} was defined to remove dependency of ambient temperature. Inside temperature of display was 35.03 °C.

In order to detect thermal effect of a single MGF1313 LED, we bypassed the selected LED2. As calculated in Equation 28 using the Table 16, the 35.47 °C increase of the junction temperature comes solely from the LED chip itself.

Table 16: Thermal Effect of a single MGF1313 LED (LED2)

<i>Test Status</i>	<i>Junction Temperature of the LED (°C)</i>	<i>Ambient Temperature (°C)</i>
<i>MGF1313-LED2-Open</i>	<i>68.95</i>	<i>23.38</i>
<i>MGF1313-LED2-Close</i>	<i>34.90</i>	<i>24.80</i>

$$\Delta T_{open} = T_{j(open)} - T_{ambient(open)} = 68.95 \text{ °C} - 23.38 \text{ °C} = 45.57 \text{ °C} \quad (26)$$

$$\Delta T_{close} = T_{j(close)} - T_{ambient(close)} = 34.90 \text{ °C} - 24.80 \text{ °C} = 10.10 \text{ °C} \quad (27)$$

$$\Delta T_{open-close} = \Delta T_{(open)} - \Delta T_{(close)} = 45.57 \text{ °C} - 10.10 \text{ °C} = 35.47 \text{ °C} \quad (28)$$

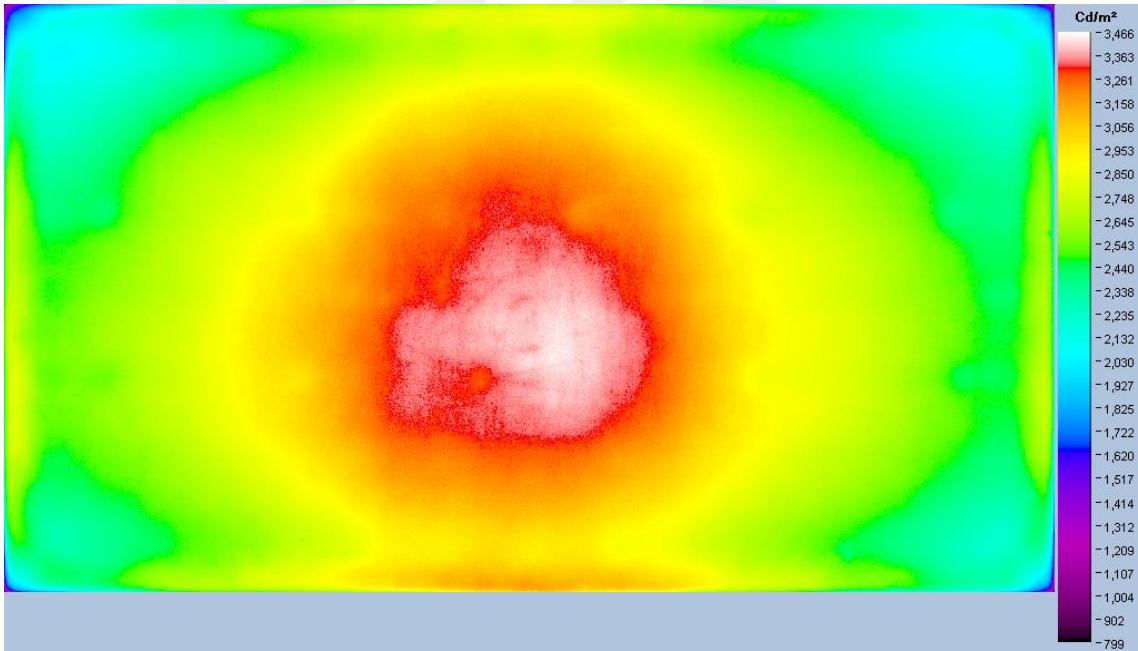


Figure 55: BLU Luminance Distribution of MGF1313

MGF1313 luminance distribution is efficient. Sides and corners of the panel are darker than YR1313. As a result, MGF coating on chip instead of YR decreases the LED beam angle. Therefore, visual performance of MGF1313 is not as good as that of

YR1313 regarding uniform distribution. Sides and corners are also worse than KSF3030 and YR3030. Cyan region has big part on BLU.

Table 17: Uniformity, Luminance and Colour Coordinates

<i>Measured System</i>	<i>¼ Uniformity Result</i>	<i>Luminance of White(nit)</i>	<i>Colour Coordinates</i>
<i>MGF1313-BLU</i>	85.95	-	-
<i>MGF1313-Display</i>	-	369	<i>x:0.255, y:0.245</i>

According to the results in Table 17, the colour coordinates are not close to target (0.280, 0.280) that we have defined at the beginning of the study. In order to compare the luminance, obtain the colour coordinates should be obtained near the target. By increasing colour x and colour y at an amount of 0.005 and 0.01 respectively, luminance improvement was 3%.

$$\text{Measured CIE Coordinates} \rightarrow x: 0.255, y: 0.245 \quad (29)$$

$$x: 0.255 + 4 \times 0.005, \quad y: 0.245 + 4 \times 0.01 \quad (30)$$

$$\begin{aligned} \text{For } x: 0.275, \quad y: 0.285 \rightarrow \text{Luminance will increase } 12\% \\ = 369.0 \times \frac{112}{100} = 413 \text{ nit} \end{aligned} \quad (31)$$

We will use the calculated value of luminance (412.7 nit) for the target colour coordinates.

Table 18: Gamut Results of the MGF1313

<i>Measured System</i>	<i>Gamut (BT2020)</i>	<i>Gamut (DCI-P3 Coverage)</i>
<i>MGF1313-Display</i>	66.36%	86.41%

The results of MG1313 shows that colour gamuts are better than YR1313 and YR3030. However, it is not close to the KSF performance since KSF's red peak is narrower than MGF. It is possible to obtain wider colour gamut. MGF conversion material provided the solution between the YR and KSF in regard to colour gamut.

As we seen from BLU spectrum of MGF in Figure 56, there is an elevation in red region. In addition, at the end of the green colour filter, the spectrum intensity decreases. These structures were different from YR1313. These effects provided the best wider colour gamut than YR1313.

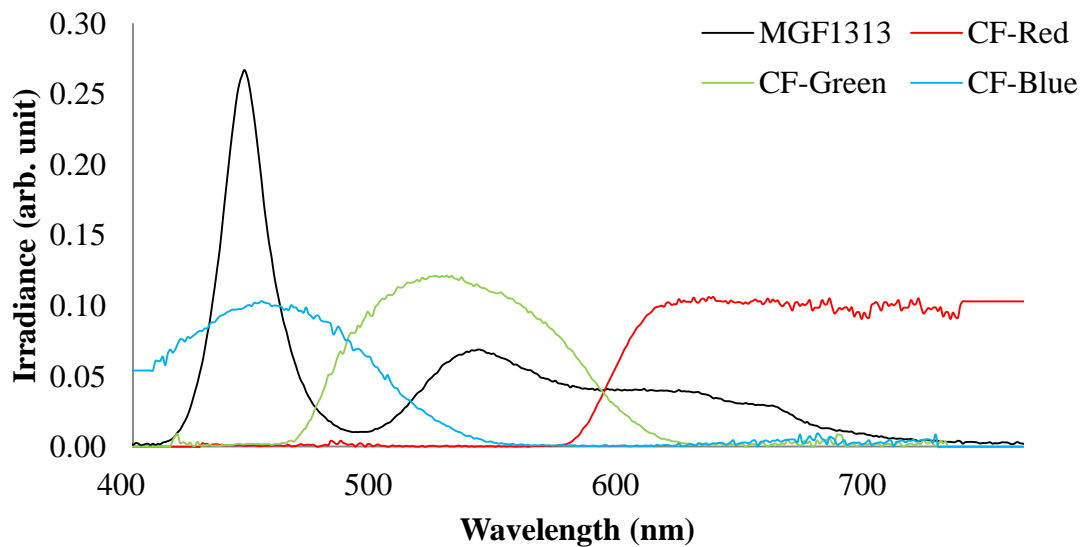


Figure 56: The BLU Spectrums of MGF1313 with CFs of Panel

In Figure 57, the red corner of the triangle is far away from that of standard according to the KSF. Therefore, improvement of MGF in red region according to the YR was not sufficient as KSF. Some improvement for DCI-P3 and BT2020 standards were achieved. However, it needs to be developed for the green and red regions.

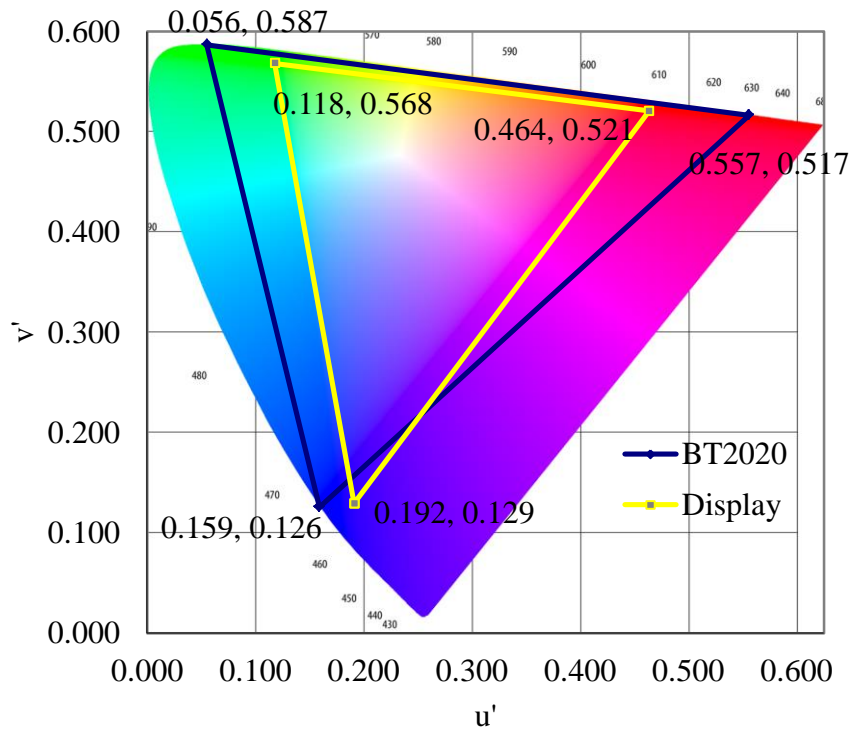


Figure 57: Colour Gamut Schema of MGF1313 on BT2020 Standard

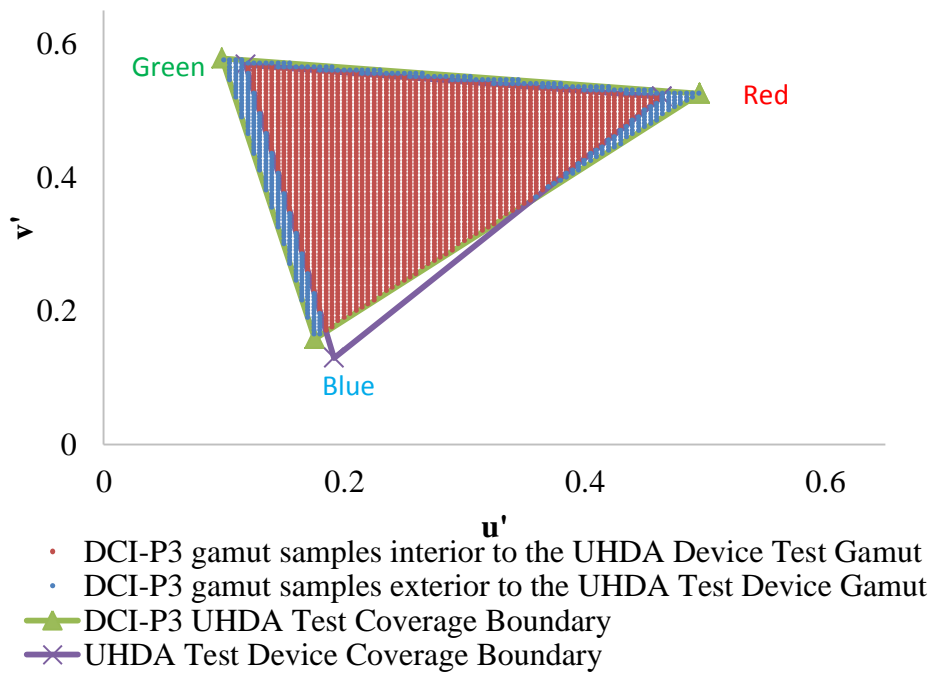


Figure 58: Colour Gamut Schema of MGF1313 on DCI-P3 Coverage Standard

Figure 57 and Figure 58, v' coordinates of blue LED decreased since low intensities were obtained between the blue and green crosstalk regions (Figure 56). For the blue LED, the green and red regions may be developed for BT2020 standards. However, colour enlargement should be improved green and red regions for both DCI-P3 coverage and BT2020 standard.

3.2 Analysis of Light Conversion Layers (Remote Solutions)

In this section, we used colour conversion film with blue LED. The coated films were integrated to BLU's optical structures (Figure 29). The thermal performance was analyzed for all of the light conversion layers since the tests were completed with the same blue LED for different light conversion layers. On the other hand, the exposed temperature of light conversion layer was measured. The light converted particles are thermally sensitive. So, two more thermocouples were added to between diffuser plate and light conversion film. Thermocouples were placed away from bottom side of the display 300mm and 700mm vertically.



Figure 59: Thermocouples Connections between Colour Conversion Layer and DP

LED's thermocouples were glued to blue LEDs 3mm away from the chip as YR1313 and MGF 1313 in Figure 60.

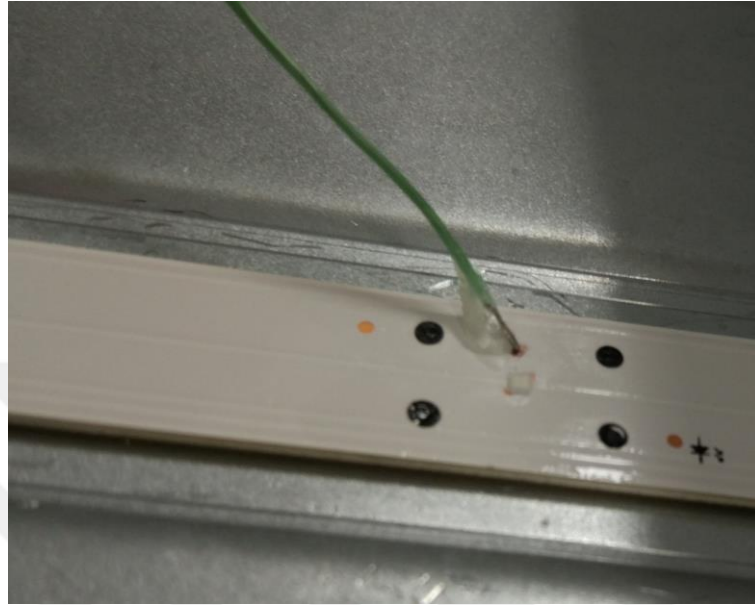


Figure 60: Thermal Test Point of 1313 Blue LED

Thermal measurements were taken 10 seconds intervals using data logger. Display was powered up at zero time.

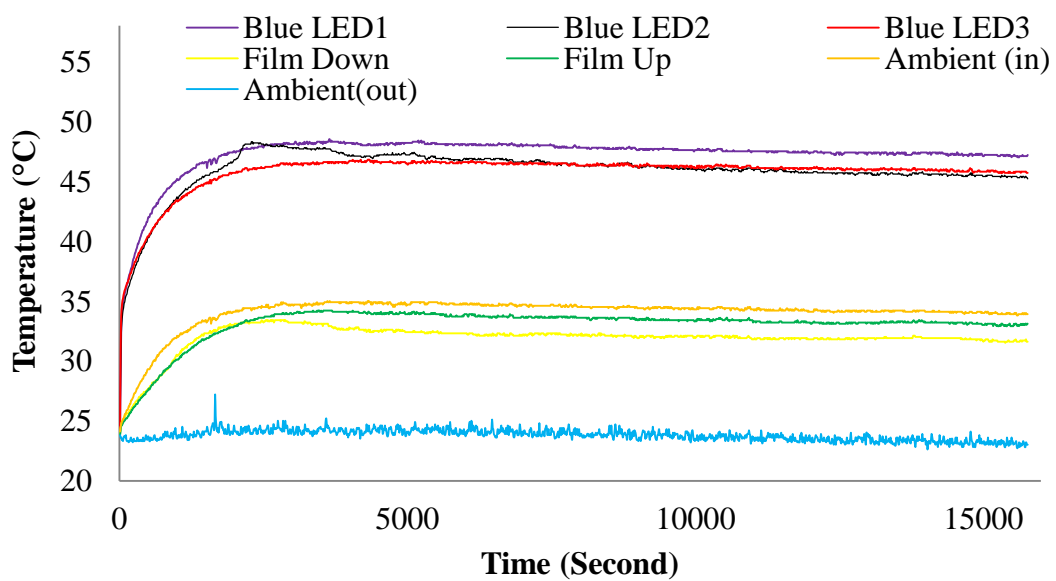


Figure 61: Blue LED 1313 Thermal Test Results

We defined the time that the system comes to steady state as 10000th second. The average thermal measurement was from 10000th to 15570th seconds. The contact on the inner assembly platform of display was specified “Ambient (in)”. The contact of the outer platform was defined as “Ambient (out)”. Thermocouples which have 300mm and 700 mm distances are called “Film Down” and “Film Up”, respectively. The results were listed in Table 19.

Table 19: Average Temperatures of Thermal Test Points

<i>Test Point</i>	<i>Average Temperature (°C)</i>
<i>Blue1313-LED1</i>	<i>47.37</i>
<i>Blue1313-LED2</i>	<i>45.70</i>
<i>Blue1313-LED3</i>	<i>46.02</i>
<i>Film Down</i>	<i>31.87</i>
<i>Film Up</i>	<i>33.22</i>
<i>Ambient (in)</i>	<i>35.03</i>
<i>Ambient (out)</i>	<i>23.38</i>

The average of three different LEDs was calculated as 46.42 °C. In order to calculate junction temperature of LED chips, Equation (2) is followed. The Rth value of the 1313 CSP was 14.5 K/W. (where I is driving current, and V_f is forward voltage)

$$T_j = 46.42 \text{ °C} + [0.450\text{A} \times 3.1\text{V} \times 14.5 \text{ K/W}] = 66.65 \text{ °C} \quad (32)$$

$$T_j - T_{\text{ambient}(\text{out})} = T_{j-a} = 66.65 \text{ °C} - 23.38 \text{ °C} = 43.27 \text{ °C} \quad (33)$$

As a result, the average junction temperature of LED was 66.65 °C at ambient temperature (23.38°C). The difference between the junction temperature and ambient temperature was found as 43.27 °C. T_{j-a} was defined to remove dependency of ambient temperature. In addition, inside temperature of display was 35.03 °C. On the other hand,

the temperatures at the bottom of light conversion layer were measured between 31.87 °C and 33.22 °C. As a result of the measurements, the conversion particles exposed to heat for light conversion film was lower than 34 °C.

In order to detect thermal effect of a single blue 1313 LED, we bypassed the selected LED2. Equation 36 using the Table 20, the 35.03 °C increase of the junction temperature comes solely from the LED chip itself.

Table 20: Thermal Effect of a single Blue 1313 LED (LED2)

<i>Test Status</i>	<i>Junction Temperature of the LED (°C)</i>	<i>Ambient Temperature (°C)</i>
<i>Blue1313-LED2-Open</i>	<i>67.70</i>	<i>23.38</i>
<i>Blue1313-LED2-Close</i>	<i>34.19</i>	<i>24.90</i>

$$\Delta T_{open} = T_{j(open)} - T_{ambient(open)} = 67.70 \text{ °C} - 23.38 \text{ °C} = 44.32 \text{ °C} \quad (34)$$

$$\Delta T_{close} = T_{j(close)} - T_{ambient(close)} = 34.19 \text{ °C} - 24.90 \text{ °C} = 9.29 \text{ °C} \quad (35)$$

$$\Delta T_{open-close} = \Delta T_{(open)} - \Delta T_{(close)} = 44.32 \text{ °C} - 9.29 \text{ °C} = 35.03 \text{ °C} \quad (36)$$

3.2.1 Cadmium (Cd) based Quantum Dot (QD) Film

In this section, we have tested Cd based QD film with blue LED in this study and the coated film with Cd based QD was analyzed with the excitation of blue LED.

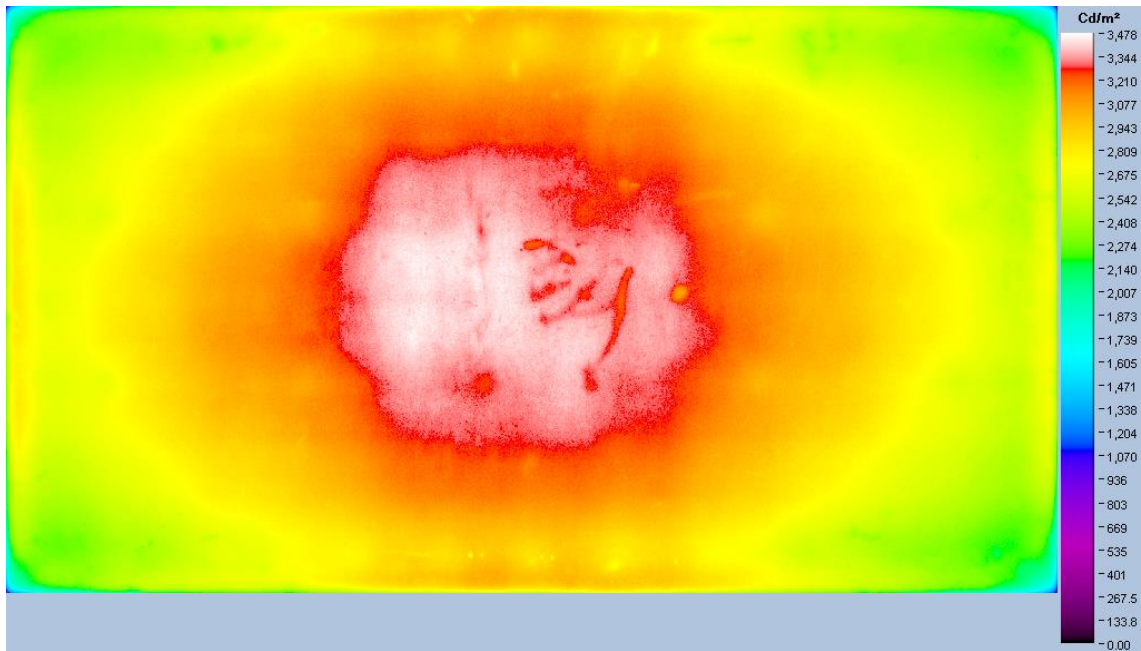


Figure 62: BLU Luminance Distribution of Cd based QD Film

The similar light distribution using YR1313 was obtained for Cd based colour conversion film in Figure 62. The yellowish area enlarged the side of the panel when compared with OCSs apart from YR1313.

Table 21: Uniformity, Luminance and Colour Coordinates

<i>Measured System</i>	<i>¼ Uniformity Result</i>	<i>Luminance of White(nit)</i>	<i>Colour Coordinates</i>
<i>Cd Based QD -BLU</i>	90.42	-	-
<i>Cd Based QD-Display</i>	-	400	<i>x:0.266, y:0.274</i>

We saw that luminance uniformity increased considering OCSs. Therefore, Cd based QD film was not only increased colour gamut but also it provided better luminance uniformity.

According to the colour coordinates in Table 21, results were close to our target (0.280, 0.280) we defined beginning of the study. However, fine tuning calculations were

better for comparisons. In order to compare the luminance by increasing the colour x and colour y amounts of 0.005 and 0.01 respectively, luminance changed by 3%.

$$\text{Measured CIE Coordinates} \rightarrow x: 0.266, y: 0.274 \quad (37)$$

$$x: 0.266 + 1 \times 0.005, \quad y: 0.274 + 1 \times 0.01 \quad (38)$$

$$\begin{aligned} \text{For } x: 0.271, \quad y: 0.284 &\rightarrow \text{Luminance increased by 3\%} \\ &= 400.0 \times \frac{103}{100} = 412 \text{ nit} \end{aligned} \quad (39)$$

We used the calculated value of luminance for our target of colour coordinates (412.0 nit).

Table 22: Gamut Results of the Cd based QD

<i>Measured System</i>	<i>Gamut (BT2020)</i>	<i>Gamut (DCI-P3 Coverage)</i>
<i>MGF1313-Display</i>	<i>76.60%</i>	<i>94.87%</i>

According to Table 22, wider colour gamut was created integrating Cd based QD film in the BLU. Cd based QD film provided the best colour gamut value when compared with OCSs. Especially, in BT2020 standard it has quite higher colour gamut than KSF3030 which has the highest colour gamut among the OCSs.

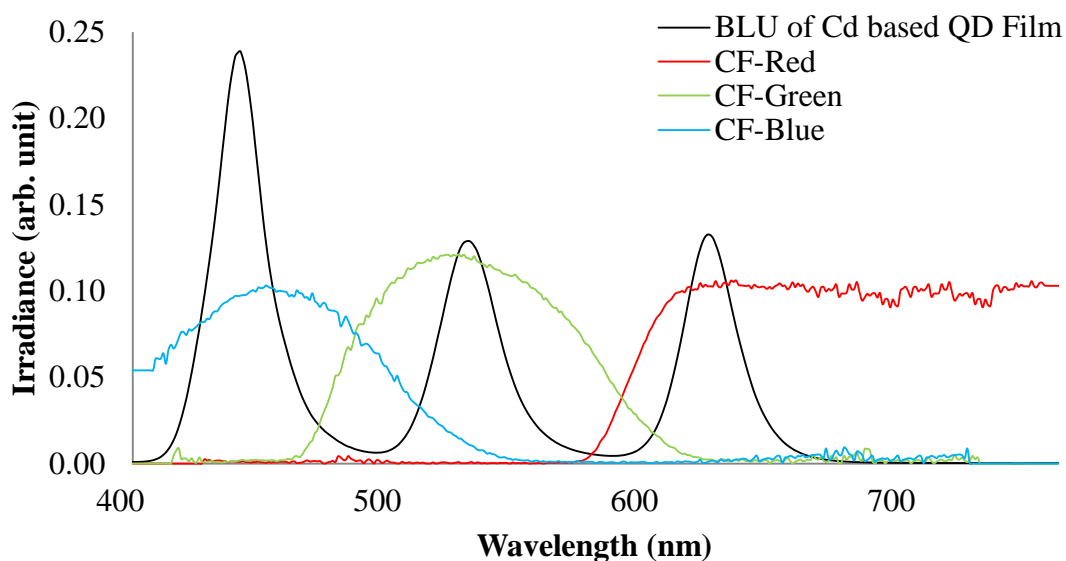


Figure 63: The BLU Spectrums of CD based QD with CFs of Panel

The spectrum of Cd based BLU in Figure 63 has narrower FWHM for green and red peaks. The FWHM of green and red are 28nm and 24 nm, respectively. The peak wavelengths of green and red for the BLU are at 529nm and 623 nm. They are compatible with CF's peak wavelengths as shown in Figure 32. The narrower peaks provide low luminance on crosstalk region. Furthermore, they create pure colours to get wider colour gamut.

The corners of triangle were closer than OCS in Figure 64. The colour gamut was calculated as 94.87 in Table 22. To obtain wider colour gamut on BT2020 standards, three colours were improved.

In Figure 65, the green and red corners of triangle had better performance than DCI-P3 standard. In order to get wider colour gamut in DCI-P3, blue chip performance should be improved. Therefore, the narrower blue peak was needed to be obtained wider colour gamut in DCI-P3 coverage.

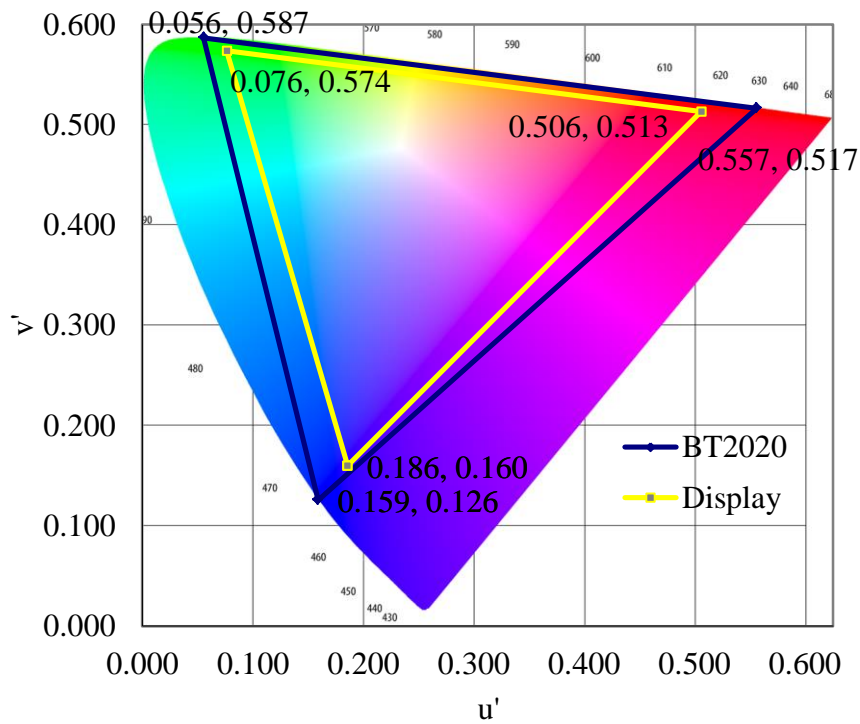
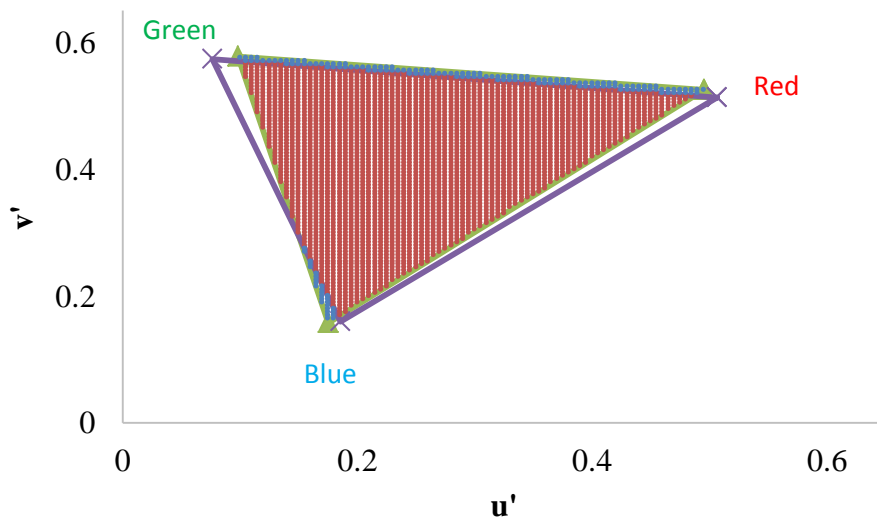


Figure 64: Colour Gamut Schema Value of Cd based QD on BT2020 Standard



- DCI-P3 gamut samples interior to the UHDA Device Test Gamut
- DCI-P3 gamut samples exterior to the UHDA Test Device Gamut
- ▲— DCI-P3 UHDA Test Coverage Boundary
- x— UHDA Test Device Coverage Boundary

Figure 65: Colour Gamut Schema of Cd based QD on DCI-P3 Coverage Standard

3.2.2 Cadmium (Cd) free Quantum Dot (QD) Film

In this section, we investigated Cd free QD film which was excited by blue LED.

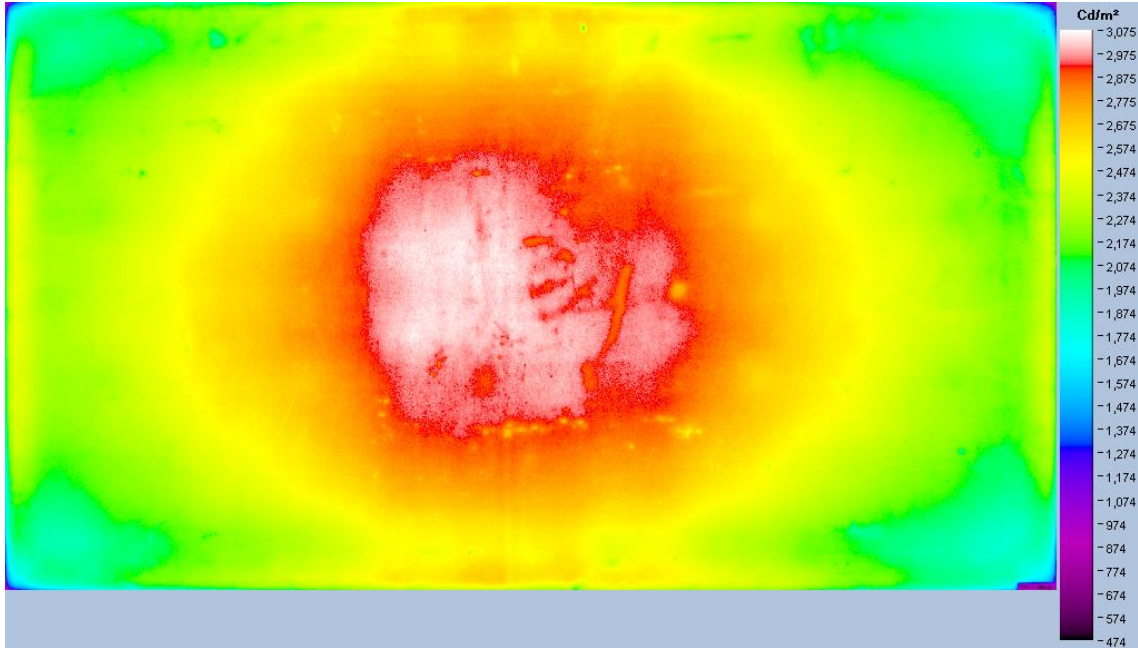


Figure 66: BLU Luminance Distribution of Cd free QD Film

The distribution performances were evaluated for Cd free colour conversion film, shown in Figure 66. The light distribution from the center to sides of the panel is not smooth as that of Cd based QD. The performance is better than MGF1313.

Table 23: Uniformity, Luminance and Colour Coordinates

<i>Measured System</i>	<i>¼ Uniformity Result</i>	<i>Luminance of White(nit)</i>	<i>Colour Coordinates</i>
<i>Cd free QD -BLU</i>	89.08	-	-
<i>Cd free QD-Display</i>	-	333	<i>x:0.281, y:0.275</i>

According to the results in Table 23, the colour coordinates are close to the target (0.280, 0.280) we defined at the beginning of the study. However, fine tuning calculations were better for comparisons. In order to compare the luminance, the colour

coordinates should be close to the target as OCSs by increasing colour x and colour y at an amount of 0.005 and 0.01 respectively, the luminance changed by 3%.

$$\text{Measured CIE Coordinates} \rightarrow x: 0.281, y: 0.275 \quad (40)$$

$$x: 0.281 + 1 \times 0.005, \quad y: 0.275 + 1 \times 0.01 \quad (41)$$

$$\begin{aligned} \text{For } x: 0.286, \quad y: 0.285 &\rightarrow \text{Luminance increased by 3\%} \\ &= 333.0 \times \frac{103}{100} = 343 \text{ nit} \end{aligned} \quad (42)$$

In Table 23, the uniformity of luminance is similar to OCS. However, the distribution is not good as Cd based QD.

Table 24: Gamut Results of the Cd based QD

<i>Measured System</i>	<i>Gamut (BT2020)</i>	<i>Gamut (DCI-P3 Coverage)</i>
<i>Cd free QD-Display</i>	<i>70.43%</i>	<i>90.81%</i>

The colour gamut of Cd free QD film is shown in Table 24. Cd free QD film provided the better solution in BT2020 standard when compared with OCSs. However, DCI P3 coverage area of KSF3030 was higher than Cd free QDs. According to Cd based Qd film, Cd free one has low colour gamut in the both standards.

The spectrum of Cd free QD BLU in Figure 67 has wider FMHM for green and red peaks than Cd based QD film. The FWHM of green and red were 44nm and 53nm, respectively. The peak wavelength of the green and red for the BLU were at 539nm and 625 nm. They were compatible with CF's peak wavelengths in Figure 32. However, the colour gamut can be increased by decreasing the wavelength of the green peak to about

530nm. On the other hand, FWHMs of the Cd free QD peaks were wider than Cd based one. This leads to differences in colour gamut.

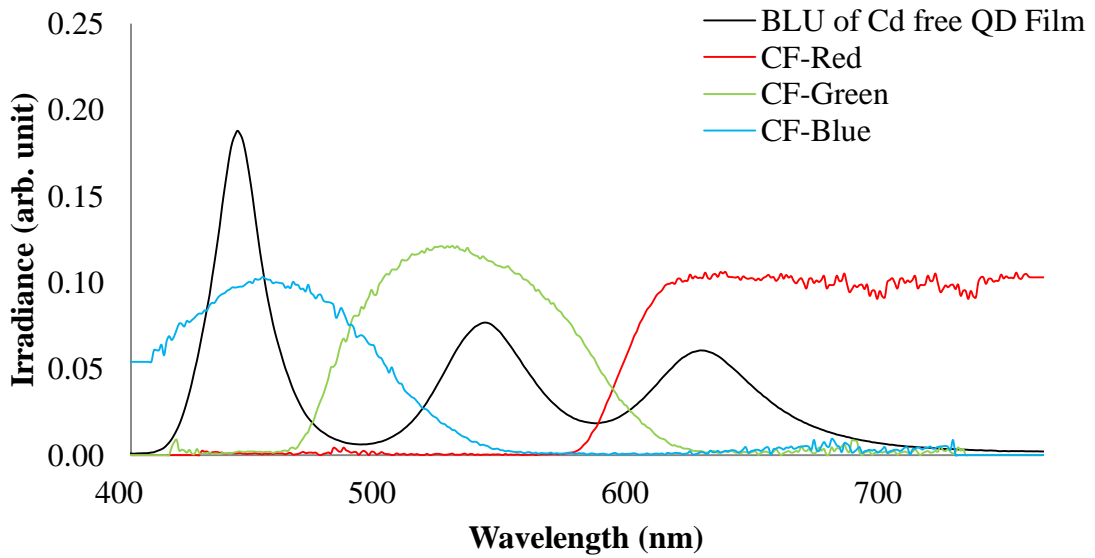


Figure 67: The BLU Spectrums of CD free QD with CFs of Panel

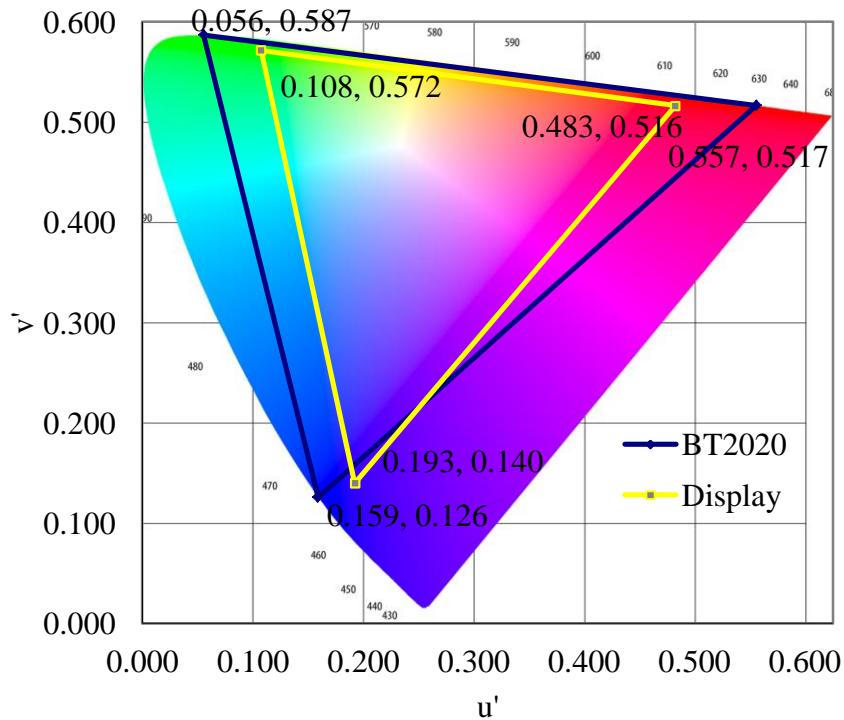


Figure 68: Colour Gamut Schema of Cd free QD on BT2020 Standard

Cd free QD provided better solutions considering OCSs in BT2020 standard (Figure 68). In order to get wider colour gamut, BLU intensity should be reduced between green and red bands on the crosstalk area of CFs.

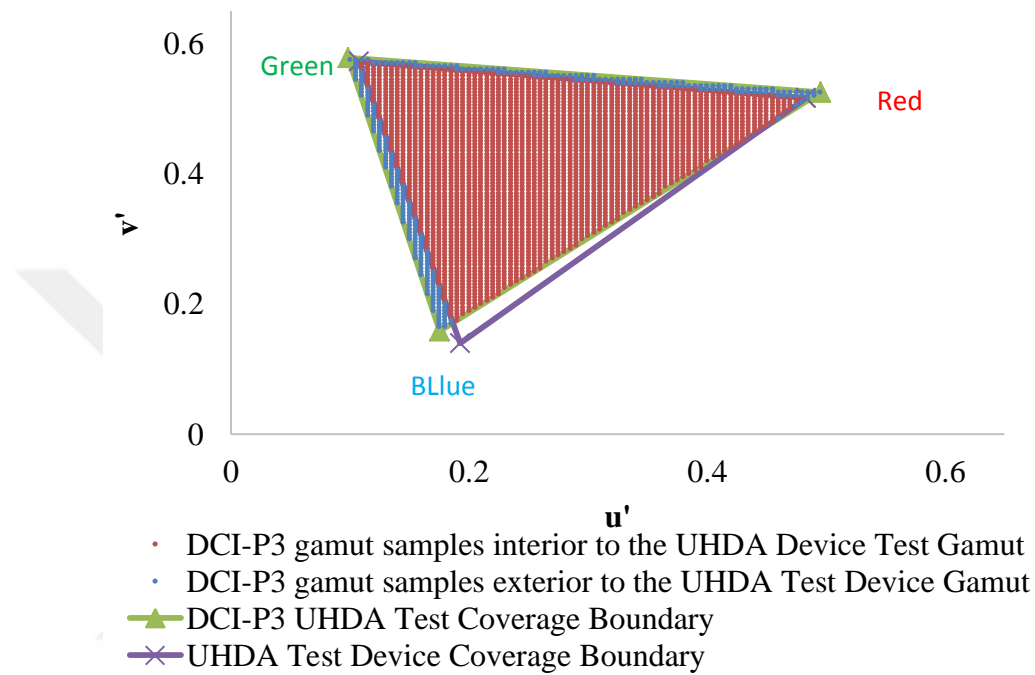


Figure 69: Colour Gamut Schema of Cd free QD on DCI-P3 Coverage Standard

The green and red corners of triangle are larger than YR and MGF. However, the performance can't catch KSF OCS in DCI-P3 standard. The exterior area of green region is not low enough to increase color gamut since the green peak of the BLU should be narrowed to develop this region.

3.2.3 Phosphor Film

In this section, we investigated coated film with red and green phosphors which is excited by blue LED.

The distribution performance was presented for phosphor colour conversion

film in Figure 70. The light distribution gave performance between Cd free QD and CD based QD. When compared the corners of the display, it was better than Cd free QD. However, QD based one has better performance. In addition, light leakage performance is better than most of the solutions.

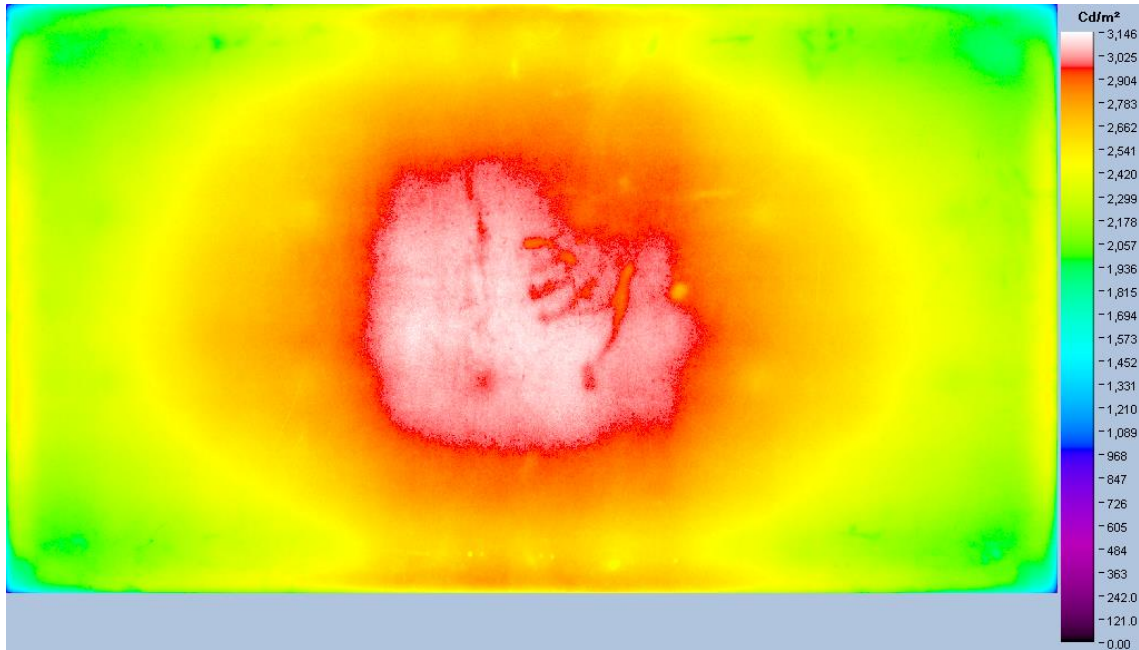


Figure 70: BLU Luminance Distribution of Phosphor Film

According to the results in Table 25, CIE-y coordinate is close to the target (0.280). However, fine tuning calculations are better for comparisons. In order to compare the luminance, the colour coordinates should be close to the target as OCSs.

Table 25: Uniformity, Luminance and Colour Coordinates

<i>Measured System</i>	<i>¼ Uniformity Result</i>	<i>Luminance of White(nit)</i>	<i>Colour Coordinates</i>
<i>Phosphor Film-BLU</i>	88.64	-	-
<i>Phosphor Film-Display</i>	-	323	<i>x:0.299, y:0.290</i>

Our CIE-y calculations could be balanced at 0.285 coordinate. Therefore, we used YR1313 as reference which is the closest to the target of CIE-y for all solutions.

By increasing colour x and colour y at an amount of 0.005 and 0.01 respectively, luminance improvement was 3%.

$$\text{Measured CIE Coordinates} \rightarrow x: 0.299, y: 0.290 \quad (43)$$

$$x: 0.299 - 0.5 \times 0.005, \quad y: 0.290 - 0.5 \times 0.01 \quad (44)$$

$$\begin{aligned} \text{For } x: 0.297, \quad y: 0.285 \rightarrow \text{Luminance will decrease 1.5\%} \\ = 323.0 \times \frac{98.5}{100} = 318 \text{ nit} \end{aligned} \quad (45)$$

In Table 25, the uniformity of luminance is similar with QD based films. However, the distribution has smaller difference than Cd based QD.

Table 26: Gamut Results of the Phosphor Film

<i>Measured System</i>	<i>Gamut (BT2020)</i>	<i>Gamut (DCI-P3 Coverage)</i>
<i>Phosphor Film-Display</i>	<i>75.59%</i>	<i>91.19%</i>

The phosphor film provides the better solution in BT2020 standard compared with other solutions, apart from Cd based QD film. Furthermore, the colour gamut performance is much close to Cd based QD.

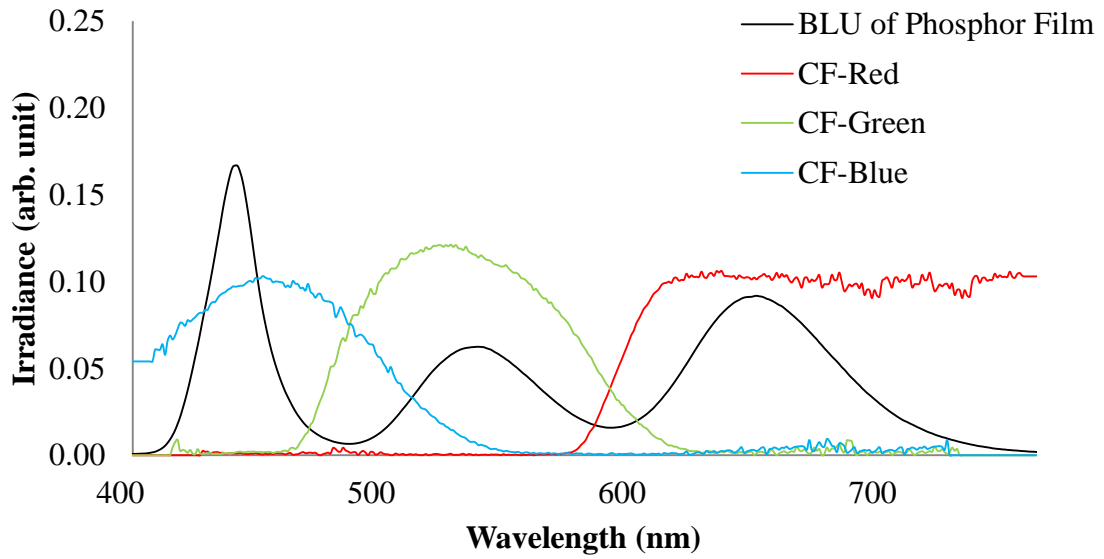


Figure 71: The BLU Spectrums of Phosphor Film with CFs of Panel

The spectrum of phosphor BLU in Figure 71 has wider FMHM for green and red peaks than Cd free QD film. The FWHM of green and red were 59nm and 67nm respectively. The Peak wavelengths of the green and red for the BLU were at 530nm and 645 nm. They were compatible with CF's peak wavelengths shown in Figure 32. However, conversion of blue light to green has low efficiency for phosphor solution. In addition, the conversions from blue to red and green light and green to red light have higher efficiencies. In this way, improvement was provided for red colour in terms of colour gamut. However, luminance was decreased since green intensity is low.

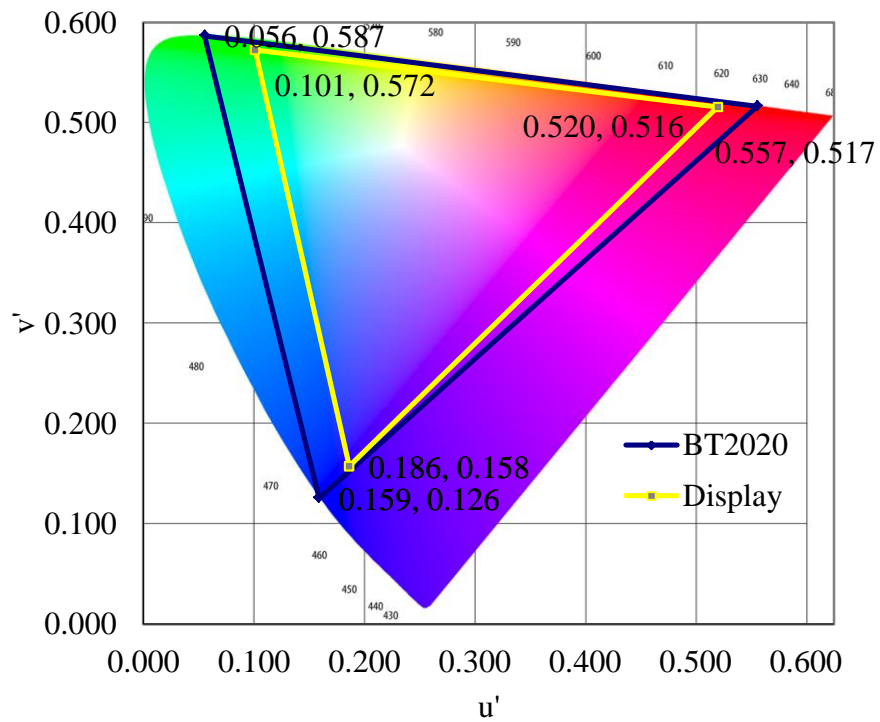
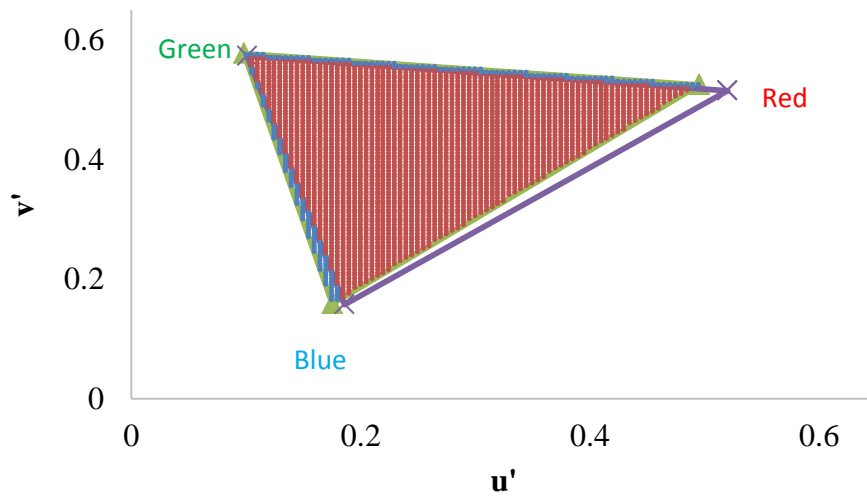


Figure 72: Colour Gamut Schema of Phosphor Film on BT2020 Standard

Phosphor film provided efficient solution considering other solutions in BT2020 standard (Figure 72). In the red region, improvement was observed. However, this conversion spectrum was decreased the luminance of display.



- DCI-P3 gamut samples interior to the UHDA Device Test Gamut
- DCI-P3 gamut samples exterior to the UHDA Test Device Gamut
- ▲— DCI-P3 UHDA Test Coverage Boundary
- ×— UHDA Test Device Coverage Boundary

Figure 73: Colour Gamut Schema of Phosphor Film on DCI-P3 Coverage Standard

As shown in Figure 73, the red corners of triangle have better performance than DCI-P3 standard. In order to get wider colour gamut in DCI-P3, green spectrum should be developed a little bit. Therefore, narrower green peak is needed to be obtained wider colour gamut in DCI-P3 coverage. However, the big improvement should be provided for blue chip in order to obtain wider colour gamut in DCI-P3 coverage standard.

CHAPTER IV

DISCUSSION

In this thesis, we analyzed the different type colour conversion layers and systems such as remote solutions and OCSs in terms of optical and thermal efficiency.

All spectrums of the solutions were shared in Figure 74.

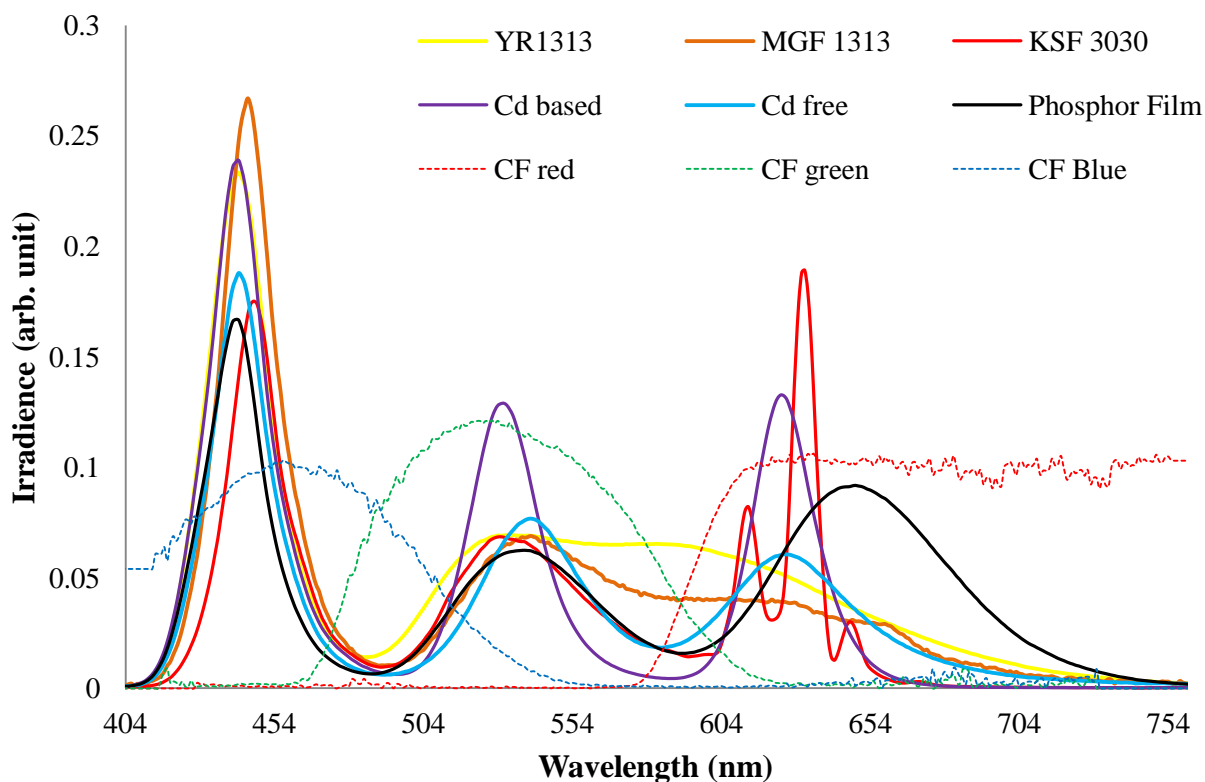


Figure 74: Spectrums of All Solutions

We aim to use the same peak wavelength for blue LED for all of the solutions. However, they had little differences because of production process such as tolerances of machines and yield rate.

MGF1313 intensity of blue is higher than other solutions from Figure 74.

Green level is similar with others apart from Cd based QD film. There is slightly increasing on the red region. However, it couldn't achieve efficient improvement on colour gamut.

Cd based QD film had second highest blue peak. Green band of Cd based QD had highest and narrowest peak. So, it provided efficient luminance and green colour. Red peak was both lower and wider than KSF3030. So, the second colour performance was observed in terms of peak specifications. Furthermore, colour conversion could be made efficiently with Cd based QD. Therefore, quantum efficiency of the structure is higher than others.

YR1313 had third highest blue peak and the broadest spectrum in the green and red bands. So, cost efficient solution YR1313 can't provide wide colour gamut. However, it had the better luminance performance since it had high intensity along the green band.

Cd free QD film has fourth highest blue peak. In green region, it had the second narrowest peak after Cd based QD film. Intensity of green peak is similar with other solutions apart from Cd based QD. In the red region, intensity of its peak is higher and narrower than YR1313 and MGF 1313.

The most characteristics band of KSF3030 solution is red which has the narrowest and highest peak. As shown in green region the similar performance with other solutions.

The phosphor film had the lowest blue peak. The green spectrum was narrower than YR1313 and MGF1313 and similar to KSF3030. The red peak of phosphor film had third highest peak. However, it didn't have narrower red peak

than KSF and Cd based QD. Furthermore, the red peak placed at right side of the others.

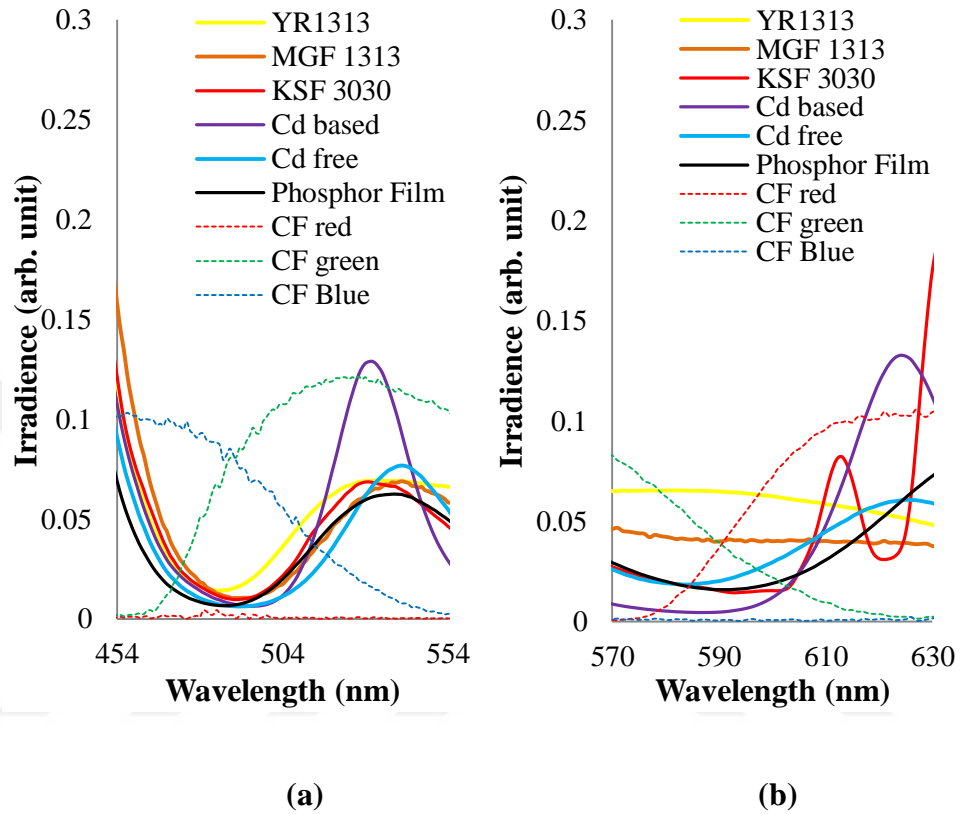


Figure 75: Crosstalk Regions (a) blue to green (b) green to red

Crosstalk regions were one of the most critical point in terms of colour gamut. Behaviors of different type solutions were analyzed between these crosstalk regions. From beginning point of green CF to end point of blue CF were called as blue to green crosstalk region. Similarly, from beginning point of the red CF to end point of green CF were called as green to red crosstalk region.

We evaluated blue to green crosstalk region firstly. In this region, YR1313 had the highest irradiance. Therefore, YR1313 presented worst performance between blue and green crosstalk region. Cd based and Cd free QDs provided better performances on this region. When calculated intensities in the green region, Cd

based QD presented higher intensity than Cd free one. Therefore, intensity ratio of green regions to crosstalk region is higher for Cd based QD. These properties and specifications are also valid for blue peaks as green peaks.

In green to red crosstalk region, MGF1313 and YR1313 have higher intensities. So, we didn't expect good performances on green and red band because of this situation. The lowest intensity was provided by Cd based QD. It shows that green and red colours performance is good. Intensity of KSF3030 was close to Cd based QD in the crosstalk region. However, one of the critical parameter is red peak intensity for KSF was higher than other solutions. Therefore, intensity ratio of only red regions to crosstalk region is higher for KSF3030. As a result of these outputs, red performance is better than the others.

We shared the test results of light distributions in Figure 76. We explained the significance and evaluation methods below the luminance distributions page 46. The Cd based QD and YR1313 were better in terms of light leakage on the right and left sides, larger light distribution and undimmed corners. YR1313 was better than Cd based QD in terms of LED visibility only. The best light leakage performances were observed on upside and bottom of the display. We can analyze it from lattice appearance which was located on middle, upside and down side of the display. The worst performance was observed on MGF1313 since it had dark corners, light leakage and dark areas. These dark areas were shown between the center and corners.

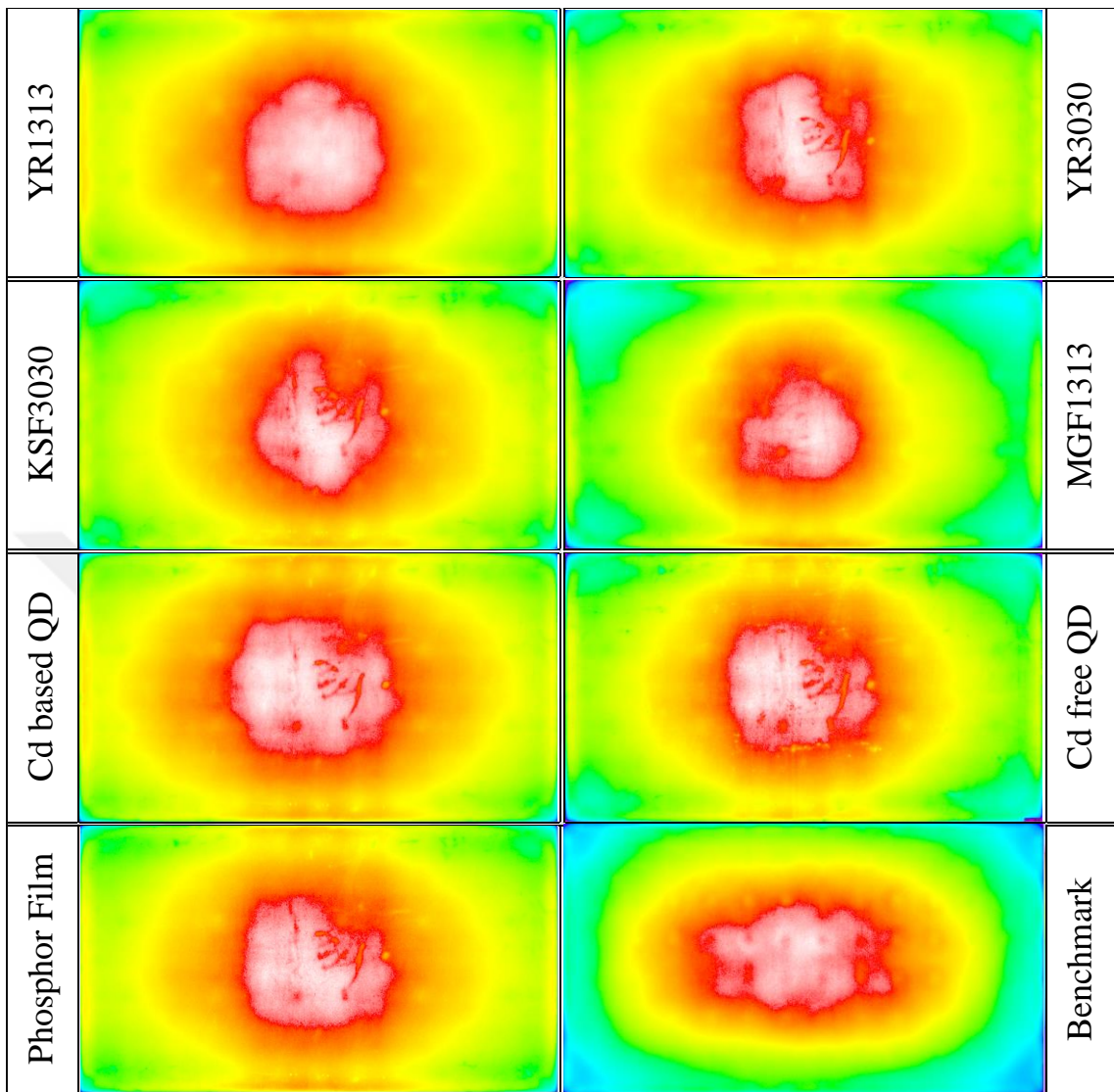


Figure 76: Visual Performances

Hisense benchmark panel was used for visual reference. Its model name is H65N5750UK. The visual performances in Table 27 are evaluated by observers using this display as reference.

The measurements results in Table 27 show that thermal performance of the blue chip is more efficient than the OCSs. Temperatures on conversion films were measured between 31.87 °C and 33.22 °C. Therefore, the temperatures of colour conversion particles can be greatly reduced using remote solution. Tj-a temperature

of YR3030 lateral chip was higher than other OCSs about 3 °C as expected. In addition, blue flip chip shared for remote solutions whose temperature was lower than coated flip chip solutions about 1.5 °C.

Table 27: Colour Gamut, Luminance, Temperatures and Visual Performances

<i>Solution Type</i>	<i>DCI P3 Coverage (%)</i>	<i>BT2020 Area (%)</i>	<i>Luminance (nit)</i>	<i>Temperature Tj-a (°C)</i>	<i>Visual Performance</i>
<i>YR1313</i>	<i>79.86</i>	<i>58.34</i>	<i>465</i>	<i>44.76</i>	<i>Much better</i>
<i>YR3030</i>	<i>78.27</i>	<i>56.89</i>	<i>470</i>	<i>47.73</i>	<i>Better</i>
<i>KSF3030</i>	<i>93.42</i>	<i>68.31</i>	<i>404</i>	<i>44.46</i>	<i>Good</i>
<i>MGF1313</i>	<i>86.41</i>	<i>66.36</i>	<i>413</i>	<i>44.54</i>	<i>Not Bad</i>
<i>Cd based QD film</i>	<i>94.87</i>	<i>76.60</i>	<i>412</i>	<i>43.27</i>	<i>Better</i>
<i>Cd free QD film</i>	<i>90.81</i>	<i>70.43</i>	<i>343</i>	<i>43.27</i>	<i>Not Bad</i>
<i>Phosphor film</i>	<i>91.19</i>	<i>75.59</i>	<i>318</i>	<i>43.27</i>	<i>Not Bad</i>

Colour gamut performances were different for DCI-P3 coverage and BT2020 standards. However, the best colour gamut was provided by Cd based QD for the both standards. The remote colour conversion layers were presented better performance than OCS. KSF3030 also provided good solution in DCI-P3 coverage standard. However, in BT2020 standard it couldn't catch the performances of remote solutions. On the other hand, YR solution presented lowest colour gamut and the highest luminance. KSF3030 and MGF1313 had better colour gamut which provided lower luminance than YR solution. However, they were higher than remote solutions apart from Cd based QD. Luminance level of Cd based QD was close to KSF3030 and MGF1313. The lowest luminance were observed on phosphor film.

CHAPTER V

CONCLUSION

In this thesis, we have studied the effect of colour conversion layer on the optical and thermal efficiency of LED based liquid crystal displays. We have designed an experimental test platform for LED based LCDs. On this platform, we have implemented OCSs and remote solutions based on phosphors or QD as colour converters. In addition, we have analyzed optical and mechanical components such as back-cover metal, LEDs, reflector sheet, diffuser plate, LCL, POP and DBEF.

Optical design of LED based LCDs is critical in determining colour gamut, luminance and visual performances. On the other hand, the selection of optical component has an effect on thermal properties of the displays. For this reason, the design should include thermal management as well. Phosphor based OCSs produce slightly more heat than the blue LED used in remote solutions. However, the temperatures of the colour converter containing films are between 30-40 °C. Since the temperature of colour converters such as phosphors or QDs has a tremendous effect on the optical performance and life time of the system, remote solutions provide a better option in terms of thermal design.

The assemble platform of the BLU is back-cover metal which was used to create the skeletal structure. GaN based LED light sources were installed on this surface. In order to direct the output of these light sources towards the LCP, a reflector sheet was used. In addition, a diffuser plate was chosen in order to distribute the LED light though the surface of the plate. LCL film was used on the

diffuser plate for remote solutions. OCS doesn't include this film. Then, we have used prism on prism in order to get higher luminance. The top layer of BLU is DBEF which provides higher luminance as well as better colour conversion for remote solution. This design is effective in improving the optical performance of the display.

Finally, we have studied the effect of optical design, light converters and colour filters on the gamut of the display, since in light-emitting diode (LED) lit liquid crystal displays (LCD), the colour gamut is related to the back-light unit (BLU) spectrum. The blue LED light is generally converted to green and red bands with light converting materials. However, the colour gamut is critically dependent on the compatibility between the converted spectra and colour filters. Quantum dot integrated display design with remote light conversion layers is a promising method, since the light conversion can be tuned by changing the QD structure. In addition, narrow band emitting phosphor blends provide an effective solution to this problem.

REFERENCES

- [1] T. Sugiura, "EBU color filter for LCDs," *SID Tech. Digest*, 2001.
- [2] Y. Shirasaki, G. J. Supran, M. G. Bawendi and V. Bulovic, "Emergence of colloidal quantum-dot light-emitting technologies," *Nat. Photonics* 7, pp. 13-23, 2013.
- [3] X. Dai, Z. Zhang, Y. Jin, Y. Niu, H. Cao, X. Liang, L. Chen, J. Wang and X. Peng, "Solution-processed, highperformance emitting diodes based on quantum dots," *Nature*, pp. 96-99, 2014.
- [4] K. Kakinuma, M. Shinoda and T. Arai, "Technology of wide color gamut backlight with RGB light-emitting diode for liquid crystal display television," *SID Tech. Digest*, 2007.
- [5] C. Ronda and A. Srivastava, "Luminescence Science and Display Materials," *The Electrochemical Society Interface*, p. 55, Spring 2006.
- [6] N. Y. Narendran, "Extracting phosphor-scattered photons to improve white LED efficiency," *Physica Status Solidi - Applications and Materials*, 2005.
- [7] S. Abe, "Hybrid remote quantum dot/powder phosphor designs for display backlights," *Light: Science & Applications*, 2017.
- [8] H. Chen, J. HE and S. Wu, "Recent Advances on Quantum-Dot-Enhanced Liquid-Crystal Displays," *IEEE Journal of Selected Topics in Quantum Electronics*, vol. 23, Iss. 5, September/October 2017.
- [9] W. Schwedler and F. Nguyen, "LED Backlighting for LCD TVs," *SID Tech. Digest*, 2010.
- [10] N. A., Jr, J. J. Wierer, Y. Ohno, W. Davis, S. R. J. Brueck and J. Y. Tsao, "Four-color laser white illuminant demonstrating high color-rendering quality," *Optics Express*, 2011.
- [11] B. Bahadur, "Liquid crystals: applications and uses," *Singapore, World Scientific*, Vols. 1,2 and 3, 1990.
- [12] L. Li and S. M. Faris, "A single-layer super broadband reflective polarizer," *SID Tech. Digest*, 1996.

- [13] Y. Cui, D.-K. Yang, R. Ma and J. J. Brown, "Characterization and modeling of light diffusing sheet," *SID Tech. Digest Tech.*, 2013.
- [14] S. K. Lim, "LCD Backlights and Light Sources," *Proceeding of Asia Display*, 2006.
- [15] D. Koseoglu, E. Bakan and K. Karsli, "Wide Colour Gamut Solutions Based on Photo-Enhanced Films," *Euro Display*, pp. 1-5, 2017.
- [16] D.-K. Yang and S.-T. Wu, "Liquid Crystal Display Components," in *Fundamentals of Liquid Crystal Devices*, Wiley, 2014, p. 514.
- [17] S. Kobayashi, S. Mikoshiba and L. Sungkyoo, LCD Backlights, John Wiley & Sons, Ltd ISBN: 978-0-470-69967-6, 2009, pp. 4,13,14.
- [18] S. Mikoshiba, "Crystal Valley Conference on LCD Backlights," pp. 3-4, 2005.
- [19] C.-C. Sun¹, 2. Moreno¹, S.-H. Chung¹, W.-T. Chien¹, C.-T. Hsieh¹ and T.-H. Yang¹, "Direct LED backlight for large area LCD TVs: brightness analysis," *1-Department of Optics and Photonics, National Central University, 320, Taiwan ; 2-Unidad Academica de Fisica, Universidad Autonoma de Zacatecas, Zacatecas 98060, Mexico*, 2007.
- [20] H. J. Round, "Electrical world," 1907.
- [21] M. A. Novikov, "Oleg Vladimirovich Losev: Pioneer of Semiconductor Electronics," *Physics of the Solid State*, vol. 46, pp. 1-4, 2004.
- [22] W. Howard, "U. of I.'s Holonyak out to take some of Edison's luster," *The Chicago Sun-Times*, 2005.
- [23] "Court dismisses inventor's patent claim but will consider reward," *The Japan Times*, 2002.
- [24] "History of Lighting," 2018. [Online]. Available: <http://www.historyoflighting.net/light-bulb-history/history-of-led>.
- [25] V. K. Khanna, Fundamentals of Solid-State Lighting-LEDs, OLEDs and Their Applications in Illumination and Displays, CRC Press, 2014, pp. 14,15-16,22,28,212-213.
- [26] S. W. R. Lee, R. Zhang, K. Chen and J. C. C. L. Lo, "Emerging Trend for LED Wafer Level Packaging," *Frontiers of Optoelectronics*, pp. 119-126, 2012.

- [27] R. Karlicek, "The Evolution of LED Packaging," p. 21, 2012.
- [28] K. Tseng and C. Tsou, "Novel Silicon-based LED Packaging Module with an Integrated Photosensing Element.," *EEE Photonics Technology Letters*, p. 515–518, 2013, March.
- [29] A. Kanemitsu, H. Iyama and T. Sakamoto, "Light Diffuser Plates for LCD-TV Backlight Systems -IT-Related Chemicals Research Laboratory," 2007.
- [30] Y. Hao, N. Bamiedakis, A. H. Hashim, R. V. Penty and I. H, "Design Study of Light-Guiding Plate in Backlighting System," *Department of Engineering, University of Cambridge, 9 JJ Thompson Avenue, Cambridge, CB3 0FA*, p. 114.
- [31] D. R. Selviah, K. Wang and X. Mo, in *Lighting and Backlighting Seminar*, UK, 2005.
- [32] C. Li, Y. Fang and M. Cheng, "Optical Express," vol. 17, 2009.
- [33] H. Okada, "Development and Trend in the Prism Sheet for Backlight," *Display Monthly, Technotimes*, p. 4, 2004.
- [34] M. F. Weber, C. A. Stover and L. R. Gilbert, "Giant birefringent optics in multilayer polymer mirrors," *Science*, 2000.
- [35] J. Castellano, "Modifying Light," *American Scientist*, 2016 September-October.
- [36] H. Mori, Y. Itoh and Y. Nishiura, "Performance of a novel optical compensation film based on negative birefringence of discotic compound for wide-view-angle twisted-nematic liquid crystal displays," *J. of Appl. Phys*, 1997.
- [37] D. F. Ross and D. M. Rao, "Developments in LCDs," pp. 7-9, 2006.
- [38] M. J. J., "Color Gamut Measurements and Mapping: The Role of Color Spaces, SPIE," *SPIE Proceedings*, vol. 3648, pp. 68-82, 1999.
- [39] J. Yurek, "Color Space Confusion," *Portrait Displays*, 2012.
- [40] O. Y. and B. P., "Chromaticity Difference Specification for Light Sources," *CIE Technical Notes*, pp. 1-3, 2014.
- [41] [Online]. Available: <https://www.handprint.com/HP/WCL/color2.html>.

- [42] K. M. C, S. Y. C., L. S. J. S. Y. R. and I. D. Kim, "Wide Gamut Multi-Primary Display for HDTV," *Second European Conference on Color in Graphics, Imaging and Vision*, pp. 248-253, 2004.
- [43] S. Mullen, "A Zero Math Understanding of Log Gamma," 2016.
- [44] Z. Luo, Y. Chen and S. T. Wu, "Wide color gamut LCD with a quantum dot backlight," *Opt. Express* 26269–26284, p. 21, 2013.
- [45] S. Coe-Sullivan, P. Allen and J. S. Steckel, "Quantum dots for LED downconversion in display applications," *ECS J. Solid State Sci. Technol.* 2, 3026–3030, 2013.
- [46] S. C. Sullivan, "Quantum dot developments," *Nat. Photonics* 3, p. 315–316, 2009.
- [47] Z. Luo, D. Xu and S. T. Wu, "Emerging quantum-dots-enhanced LCDs," *J. Disp. Technol.* 10, pp. 526-539, 2014.
- [48] Q. HONG, K.-C. LEE, Z. LUO and S.-T. WU, "High-efficiency quantum dot remote phosphor film," *The College of Optics and Photonics, University of Central Florida, Orlando, Florida 32816, USA 2Display Technology Center, Industrial Technology Research Institute*, 2015.
- [49] T. Güner, D. Köseoğlu and D. M. M., "Multilayer Design of Hybrid Phosphor Film for Application in LEDs," *Optical Materials*, vol. 60, pp. 422-430, 2016.
- [50] Y.-C. Lin, Y. Zhou, N. T. Tran and F. G. Shi, "LED and Optical Device Packaging and Materials," in *Materials for Advanced Packaging* , USA, 2009, pp. 629-677.

VITA

Emrah Bakan is born in 1987, in Zonguldak, Turkey. He graduated from Physics Department of Hacettepe University in 2011. He has been working at VESTEL as Senior Optical Design Engineer since 2013. He started his M.Sc.education at Ozyegin University in 2015. His current research interests are in quantum dots, phosphor, LEDs and optical system design.

